



Universität Hamburg

DER FORSCHUNG | DER LEHRE | DER BILDUNG

Characterization of reactive systems for lignin-based materials

Dissertation

with the aim of achieving the doctoral degree
at the Faculty of Mathematics, Informatics and Natural Sciences

Department of Chemistry

University of Hamburg

Submitted by

Paulina Georgia Maria Weidmann

2025

1st Assessor: Prof. Dr. G. A. Luinstra

2nd Assessor: PD Dr. C. Wutz

Oral defense committee: Prof. Dr. G. A. Luinstra

Prof. Dr. W. Maison

Dr. T. Lemcke

Date of Oral Defense: 05.09.2025

Date of Approval to Publish: 17.09.2025

The work presented in this thesis was carried out from November 2019 to April 2023 in the working group of Prof. Dr. G. A. Luinstra in the Institute for Technical and Macromolecular Chemistry at Hamburg University.

Financial support for this thesis given by Deutsches Bundesministerium für Wirtschaft und Energie (BMWi, ZIM) following a decision of Deutscher Bundestag as well as by a scholarship of University of Hamburg is gratefully acknowledged.

Some results were obtained in corporation with the working groups of Prof. Dr. I. Smirnova (Institute for Thermal Separations, Technical University Hamburg-Harburg) and Prof. Dr. F. Lieber (Institute of Chemistry of Renewable Resources, University of Natural Resources and Life Sciences, Vienna) as part of the research project POLIGOM (Porous Lignous Organic Materials - Hochporöse Ligninmaterialien).

Parts of the experimental work was carried out by Torben Duhm, Tim Domroes and Frederick Leube as part of their bachelor thesis and internships.

DeepL was used to revise spelling and grammar for parts of this work.

Abstract

Lignin is the second most abundant biopolymer on earth but is rarely used as polymeric aromatic source because of its high structural variety. Two different approaches are studied in this work for the valorization of lignin, both of them give a perspective to add a sustainable resource for material synthesis.

Oxypropylation, e.g. the modification of lignin with propylene oxide, yields liquid polyol mixtures suitable for the synthesis of polyurethane foams. Poly(propylene glycol) is formed as a side product, reducing the overall lignin content in the final foam. The extent of this side reaction was found to be highly sensitive to the type of catalyst. Potassium *tert*-butoxide as catalyst gives 10% less side product than the usually used potassium hydroxide. Formation of side products is even lower using the amidine 1,8-Diazabicyclo[5.4.0]undec-7-ene as catalyst. Combined use of propylene oxide and cyclic propylene carbonate as modifiers lead to presence of carbonate linkages in the polymer chains grafted to lignin. The properties of lignin-based polyols can thus be tailored for a desired application.

Mechanically stable organic aerogels are prepared from an acid-catalyzed polycondensation of a mixture of 40 *wt%* resorcinol and 60 *wt%* lignin and an appropriate amount of formaldehyde. Gels form within a few minutes. Dimethyl sulfoxide/H₂O is the best solvent system for the preparation of stable gels with low shrinkage and without the need for supercritical drying. Scale-Up allows for production of monolithic gels with dimensions of 15x15x3 cm or below. The obtained detailed understanding in form of a structure-property relationship makes it possible to tailor the amount of acid and formaldehyde appropriate for a certain application.

Zusammenfassung

Lignin ist das am zweithäufigsten vorkommende Biopolymer der Erde, wird aber aufgrund seiner großen strukturellen Vielfalt nur selten als aromatischer Rohstoff in Polymeren verwendet. In dieser Arbeit werden zwei verschiedene Ansätze untersucht, die eine Wertschöpfung von Lignin ermöglichen und die so die Perspektive eröffnen, einen zusätzlichen nachwachsenden Rohstoff für die Materialsynthese zu etablieren.

Die Oxypropylierung, d.h. die Modifizierung von Lignin mit Propylenoxid, führt zu flüssigen Polyolmischungen, die sich für die Synthese von Polyurethanschäumen eignen. Als Nebenprodukt entsteht Poly(propylenglykol), das den Gesamtgehalt an Lignin im fertigen Schaum verringert. Der Anteil dieser Nebenreaktion ist stark abhängig von der verwendeten Katalysatorart. Kalium-*tert*-butanolat als Katalysator verringert die Menge des Nebenprodukts um 10% im Vergleich zu dem üblicherweise verwendeten Kaliumhydroxid. Die Verwendung der Amidinbase 1,8-Diazabicyclo[5.4.0]undec-7-en als Katalysator verringert die Bildung von Nebenprodukten noch weiter. Die kombinierte Verwendung von Propylenoxid und cyclischem Propylencarbonat als Modifikator führte zur Bildung von Carbonatbindungen in den Polymerketten. Eigenschaften von Polyolen auf Ligninbasis können dadurch an die gewünschte Anwendung angepasst werden.

Mechanisch stabile organische Aerogele werden aus einer säurekatalysierten Polykondensation einer Mischung aus 40 *wt%* Resorcin und 60 *wt%* Lignin sowie einer entsprechenden Menge Formaldehyd hergestellt. Die Gele bilden sich innerhalb weniger Minuten. Dimethylsulfoxid/H₂O ist das beste Lösungsmittelsystem für die Herstellung stabiler Gele mit geringem Schrumpfverhalten, ohne dass eine überkritische Trocknung erforderlich ist. Eine Maßstabsvergrößerung führt zur Herstellung monolithischer Gele mit Abmessungen von 15x15x3 cm oder weniger. Das gewonnene detaillierte Verständnis in Form einer Struktur-Eigenschafts-Beziehung ermöglicht es, die benötigten Mengen an Säure und Formaldehyd auf die gewünschte Anwendung abzustimmen.

Table of Contents

1	Introduction.....	1
1.1	Lignin.....	3
1.1.1	Structure and Properties	3
1.1.2	Recovery of Lignin from Biomass.....	4
1.1.3	Valorization of Lignin.....	8
2	Objectives of the thesis	10
3	Lignin-based Polyols.....	11
3.1	Background	11
3.1.1	Lignin as Polyol for Polyurethane Synthesis.....	11
3.1.2	Modification of Lignin with Propylene Oxide	12
3.1.3	Modification of Lignin with Propylene Carbonate	15
3.2	Scope of this work.....	18
3.3	Results and Discussion.....	19
3.3.1	Oxypropylation of Lignin	19
3.3.2	Influence of Different Catalysts on the Oxypropylation of Lignin	22
3.3.3	Oxypropylation of Different Types of Lignin	29
3.3.4	Oxypropylation with Propylene Carbonate	30
3.3.5	Oxypropylation with Propylene Oxide and Propylene Carbonate	33
3.4	Summary	40
4	Lignin-based Aerogels.....	42
4.1	Background	42
4.1.1	Aerogels – Preparation and Theoretical Models.....	43
4.1.2	Resorcinol-Formaldehyde Aerogels	45
4.2	Scope of this work.....	54
4.3	Results and Discussion.....	55
4.3.1	Gels with various Lignin Contents	56
4.3.2	Gels with Different RC	61
4.3.3	Gels with Different M/F.....	62

4.3.4	Gels with Different M/C	63
4.3.5	Gels Synthesized in various Solvent Systems	66
4.3.6	RLF Aerogels from Non-Soluble Lignin	69
4.3.7	Acetone/H ₂ O as Solvent System.....	70
4.3.8	DMSO/H ₂ O as Solvent System	73
4.3.9	Solid Content Reduction using a higher Viscosity of the Formulation	76
4.3.10	Combination of Base and Acid as Catalyst for RLF Gels.....	77
4.3.11	Property Optimization by Design of Experiments	80
4.3.12	Scale-Up of Promising Formulations.....	85
4.4	Summary.....	91
5	Conclusions	93
6	Experimental Details	95
6.1	Materials	95
6.2	Oxypropylation of Lignin.....	96
6.3	Preparation of RLF Aerogels.....	99
6.4	Sample Characterization	101
	Chemicals and Safety	104
	References.....	107
	Appendix	114
	Publications	131
	Acknowledgements.....	132
	Declaration of Academic Integrity	133

Index of Abbreviations

C	Catalyst
cPC	Cyclic Propylene Carbonate
Đ	Dispersity
DBU	1,8-Diazabicyclo[5.4.0]undec-7-en
DMSO	Dimethyl Sulfoxide
DoE	Design of Experiments
DP	Degree of Polymerization
EtOH	Ethanol
F	Formaldehyde
FTIR	Fourier Transform Infra-Red
HL	Hydrolysis Lignin
KL	Kraft Lignin
KOH	Potassium Hydroxide
KOtBu	Potassium <i>tert</i> -Butoxide
L	Lignin
L/PO	Ratio of Lignin to Propylene Oxide
M/C	Molar ratio of monomer to catalyst
M/C_a	Molar ratio of monomer to acid catalyst
M/C_b	Molar ratio of monomer to acid catalyst
M/F	Molar ratio of monomer to formaldehyde
M_n	Number average molar mass

M_w	Weight average molar mass
NMR	Nuclear Magnetic Resonance
OSL	Organosolv Lignin
pK_a	Acidity constant
PO	Propylene Oxide
PPG	Poly(Propylene Glycol)
PU	Polyurethane
R	Resorcinol
RC	Reactive Content
RF	Resorcinol – Formaldehyde
RLF	Resorcinol – Lignin – Formaldehyde
ROP	Ring Opening Polymerization
SEC	Size Exclusion Chromatography
SEM	Scanning Electron Microscopy
SL	Soda Lignin
T_{max}	Maximum Reaction Temperature
wt	weight

1 Introduction

In 1956, a speech held at a meeting of the American Petroleum Institute sparked an outcry. It was given by American geologist and geophysicist M. King Hubbert, who predicted the peak of the US petroleum production between 1965 and 1970.^[1] His prognosis, at first met with harsh criticism, proved to be accurate, as oil production in the US declined for some time after 1970. While technological advances and newly discovered oil reserves led to a deviation from the predicted curves at the beginning of the 21st century,^[2] Hubbert was one of the first scientists to point out a critical problem – fossil resources will eventually run out.

Depletion of natural reserves is a major challenge of today's society, calling for a shift from fossil to more renewable resources.^[3] Gas, oil and coal are mostly used for energy production but are also the main carbon source for the chemical industry and with that for the plastics industry.^[4] The advantages of polymer materials in daily life are plentiful, but their use also raises environmental concerns.^[5]

Changing from petrol-based to plastics from renewable resources is a key challenge for polymer scientists.^[6–8] This topic is also addressed on the political stage - alternative feedstocks for plastics production are part of the European Union's *European Strategy for Plastics in a Circular Economy*.^[9] In 2021, only 1.5 % of the world plastics production were bio-based materials. Although this is still a very small percentage, the amount has almost doubled since 2018.^[10]

One example of a renewable resource with promising applications in polymer synthesis is lignin.^[11–16] This phenolic macromolecule is a main component of wood and other plants. Large quantities of lignin are resulting as a byproduct in the paper industry. The availability on a large scale makes this renewable resource a potential substitute for (a part) of petrol-based substances. Nowadays, the major part of around 98 % of lignin is burned for energy recovery and only a small part is isolated for further valorization. Because of the overall high amount of lignin that is processed these 2 % still amount to over 1 million tons per year.^[17]

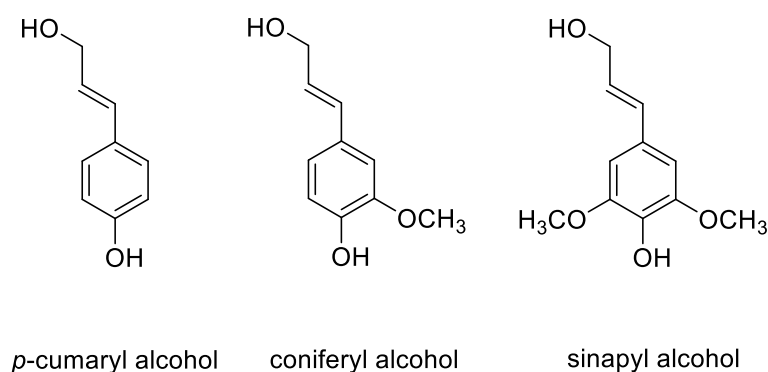
The concept of biorefineries has added to a growing focus on lignin valorization.^[17,18] Separating lignin from the other components is a key aspect of the biorefinery cycle, which aims to convert all parts of biomass to high-value products.^[12,19,20] Every liter of cellulosic ethanol (EtOH) produced as renewable fuel in biorefineries generates about 0.5 – 1.5 kg of lignin of which only around 40 % is needed to cover the energy demand of the production.^[18] It is estimated that 60 billion gallons of biofuel will be produced in the US in 2030.^[21] This amount would require 750 million tons of biomass and would leave 22.5 million tons of lignin available. These numbers highlight the substantial amount of lignin that could be available as feedstock.

However, lignin is not a simple compound; it also has been considered worthless because of its high structural complexity. “You can make everything from lignin, except money” – this alleged quote of the pulp industry represents the negative view on this topic.^[22,23] Fortunately, the opinion has changed and an immense amount of scientific publications reflect the effort to utilize this potential.

1.1 Lignin

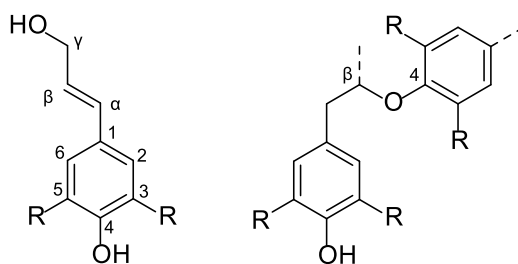
1.1.1 Structure and Properties

Lignin is the most abundant natural polymer on earth after cellulose. It is a crosslinked phenolic macromolecule that adds strength and rigidity to plant cell walls. It is also important for the transport of water and nutrients inside the plants and as a protection against UV radiation because of its aromatic character. The name lignin is derived from the Latin word for wood, *lignum*.^[24] The structure of lignin has been of interest for quite some time.^[25] It is based on substituted phenylpropanoids, the monolignols. Three different monolignols have mainly been identified: *p*-cumaryl alcohol, coniferyl alcohol and sinapyl alcohol (Scheme 1). The resulting units of the lignin molecule are referred to as *p*-hydroxyphenyl (H), guaiacyl (G) and syringyl (S) unit.^[26,27]



Scheme 1. Structure of monolignol units *p*-cumaryl, coniferyl and sinapyl alcohol.

Oxidative phenolic coupling of those units leads to a broad structural variety in lignin. Monolignols are linked by ether and carbon-carbon bonds. The most common bond is the β -O-4 type. For bond classification carbon atoms of the side chain are labeled α ; β and γ whereas the carbon atoms of the aromatic ring are numbered 1-6. An ether bond is indicated by the addition of the letter 'O' (Scheme 2).^[19]



Scheme 2. Exemplary labeling of atoms in a monolignol unit and structure of a β -O-4 bond.

Relative amount of H-, G- and S-units and types of linkages depend on the plant species lignin is extracted from. Differences in composition can also be noted between different plants or even different parts of the same plant. Softwood lignin consists mostly of G-units, hardwood lignin of G- and S- units and grass lignin of all three units.^[14,19,26] Lignin contains different functional groups. Most common are hydroxy groups, both aliphatic and aromatic. Other present functionalities are methoxy, carbonyl and carboxyl groups. High structural variance makes it difficult to establish a defined structural formula for lignin.

1.1.2 Recovery of Lignin from Biomass

Lignin is present in nature in form of lignocellulosic biomass. The ratio between lignin, hemicellulose and cellulose in the biomass depends on the type of plant. The main components need to be separated for a valorization in the best possible way.^[12] The way of separation has an influence on the structure of the resulting lignin.^[27] Various separation processes have been established (Figure 1). Two groups can be distinguished: processes leading to lignin that contains sulfur and sulfur-free processes.^[12] The aim of the separation has mostly been the conversion of lignin and hemicellulose to a soluble form to separate them from the cellulose. The latter is then used for paper production.

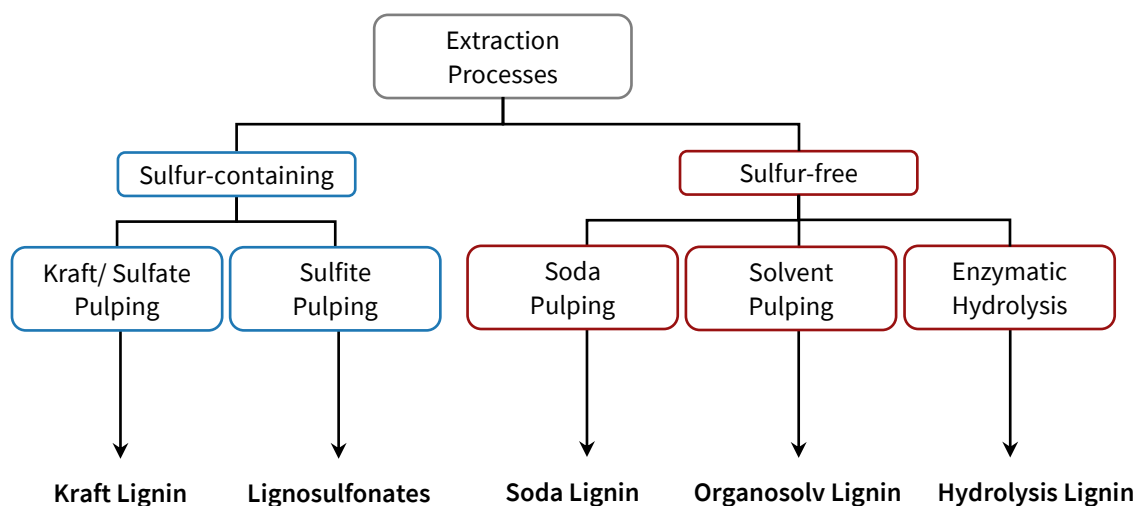
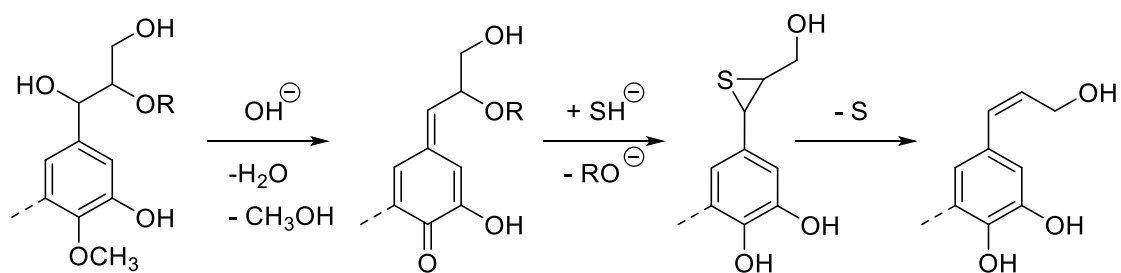


Figure 1. Processes for lignin isolation.

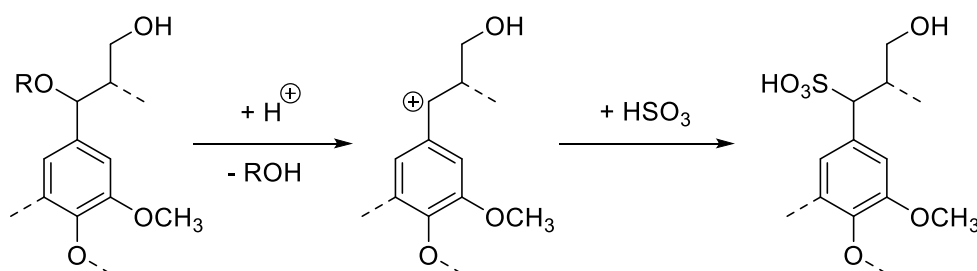
Sulfate pulping was patented in 1884.^[28] The process is known as the “Kraft” process after the German word for “strong” because the resulting paper showed high strength.^[29] This name is nowadays still used and the resulting lignin is called Kraft lignin (KL). Strong alkaline conditions are used to cleave ester bonds between hemicellulose and lignin.^[19] An aqueous solution of sodium hydroxide and sodium sulfide is used at temperatures between 150- 180 °C.^[14,17,30] Several reactions take place beside the ester cleavage and result in episulfides. Elimination of sulfur leads to conjugated structures and explains the presence of both elemental and bound sulfur in KLs (Scheme 3).



Scheme 3. Typical reactions during Kraft pulping leading to episulfide structure and conjugated structure after elimination of sulfur.

Sulfite pulping uses aqueous solutions of sulfite or bisulfite at temperatures between 140-170 °C.^[30] This process comprises an acidic cleavage of lignin ether bonds.

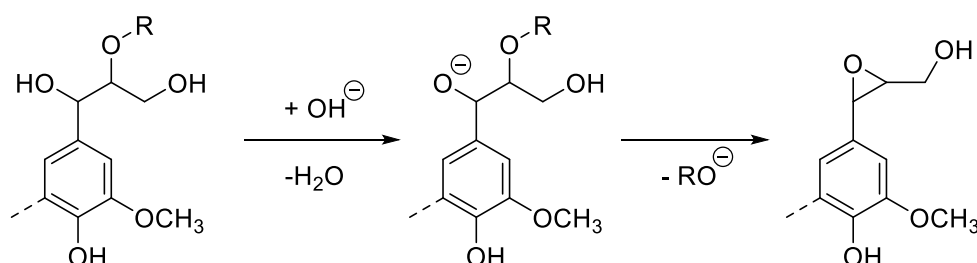
A sulfonation of aliphatic lignin parts takes place and a loss of alkoxy groups is observed. The resulting products are called lignosulfonates (Scheme 4).^[19] Lignosulfonates are soluble in water.^[27] The relevance of sulfite pulping is declining because the more versatile and robust Kraft process is commercially preferred.^[15]



Scheme 4. Typical reactions during sulfite pulping leading to formation of lignosulfonates.

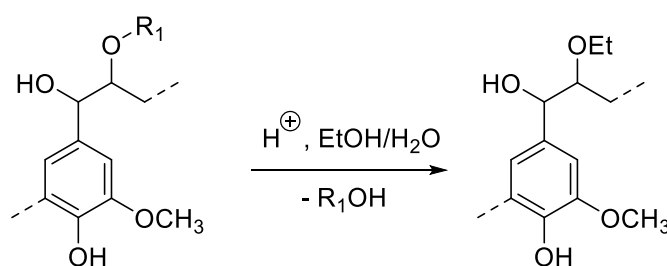
High sulfur content present after extraction is a disadvantage for further lignin processing because of the occurring yellowing of the products, the odor and interference with further reactions.^[31] Sulfur-containing lignins, especially KL, are mostly burned to generate energy for the pulping mills.^[14,31]

The alternative Soda process uses aqueous sodium hydroxide at a temperature of 160 °C for separation of the components of wood.^[30] Ester bonds of lignin are cleaved under formation of epoxides (Scheme 5). Resulting Soda lignin (SL) is soluble in water and precipitates from the pulp after acidification.^[27] This process is mostly used for annual grown non-wood sources such as straw and bagasse.^[12]



Scheme 5. Typical reactions during Soda pulping leading to epoxide-containing structures.

A further source of lignin comes from biomass in the Organosolv process. Therein solvents like primary alcohols at temperatures around 180 °C are applied.^[19] Cleavage of ether bonds takes place under acidic conditions and results in fragmentation (Scheme 6). Organosolv lignin (OSL) is soluble in many organic solvents but insoluble in water.^[12] The use of low-boiling solvents facilitates the recovery and concomitantly gives a lower energy consumption. Odor produced by heating of sulfur components of the lignin from KL and other processes can be avoided and the resulting lignin is of high purity. This opens the possibility for an easier lignin valorization. The first Organosolv process was patented in 1971.^[32] Since then various similar processes based on various solvents have been developed. However, none of them have been established on a large industrial scale.^[24]



Scheme 6. Typical cleavage of an ether bond during Organosolv pulping with EtOH.

Hydrolysis lignin (HL) is a byproduct of the bioethanol production.^[33] Pretreatment of biomass with enzymes and catalytic amounts of acid leads to hydrolysis and is needed for the separation of the carbohydrate component. The residual lignin can be recovered by downstream extraction.^[11]

In the past, recovery and valorization of lignin was not the main objective of the pulping processes established in the paper industry and the obtained lignin was mostly unsuitable for further processing.^[24,31] Nowadays, with increasing relevance of bio-based chemicals within the approach of green chemistry, consideration of lignin as a simple waste product is no longer appropriate. Recent research therefore focusses on revising and adapting existing processes to enable easy valorization of lignin.^[18,34–36]

1.1.3 Valorization of Lignin

The production of commercial lignin worldwide was estimated at 1.7 million tons in 2018.^[35] The largest amount were lignosulfonates (approx. 80 %), followed at some distance by KL (15 %). SL and HL make up the smallest fraction (5 %). OSL is produced only on pilot scale.^[17] Other processes like hydrolysis or steam explosion yield also lignins with high purity, but those techniques still remain at a very low production level.

The available quantity in combination with the high content of hydroxy groups make lignin an interesting educt for simple chemical derivatizations.^[14,15,23,37] The dependence of the lignin structure from source and extraction method results in a diversity of chemical behavior and generally an “inconsistent” performance.^[30] Solubility and reactivity of a given lignin will differ from batch to batch. The presence of sulfur in some types of lignin can additionally be problematic because of its odor and possible yellowing of the product. The dark brown color of lignin itself is disadvantageous for certain applications. Nonetheless, a larger number of publications deal with the application of lignin in diverse material classes. Possible fields of applications include drug release and tissue engineering^[38,39] or as electrodes and for energy storage.^[40,41] A variety of approaches to produce lignin-containing polymeric materials has been published and reviewed in the last years.^[13,14,42–44] Replacement of phenolic components in resins by lignin is the most evident choice because of structure similarity.^[15,30] The limited reactivity of lignin compared to phenol remains an obstacle in this approach. Lignin depolymerization and catalytic valorization is another vast field of research but shall not be addressed here any further.^[45–47]

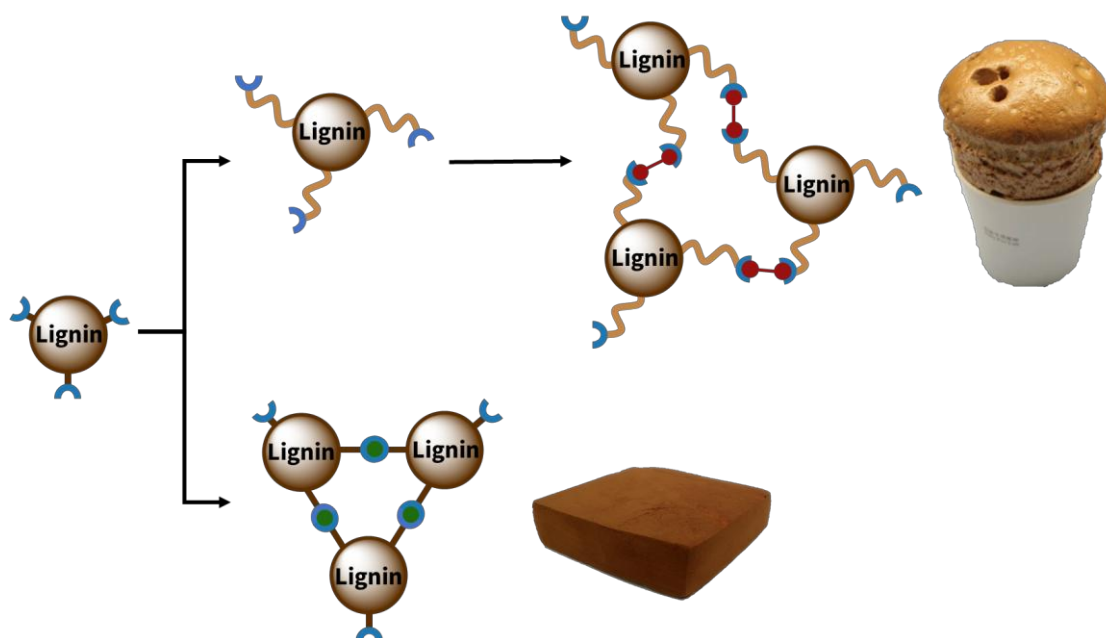
The use of lignin as (reactive) filler in composites has also been studied.^[30,48,49] Low compatibility with other polymers is a limiting factor here. Modification of lignin is thus often advantageous prior to application.^[11,12] The incorporation of lignin into other polymers can also be achieved by grafting from or onto the different hydroxy groups inside the molecule.^[50,51]

The challenges described above have so far limited the valorization of lignin on a larger scale.^[15,52] The need for chemical modification prior to the material synthesis additionally

limits the economic viability. However, some applications have been brought to a semi-commercial level, including melt-blown or injection-molded polymer blends and lignin-containing resins for plywood and fiberboards.^[53–56]

2 Objectives of the thesis

This thesis focuses on two approaches for the valorization of lignin in polymeric materials (Scheme 7). The first approach is the modification of lignin by oxypropylation. This method enhances the reactivity and compatibility of lignin and permits its use as polyol component for polyurethanes, e.g. in form of rigid foams. The second approach uses lignin without modification for the synthesis of aerogels. These porous structures have various promising fields of interest, e.g. use as insulation materials or as substrates with high surface area.



Scheme 7. Valorization of lignin by substitution and incorporation into a PU network (top) and direct incorporation of lignin into aerogels (bottom).

3 Lignin-based Polyols

3.1 Background

3.1.1 Lignin as Polyol for Polyurethane Synthesis

An urge for a change from petrol-based resources to renewable ones can be observed in all parts of the chemical industry. This includes production of polyurethanes (PUs), a major class of polymeric materials and sixth in volume of the most produced plastics in Europe.^[10] The two main components in PU synthesis are isocyanates and hydroxyls. Lignin contains both aliphatic and aromatic hydroxy groups, which makes it applicable as polyol. Various approaches to incorporate lignin into PU materials, especially PU rigid foams, have been evaluated and reviewed in detail.^[33,37,57–59] The natural properties of lignin could also enhance the moisture and flame resistance of derived PU materials.^[60,61]

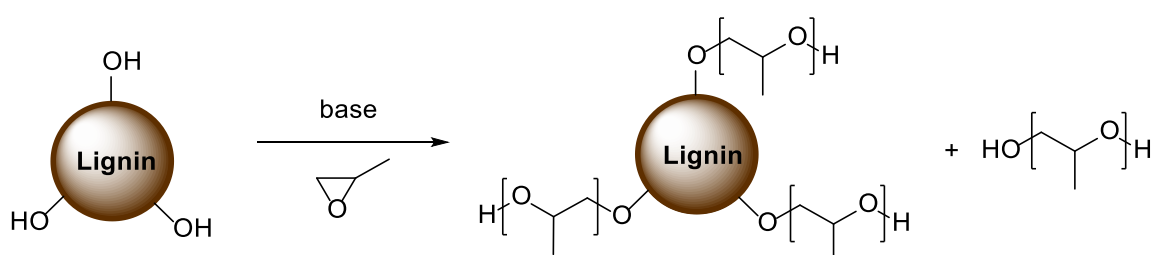
The incorporation of native lignin, i.e. without chemical modification, showed general limitations in its ability to yield PU-foams with application adequate properties.^[62–65] The low miscibility of lignin with polyol mixtures affected the cell structure of foams and led to higher thermal conductivities and substandard mechanical properties. The lignin content was limited as high loading leads to a drastic viscosity increase of the polyol component.^[66] Lignin agglomeration resulted in a lower conversion of OH groups because they were inaccessible.^[33] The best results in the above context were obtained with lignin types with higher solubility, such as OSL.^[62,65,67] Several approaches were used to enhance the compatibility of other lignin types with commercially available PU systems.^[68,69] One possibility is chemical modification by grafting propylene oxide (PO) to lignin by a ring opening polymerization, the so-called oxypropylation.

Ring opening polymerization (ROP) of PO is a common route to obtain polyether polyols, e.g. for the synthesis of PU materials.^[70] Starter molecules with various amounts

of hydroxy groups, e.g. glycerin or sugars, are used to generate polyols with concomitant functionalities. Thus, different kinds of PU materials become assessable in dependence of the type of polyols obtained from the starters and their functionalization by the ROP. Both bases and acids can be used as catalysts for the ROP. Potassium hydroxide (KOH) is the most commonly used catalyst on industrial scale and has been studied detail.^[71–73] Acid catalysts are not used on a larger scale because of the high amount of cyclic byproducts.^[74] A class of catalysts called Double Metal Cyanides (DMCs) show higher efficiency and are used for the synthesis of a plethora of polyols, thereunder those of high molecular weight.^[75–77]

3.1.2 Modification of Lignin with Propylene Oxide

Oxypropylation has been applied to functionalize biomass^[78–80] thereunder also of several lignin types.^[61,81–83] Such biomolecules can be used as starter molecules as long as they contain OH groups. Hydroxy groups of lignin are used as starters in the anionic ring opening polymerization (Scheme 8). The hydroxy groups are deprotonated by a base and the resulting alcoholate groups mostly attack the secondary α -carbon atom of the PO ring. An attack on the tertiary β -carbon is also possible but less likely because of higher steric hindrance.^[74]



Scheme 8. Reaction equation of oxypropylation of lignin with PO yielding modified lignin and PPG.

Chain transfer reactions and other nucleophiles present in the mixture cause a simultaneous formation of poly(propylene glycol) homopolymers (PPGs).^[79] Nucleophiles leading to homopolymerization can be alcoholates formed from residual

solvents like EtOH or methanol from the lignin extraction processes. Base catalysts themselves can also be starter nucleophiles. Homopolymer content can vary between 10 % and 60 % depending on the reaction conditions.^[61] Modified lignin and homopolymer can be separated by extraction.^[84]

Oxypropylation leads to lignin containing hydroxyl with an enhanced reactivity, especially those resulting from phenolic moieties.^[61] Grafting of PPG chains from OH groups resembles an extension of these groups and results in better accessibility by some release of steric and electronic constraints (phenols are less reactive toward isocyanates).^[85,86] Oxypropylation also improves the solubility of lignin in the polyol/isocyanate medium.^[87]

Oxypropylation of lignin is commonly carried out in pressure reactors at temperatures above 150 °C and at pressures up to 20 bar. Reaction times from 30 minutes to multiple hours are reported.^[61,82,88] Oxypropylation under mild reaction conditions, i.e. lower temperature and pressure seems possible but reaction times of several days are necessary.^[89]

A handful of studies were focused on the oxypropylation of lignins in the context of their application to yield PU foams. Oxypropylated Kraft, Soda and Organosolv lignins give liquid polyol mixtures and could be transformed into foams without significant deterioration in the properties.^[61,82,83,90–92] Lignins will span a range of properties in dependence of their origin and may therefore show differences in their reactivities. One example is the oxypropylation of KL, which can be unproblematic or give undesired solid residues under seemingly identical conditions.^[61,82]

Bottom line of several research groups is the agreement on two main influential parameters: the amount of catalyst (usually given in *wt%*) and the ratio of lignin to PO (L/PO; usually given as ratio weight/volume).^[61,82,88] General trends have been established describing the dependence of reaction time, maximum reaction temperature, homopolymer content, polyol viscosity, molecular weight M_n and dispersity \bar{D} from these two parameters (Scheme 9).

Scheme 9. Dependencies of L/PO ratio and catalyst concentration on reaction time, maximal temperature, homopolymer content, polyol viscosity, M_n and \bar{D} .

	reaction time	max. temperature	homopolymer content	polyol viscosity	M_n	\bar{D}
higher ratio L/PO	↓	↑	↓	↑	↓	↑
higher catalyst amount	↓	↑	⇒	⇒	↓	↓

High ratio L/PO resulted in shorter reaction times for PO conversion and a higher maximum reaction temperature. The higher maximum temperature is taken as the higher rate of the exothermal PO ring opening (polymerization). Homopolymer content was lower and polyol viscosity was higher when more lignin was used, and the apparent molecular weight was lower and dispersity was higher. Lower M_n is a result from the formation of shorter chains because less PO is available per OH group. A higher dispersity is the logic result for lower molecular weight products, where the lignin dispersity is more dominant. In addition, the original hydroxyls on lignin and the oxypropylated ones are bound to have different reactivities, also leading to a broadening. The higher viscosity is most likely associated with the overall higher amount of hydrogen bonds.

Homopolymer content and polyol viscosity were independent of catalyst concentration. M_n and \bar{D} were lower because more but shorter chains were formed and a more uniform growth can be expected for higher catalyst concentration and the resulting higher reaction temperature. Analysis of modified lignin by ^1H NMR gave the average amount of repeating units per OH group between 3 and 6 for oxypropylation with a L/PO ratio of 30/70.^[82]

Incorporation of oxypropylated lignins into PU rigid foam is majorly limited by their viscosities, with partly inhomogeneous (viscous) products as result. Foams were

produced from oxypropylated lignins with a L/PO between 20/80 and 40/60 and using catalyst concentrations of 2 - 5 wt%. The highest overall lignin content in a foam was obtained by using a reaction product with L/PO of 40/60 as polyol.^[88] Such foams had properties comparable to foams based on fossil polyols.

The modified lignin and homopolymer were not separated for the synthesis of PU foams. A separation step is not necessary because both oxypropylated lignin and PPG are polyols and react with isocyanates. A certain amount of homopolymer is even useful to enhance processability. Polyol mixtures have mostly homopolymer contents between 40 % and 50 %. The resulting foams consequently have a rather low lignin content. Reduction of the homopolymer content would thus be useful to achieve a higher content of renewables. However, an isolated lignin fraction may end up to be too viscous for homogeneous mixing with standard isocyanates.

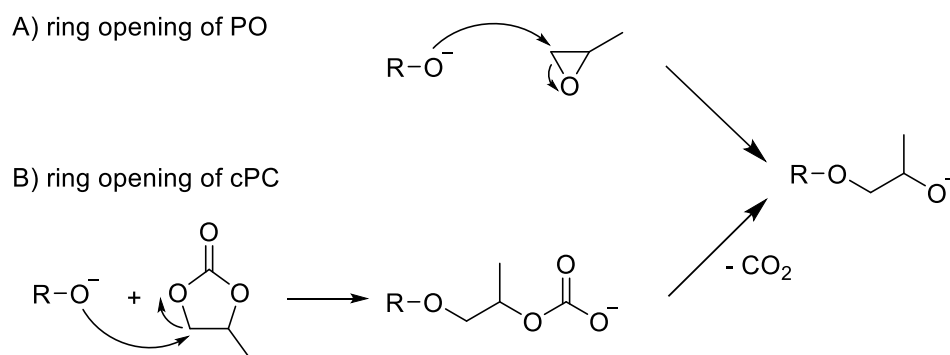
The homopolymer content is likely dependent on the catalyst type: at least a basic catalyst can also be a nucleophile, starting the ring opening polymerization of PO and thus giving PPG. However, little seems to have been published on the influence of the diverse basic catalysts on the formation of homopolymer in a mixture with lignin. The use of catalysts other than KOH in the oxypropylation of lignin thus remains an open field.

It is known that homopolymer content could be drastically reduced by using THF as solvent (and co-monomer) and also by using boron trifluoride etherate as Lewis acidic catalyst.^[93,94] Tertiary amines as catalyst led to a slower oxypropylation than hydroxides in the oxypropylation of sugar beet pulp.^[78] Full conversion of PO was not observed, indicating a loss of catalytic activity during the reaction. Higher water content during the oxypropylation was shown to lead to higher amounts of PPG. No reaction took place when drying the biomass in a dynamic vacuum, removing most of the water.

3.1.3 Modification of Lignin with Propylene Carbonate

Propylene carbonate (cPC) is a possible reagent for substituting PO in the oxypropylation of lignin. It is less toxic than PO. cPC is available as a side product of

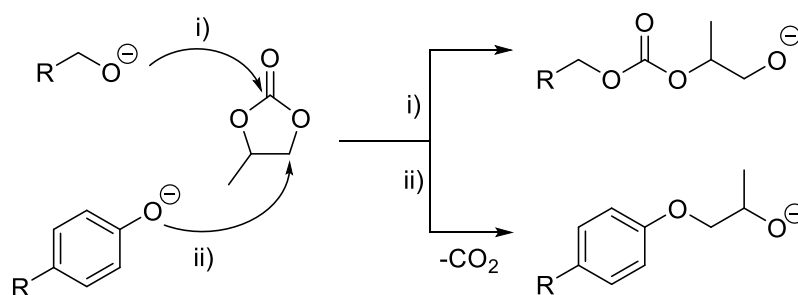
polycarbonate production from CO_2 and PO but also is produced from PO and CO_2 , using a zinc / ammonium bromide catalyst system.^[95,96] The reaction product from the reaction of lignin and cPC may be the same as for the ring opening of PO (Scheme 10, A). A nucleophilic attack under ring opening of cPC and subsequent decarboxylation (Scheme 10, B) yields a secondary hydroxyl. The oxypropylation of Organosolv lignin with cPC and K_2CO_3 as catalyst was reported.^[97] Follow-up studies showed that oxypropylation is also possible for KL and SL, with other cyclic carbonates and with organic bases like DBU.^[98–102]



Scheme 10. Ring opening of A) PO and B) cPC by a nucleophile.

Oxypropylation with cPC takes place both on aliphatic and aromatic OH groups of lignin but is significantly slower for the aliphatic ones.^[98] Higher degree of substitution and longer chains were obtained at higher temperatures, higher catalyst concentrations and with more equivalents of cPC. Longer reaction times showed the same effect but also favored side reactions. A strong increase of molecular weight indicated coupling of different lignin molecules, e.g. by a transesterification of intermediate carbonates.

Aromatic and aliphatic OH moieties will react differently with cPC (Scheme 11). Aliphatic OH groups preferably react at the carbonyl group of cyclic carbonates and therefore lead to the formation of carbonate linkages inside the polymer chains.^[98,102] The formation of carbonate linkages was reported to be favored for longer reaction times, higher catalyst content and more equivalents of cPC.



Scheme 11. Reaction of propylene carbonate with i) a deprotonated aliphatic OH group and with ii) a deprotonated aromatic OH group.

Average number of propyl units per OH group was lower for oxypropylation with cPC then with PO.^[99,101] An approximate DP = 2 was reported for KL.^[102] SL only allowed for an approximate DP = 1.5 after a reaction time of 24 h.^[100] The highest DP of 4.5 was reported for OSL.^[98] An excess of 10 eq cPC was used in this reaction.

Homopolymerization is only observed to minor degree, but the reaction product contains unreacted cyclic carbonates.^[59] First studies have shown that incorporation of crude reaction products from oxypropylation with cPC in PU foams is possible.^[103] However, the overall lignin content in the foam was limited to 20 *wt%* and material properties were overall worse than for reference materials without lignin. A full assessment has not been conducted, and a set of questions remain open in the usefulness of the functionalization of lignin with cPC for PU foams.

3.2 Scope of this work

Oxypropylation is regarded as the most promising modification for incorporation of lignin into PU materials. Until now, oxypropylated lignin has not made its way to industrial scale, showing the need for further developments. Two remaining drawbacks in that context will be addressed in this work:

- Reduction of the amount of PPG formed as side product will be targeted by a change in catalyst. Potassium *tert*-butoxide and the amidine 1,8-Diazabicyclo[5.4.0]undec-7-ene will be considered as alternative to KOH because of their different basicity and nucleophilicity. The aim is to control the formation of byproducts.
- A more benign approach is using cPC for functionalizing lignin. Reaction conditions will be varied with the objective to obtain suitable polyols for foam production. A combined use of PO and cPC is proposed too and the effects of the ratio of these two reagents on the polyol properties will be mapped.

3.3 Results and Discussion

3.3.1 Oxypropylation of Lignin

Oxypropylation of lignin, i.e. the grafting of PPG chains to lignin OH groups was carried out in a batch reactor. A ratio of lignin to PO of 30/70 (*wt/wt*) was used in all reactions. OSL and catalyst were dissolved in PO and the reaction was started by heating to 150 °C. This process converted solid lignin to a liquid lignin-containing polyol (Figure 2).



Figure 2. Unmodified solid lignin before and liquid lignin-containing polyol after oxypropylation.

The crude product consisted of modified lignin and byproduct free of lignin. Both components could be separated by extraction. Successful oxypropylation was confirmed with FTIR and ^1H NMR spectroscopy of the isolated lignin fraction as described in literature.^[61,82,91] The byproduct could be identified as PPG by FTIR spectroscopy in agreement with previous studies.^[61]

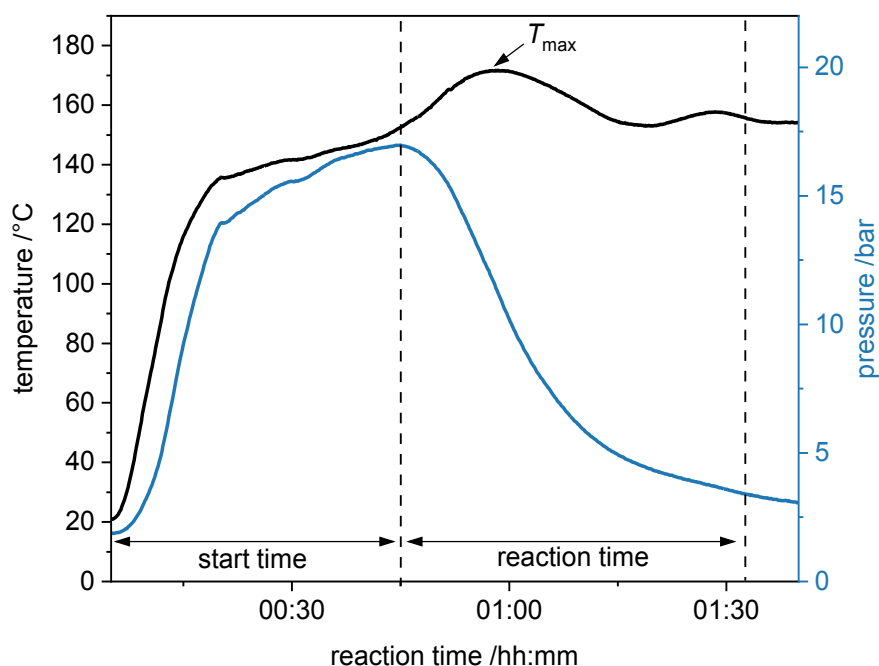


Figure 3. Exemplary course of temperature (black) and pressure (blue) inside the reactor during the oxypropylation of lignin. Start time, T_{\max} and reaction time are indicated.

Temperature and pressure profiles in the reactor were similar for all oxypropylations (Figure 3). Both parameters rose in the beginning because the mixture was heated (over the reactor wall by a heating mantle set to 150 °C). An increase over this temperature indicates the beginning of the exothermic PO ring opening. This time was marked as start time. The pressure decrease observable after the reaction start is caused by conversion of PO into a liquid polyol, lowering the partial pressure over the liquid reaction medium. The return to a pressure near to the initial value corresponds to a full consumption of PO and marks the end of the reaction. This time was set as reaction time. Deviations of the temperature from 150 °C after the first increase were caused by intermittent heating of the external heat supply. Start time, reaction time and T_{\max} (highest temperature reached) can be used to describe and compare oxypropylation reactions.

Oxypropylation with OSL and 5 % KOH was performed to validate the reactor setup. The system was chosen because it is an established benchmark. The reaction with OSL and 5 wt% KOH was repeated five times to test reproducibility (Figure 4). The profiles of different reactions show minor differences. Reaction times have a larger but still

reasonable standard deviation (Table 1). The overall results indicate a good reproducibility and allows the comparison of the abovementioned parameters for different reaction conditions in the following.

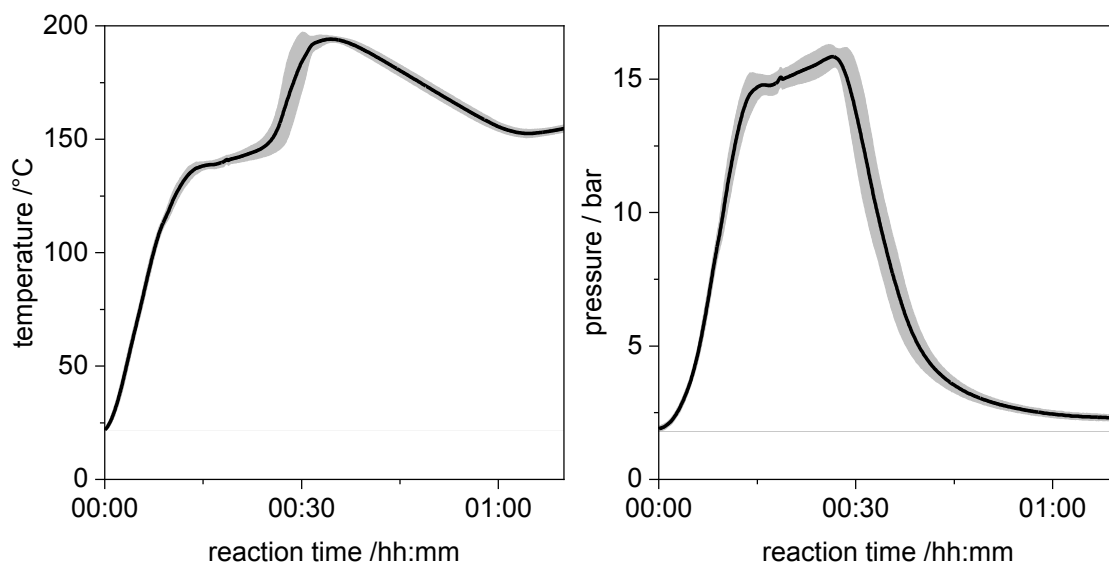


Figure 4. Temperature profile (left) and pressure profile (right) of oxypropylation of OSL with 5 wt% KOH. Average data of five experiments is shown in black with standard derivation indicated in grey.

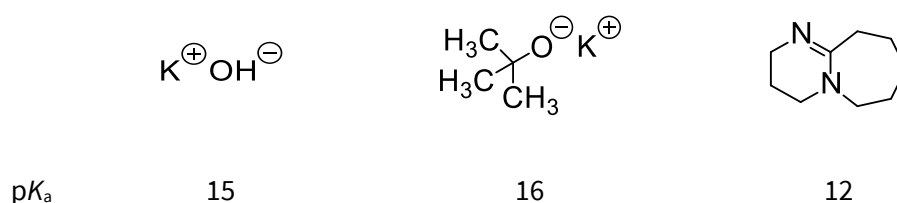
Table 1. Oxypropylation reactions of OSL with 5 wt% KOH.

	start time / min	reaction time / min	T_{\max} / °C
	22	54	197
	22	48	195
	22	36	194
	24	47	195
	25	44	193
average	23 ± 2	46 ± 8	195 ± 2

3.3.2 Influence of Different Catalysts on the Oxypropylation of Lignin

Two different reactions take place during treatment of lignin with propylene oxide. Control over the ratio of these reactions is essential to obtain a polyol suitable for a given application. The first reaction is the intended modification of lignin by grafting PO from OH groups present. The other one is the homopolymerization of propylene oxide to PPG. Homopolymer formation is caused by the presence of nucleophiles other than deprotonated OH groups of lignin. One possible source of nucleophiles is the base catalyst itself. Variation of catalyst is therefore expected to affect the homopolymer content.

Three different base catalysts were used: potassium hydroxide (KOH), potassium *tert*-butoxide (KOtBu) and 1,8-Diazabicyclo[5.4.0]undec-7-ene (DBU). They differ in their basicity as indicated by the acidity constant $pK_a^{[101,104]}$ (Scheme 12). Oxypropylation was performed at catalyst concentrations of 2.5 *wt%*, 5 *wt%* and 10 *wt%*. Higher amounts of catalyst led to shorter start time and higher T_{max} (Figure 5 and Table 2).



Scheme 12. Structural formulas and pK_a of KOH, KOtBu and DBU.

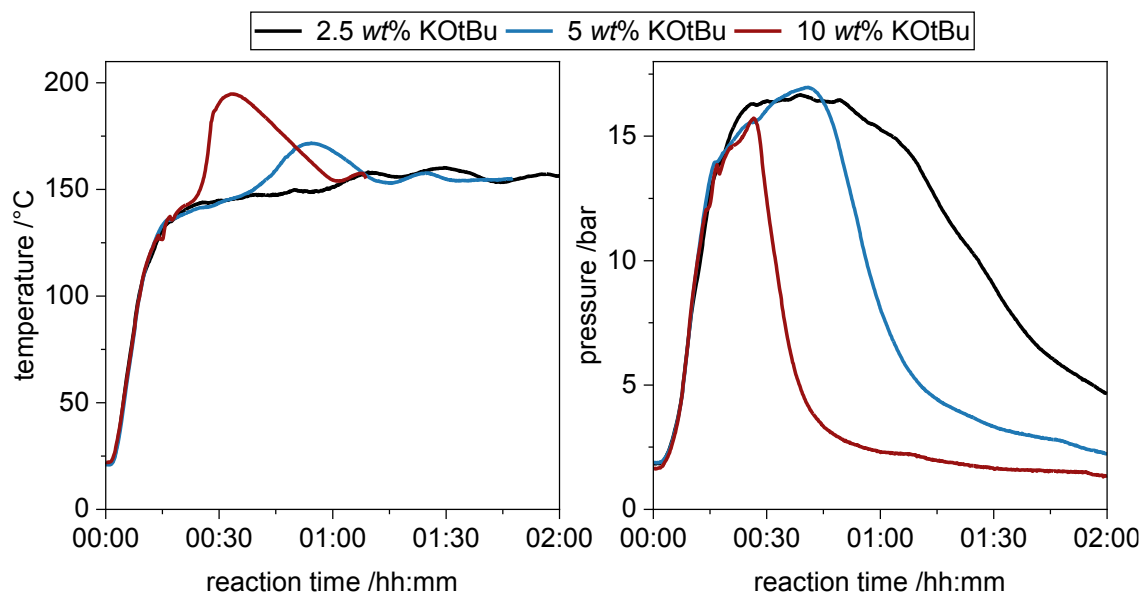


Figure 5. Temperature profile (left) and pressure profile (right) of oxypropylation with 2.5 wt% (black), 5 wt% (blue) and 10 wt% (red) KOtBu.

Table 2. Start time and T_{\max} for oxypropylation with different concentration of KOH and KOtBu.

KOH			KOtBu	
concentration	start time	T_{\max}	start time	T_{\max}
/wt%	/min	/°C	/min	/°C
2.5	42	163	50	/
5	32	195	35	172
10	19	209	23	195

No distinct temperature increase was observed when using 2.5 wt% of KOtBu. The start time and T_{\max} could not be determined as described before. A decrease of (PO partial) pressure was observed after 50 minutes and therefore start time can be estimated in this range. The reaction with 5 wt% of KOtBu had a start time of 35 minutes with a $T_{\max} = 170$ °C. KOtBu at the level of 10 wt% caused a rise in temperature after 23 minutes to $T_{\max} = 195$ °C. The same trend was observed for KOH (Figure A1, appendix). No exothermal peak was observed for DBU (Figure A2, appendix). Shorter start times can

be explained by faster conversion induced by more active sites as more OH groups of lignin are deprotonated. Each active site can open PO rings. The exothermic reaction at the same time causes a stronger increase in temperature when the rate is higher. This logic also explains the lack of exothermal peak for the slow reaction using the lowest catalyst concentration. The use of K_{OT}Bu instead of KOH leads to longer starting times and also a lower T_{\max} . A possible explanation for this is its lower basicity which leads to lower degree of lignin deprotonation.

The reaction time for PO conversion was shorter at higher catalyst concentration. Reaction time is longer for reactions with K_{OT}Bu as catalyst than for those with KOH (Figure 6). The reaction with 5 wt% of DBU was even slower. Only 25 % conversion was reached after a reaction time of 12 h (Figure A2, appendix).

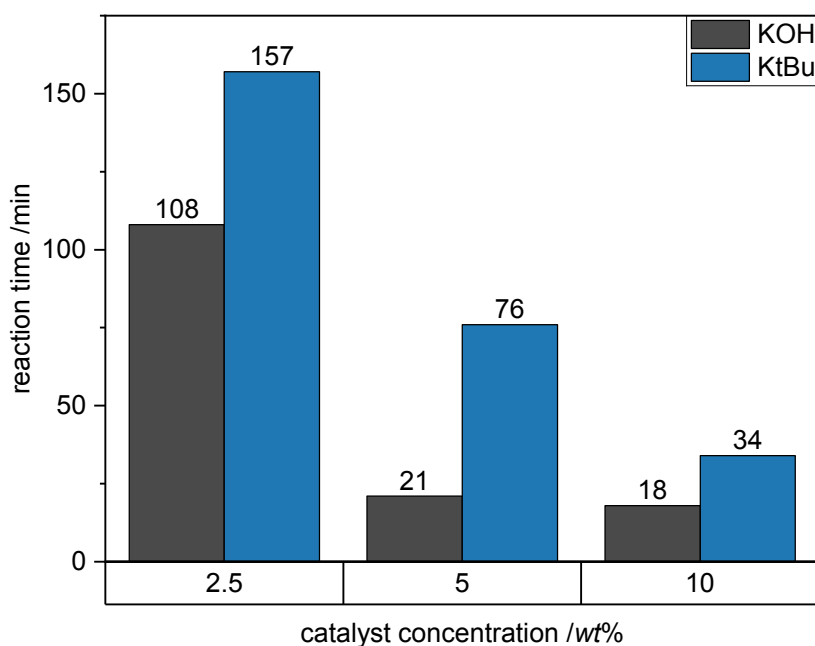


Figure 6. Reaction time for PO conversion in dependence of catalyst concentration.

Using a higher amount of catalyst leads to higher numbers of growing chains as indicated by the faster consumption of PO. Also, reaction time was shorter for more nucleophilic catalysts with a faster rate of initiation by PO ring opening polymerization. More nucleophilic ring openings lead to a higher number of homopolymer chains in addition to the chains grafted from lignin and further increases the rate of PO

consumption. Reaction with DBU was significantly slower than with KOH and K₂OtBu. DBU as a non-nucleophilic base possibly only causes deprotonation of OH groups in lignin, but no additional reactive chain ends are formed by ring opening. Less initiation would result in a lower homopolymer content.

Homopolymer content was lower for reactions with K₂OtBu than for reactions with KOH. Almost no homopolymer was formed with DBU (Figure 7).

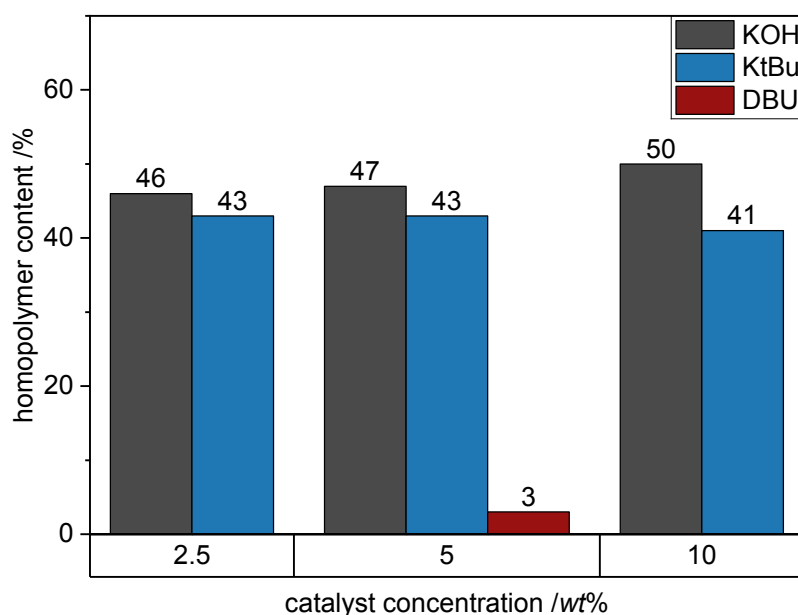


Figure 7. Homopolymer content in dependence of catalyst type and concentration.

The lower homopolymer content supports the assumption that modification of lignin is favored over homopolymerization in case of applying less nucleophilic catalysts. The (minor) homopolymer formation observed for the non-nucleophilic base DBU could be caused by nucleophilic impurities like H₂O or EtOH present in lignin. No clear dependence of homopolymer content on catalyst concentration was observed within the scope of accuracy of this method.

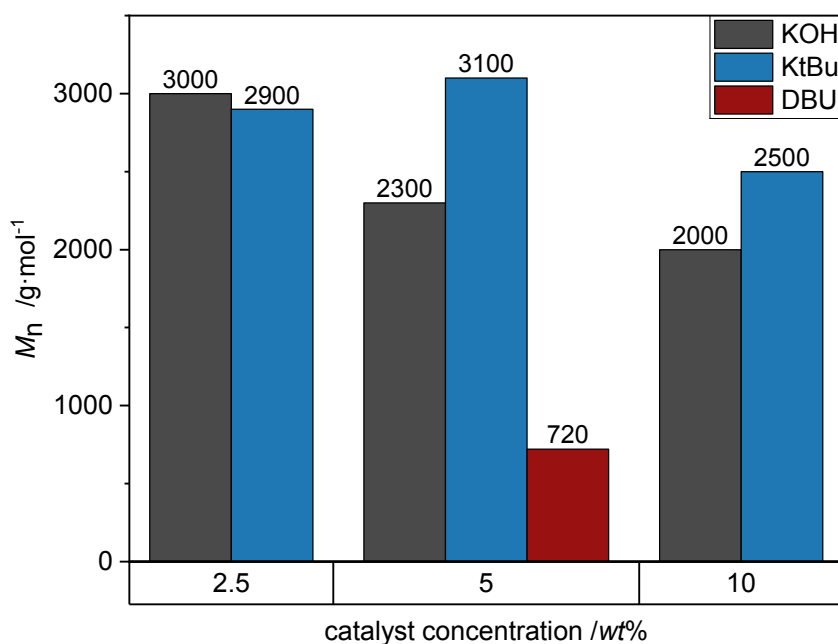


Figure 8. Molecular weight of modified lignin as function of catalyst concentration and type. Molecular weight of unmodified lignin was 480 g·mol⁻¹.

Higher catalyst concentration resulted in lower molecular weight (Figure 8, Figure A3 - Figure A5, appendix). The same amount of monomer is distributed over more active sites, leading to overall shorter chains and a more compact polymer.^[61] Molecular weight of modified lignins is higher in products from reactions with K^tOBu than with KOH. The difference in molecular weight again indicates that using K^tOBu favors modification of lignin over homopolymerization. Molecular weight is low for reactions with DBU because the reaction was terminated before full conversion of PO was reached.

M_n is similar for KOH and K^tOBu for 2.5 wt% catalyst. This observation indicates a lower influence of nucleophilicity at lower catalyst content. It seems that most of the catalyst reacts with lignin and thus that an overall smaller amount of catalyst reduces the number of free nucleophiles: side reactions such as PPG formation become less relevant.

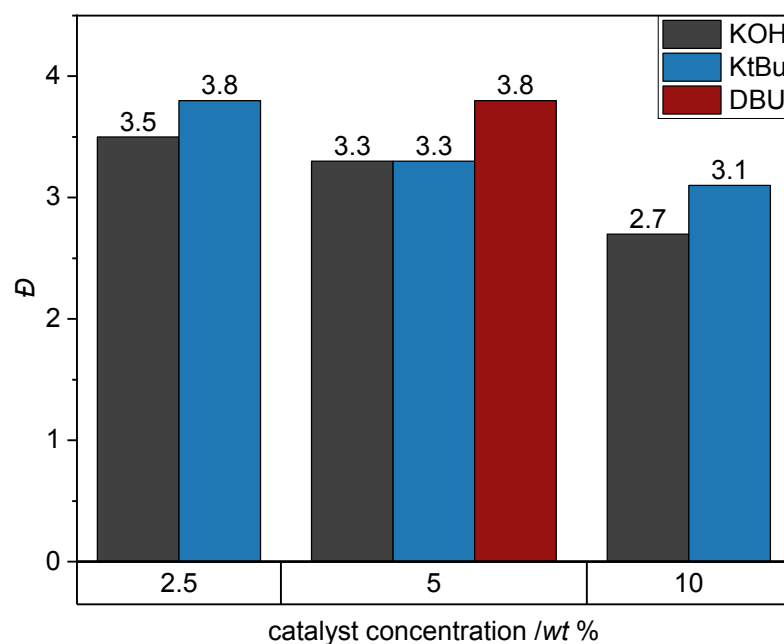


Figure 9. Dispersity D in dependence of catalyst concentration. Dispersity of unmodified lignin was 2.5.

The polydispersity D of lignin was higher after oxypropylation. Chromatograms show a broadening towards lower molecular weights. The structural variety of lignin itself possibly amplified by uneven distribution of active sites may be an explanation for broadening of molecular weight distribution – not all molecules are oxypropylated to the same extend. D was higher for lower amount of catalyst and higher for KOtBu than for KOH. A low molar ratio of catalyst to OH groups in lignin is used in all reactions, leading to simultaneous activation of only a small percentage of OH groups. Oxypropylation of a given lignin molecule additionally leads to higher solubility in the reaction system and higher availability for further addition. This could result in a preferred addition of PO to longer chains and therefore result in uneven distribution between the chains and higher polydispersity. The larger dispersion when using KOtBu is possibly to be related to the lower molar content at the same weight percentage. Another possible explanation is the longer reaction time, leading to inhomogeneity because of increasing viscosity during the course of the reaction, which might cause uneven distribution of reactants.

Oxypropylation with DBU also led to a high D (Figure 9). This could result from the long reaction time favoring side reactions as mentioned before. Basicity of DBU could also be lower than the new chain end of a formed polymer chain, resulting in abstraction of a proton, termination of this growing chain and the initiation of chain growth in a different position.

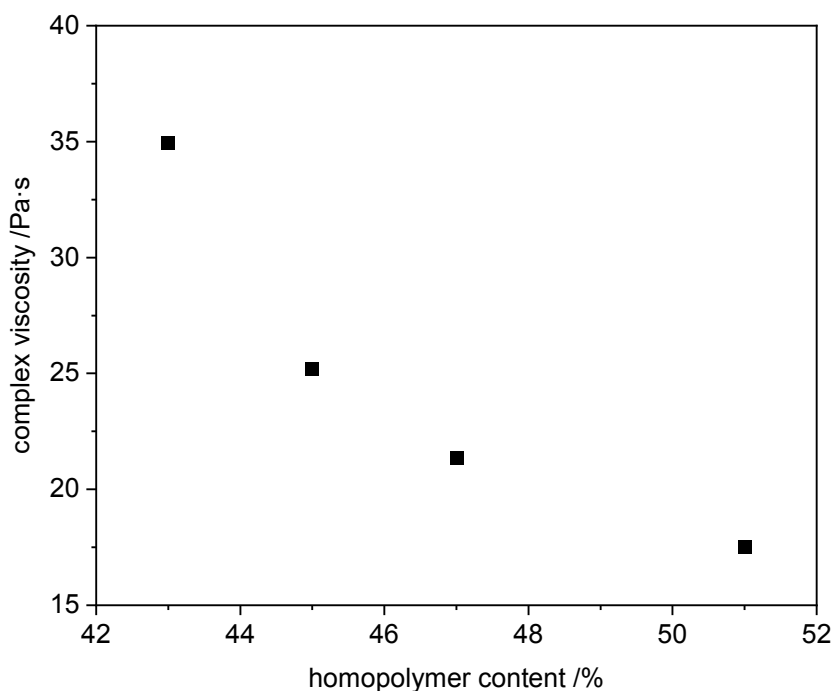


Figure 10. Complex viscosity for crude oxypropylation products with different homopolymer content.

Viscosity of lignin polyols could be tuned by controlling homopolymer content. PO-modified lignin (with no PPG) has a high viscosity being in an almost solid product. Lower viscosities were obtained for high homopolymer content (Figure 10). A higher content of the compound with low viscosity in the polyol mixture results in an overall lower viscosity. Higher molecular weight of PPG side products can also be the reason for a higher viscosity, but this effect has been identified as a smaller effect for PPG contents < 40 %.^[61] PPG with low molecular weight has a low viscosity. Complex viscosity of Lupranol 1200 (PPG with average molecular weight of $450 \text{ g}\cdot\text{mol}^{-1}$) as reference was determined as $0.0734 \text{ Pa}\cdot\text{s}$.

Oxypropylation with 5 *wt%* DBU inhibited the formation of homopolymer. A solid product was obtained. It showed good solubility in PPG and commercially available polyols. Higher solubility offers the possibility to adjust viscosity of the lignin polyol to a desired value. A major drawback when using DBU is the long reaction time. A reaction with 20 *wt%* DBU showed that higher catalyst concentration accelerated the reaction - full conversion of PO was reached after 8 hours. The crude product was highly viscous with a homopolymer content of only 15 %, but also with residual DBU. These results indicate that organic, low nucleophilic bases may generally be useful catalysts to obtain oxypropylated lignin with low homopolymer content, paving the way to foams with high lignin content without the effort of separating off PPG.

3.3.3 Oxypropylation of Different Types of Lignin

Oxypropylation of KL, SL and OSL using a lignin/PO ratio of 30/70 (*wt/wt*) and 5 *wt%* KOtBu as catalyst resulted in a liquid polyol mixture without a solid residue. ¹H NMR spectra (Figure A6- Figure A8) and FTIR spectra (Figure A9 - Figure A11, appendix) indicated the modification of lignin. The byproduct was identified as PPG by FTIR spectroscopy and was the same for all three reactions (Figure A12, appendix).

Table 3. Data on the oxypropylation of KL, SL and OSL 5 *wt%* KOtBu.

	KL	SL	OSL
start time /min	26	19	36
T_{\max} /°C	175	178	172
reaction time /min	113	59	99
homopolymer content /%	42	43	43
average DP per OH	5	6	3

The general reaction profile of the oxypropylation was similar for all lignin types, showing a temperature increase indicating reaction start followed by a decrease in pressure (Figure A13, appendix). The same amount of PO and lignin was taken in each reaction. The same mass of catalyst was used for all reactions but OH_{total} is different for different lignins (Table A1, appendix). This results in the highest catalyst concentration per OH group in SL followed by KL and OSL and thus also of active centers. The same order indeed is found for the start times (ranging from 19 min for SL to 26 min for KL and 36 min for OSL) and for the maximum temperature (Table 3).

Reaction time for PO conversion was shortest for SL (59 min) followed by OSL (99 min) and KL (113 min). This order is only partially following the amount of catalyst per OH group. The faster oxypropylation of OSL could relate to higher solubility of this lignin, leaving OH groups more accessible, but other factors cannot be excluded.

All crude products had a homopolymer content of 42-43 %. The homopolymer content is in accordance with previous results indicating no dependence of homopolymer content on catalyst concentration. OSL had the lowest average DP per OH group, followed by KL and SL (by 1H NMR spectroscopic analysis). The average DP is lower for lignin with the higher OH content. Distribution of the same quantity of monomers on a higher number of active centers results in fewer repeating units per chain.

3.3.4 Oxypropylation with Propylene Carbonate

Cyclic propylene carbonate (cPC) was also considered for functionalizing lignin, a viable alternative for PO.^[97,98,101,102] The reaction between cPC and lignin was carried out with various lignin types (OSL, KL, SL), catalysts (K_2CO_3 , KOtBu, DBU), amounts of cPC (10, 20, 30 eq.) and reaction times (2 h, 6 h, 12 h). All reaction products contained residual cPC and after removal, the lignin fraction was obtained as a powder. Analytic results were similar for all reactions and are shown exemplarily for the modification of OSL with DBU as catalyst in the following.

FTIR spectra of lignin fractions after the reaction with cPC confirmed the oxypropylation^[61] and indicate a similar product as for the lignin fraction after reaction with PO (Figure 11). The increasing band intensity between 2700 – 3000 cm^{-1} corresponds to stretching of aliphatic CH_3 , CH_2 and CH groups. This is expected for a compound with a higher number of methyl groups caused by grafting of isopropoxy units to the OH groups of lignin. Another band appeared at 1370 cm^{-1} , typical for CH_3 groups. The carbonyl band at 1710 cm^{-1} decreased. All changes were less pronounced in the lignin fraction after oxypropylation with cPC than with PO, suggesting a smaller number of repeating units added.

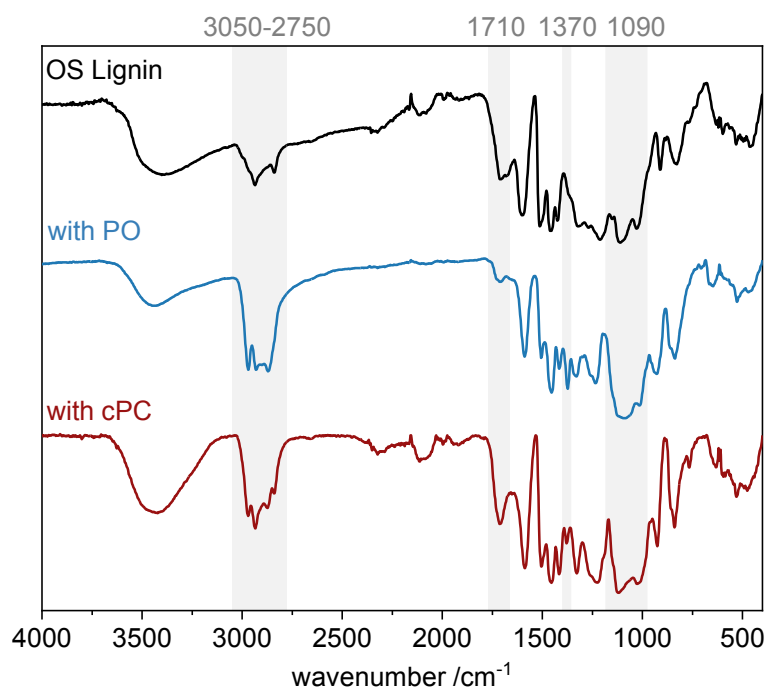


Figure 11. FTIR spectra of OSL before modification (black) of lignin fraction after oxypropylation with PO (blue) and of lignin fraction after oxypropylation with cPC (red).

The same observation was made in ^1H NMR spectra of lignin fractions after oxypropylation with either PO or cPC (Figure 12). New signals appeared between 0.8 – 1.4 ppm and 3.0 – 4.1 ppm, corresponding to methyl and/or methylene/methine entities of the isopropyl group. Aromatic protons of the lignin backbone are showing the characteristic shifts between 6.1 – 7.2 ppm.

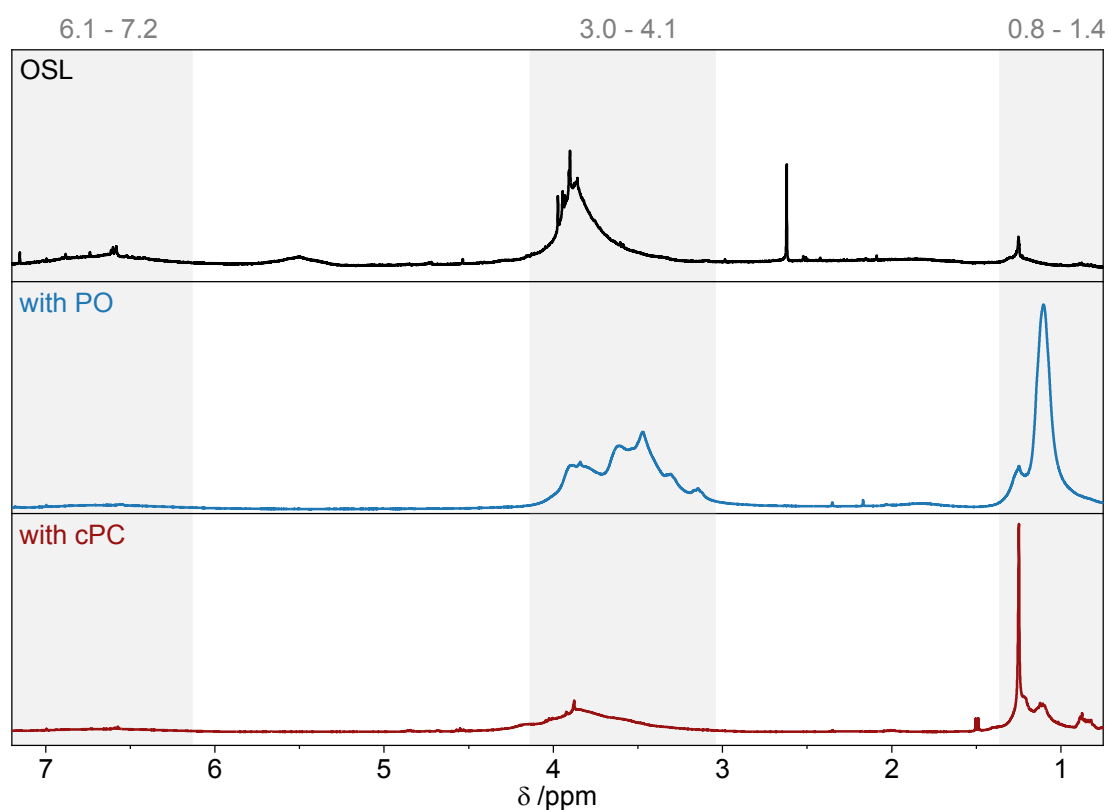
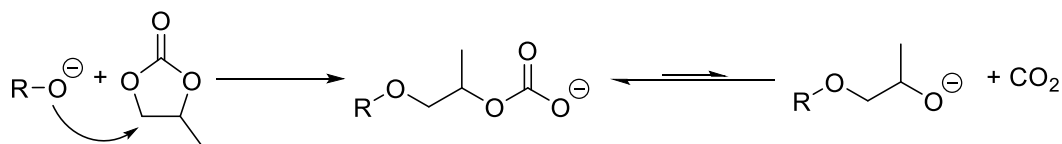


Figure 12. ^1H NMR spectra of OSL (black) of lignin fraction after oxypropylation with PO (blue) and of lignin fraction after oxypropylation with cPC (red).

Evaluation of this signals resulted in an average DP of 1.6 per OH group for reaction with cPC and of 3.2 for oxypropylation with PO (Figure A6 and Figure A14, appendix). Solubility of the reaction product of the oxypropylation with cPC was low in CDCl_3 and a solid residue was present. The low solubility implies that the average DP was even lower. Low average DP indicates that each OH group in lignin was modified with cPC once but almost no consecutive addition took place after that.

Hydroxy groups in lignin preferably attack the alkylene carbon atom of cPC, leading to carbonato intermediates. Decarboxylation would lead to a secondary alcoholate comparable to the one formed during ROP of PO. However, under the given reaction conditions, the carbonato intermediate is favored and no further addition of cPC takes place. In accordance, it is not possible to polymerize cPC to the corresponding polycarbonate.



Scheme 13. Proposed reaction of lignin OH groups with cPC.

This low DP is presumably the reason why the lignin fraction was solid. Liquification by dissolution was not possible because solubility in commercial polyols or PPG was low. A higher DP is preferable because a liquid or at least a soluble lignin component shows better compatibility with the other reactive components in PU synthesis.

A certain lignin type could possibly react with cPC to a higher DP by optimization of reaction conditions. However, this would probably require high amounts of cPC. Isolation of modified lignin from unreacted cPC and short oligomers requires multiple washing steps and is elaborate and expensive. The use of the crude reaction product as polyol in PU foams is possible according to literature, but results in a low overall lignin content.^[105] The combination of those drawbacks leads to the conclusion that the reaction products after oxypropylation with cPC are not attractive to synthesize PU foams with high lignin content in a simple and cost-efficient manner.

3.3.5 Oxypropylation with Propylene Oxide and Propylene Carbonate

A further set of experiments for lignin oxypropylation was with a combination of PO and cPC, again with the objective to obtain a liquid polyol (while reducing the amount of toxic PO). Lignin was thus first dissolved in cPC and base catalyst was added. The mixture was then subjected to the same reaction conditions as described in chapter 3.3.1 for oxypropylation with PO. The product was a dark brown liquid. The crude product could be separated into a brown lignin fraction and a yellow homopolymer fraction. The homopolymer was identified as PPG by ¹H NMR spectroscopy (Figure A15, appendix).

FTIR spectra of the lignin fraction is consistent with an oxypropylation. New bands at 1260 cm⁻¹ and 1740 cm⁻¹ appear in the spectra in addition to the ones described before. (Figure 13). Those bands can be assigned to C=O bond stretching of carbonate groups.^[98]

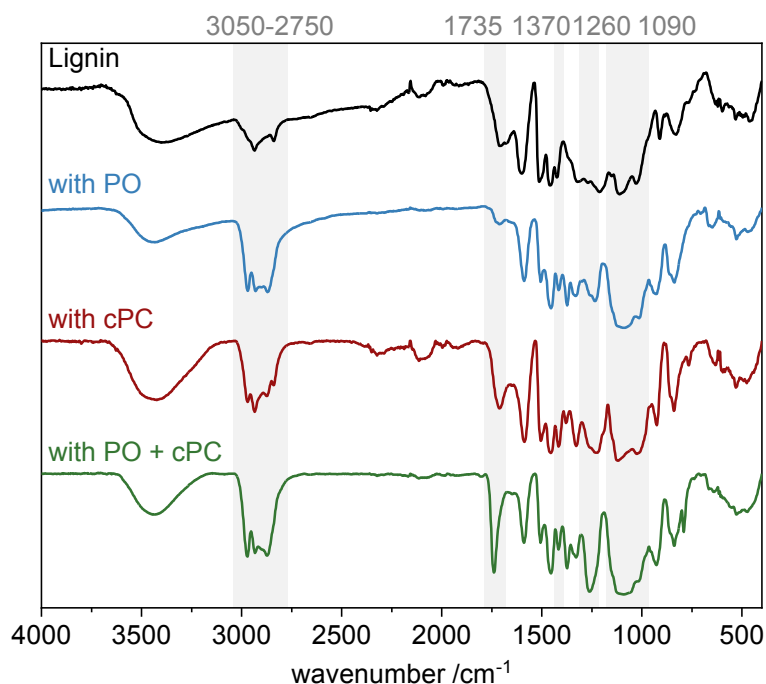


Figure 13. FTIR spectra of OSL before modification (black) after modification with PO (blue), with cPC (red) and PO and cPC (green).

Multiple washing steps were performed to remove excess cPC. Purification of crude product was verified by FT-IR and ¹H NMR spectroscopy (Figure A16 and Figure A17, appendix). The spectra after purification confirm that the origin of this band is not residual cPC but originate from carbonate linkages in the modified lignin. The formation of this linkage is caused by nucleophilic attack on the carbonate carbon of cPC.

Incorporation of cPC into the homopolymer was also observed. The FTIR spectrum of the obtained homopolymer also shows characteristic bands for the carbonyl group at 1260 cm⁻¹ and 1735 cm⁻¹ which were not present in the spectrum of homopolymer from reaction with only PO (Figure 14).

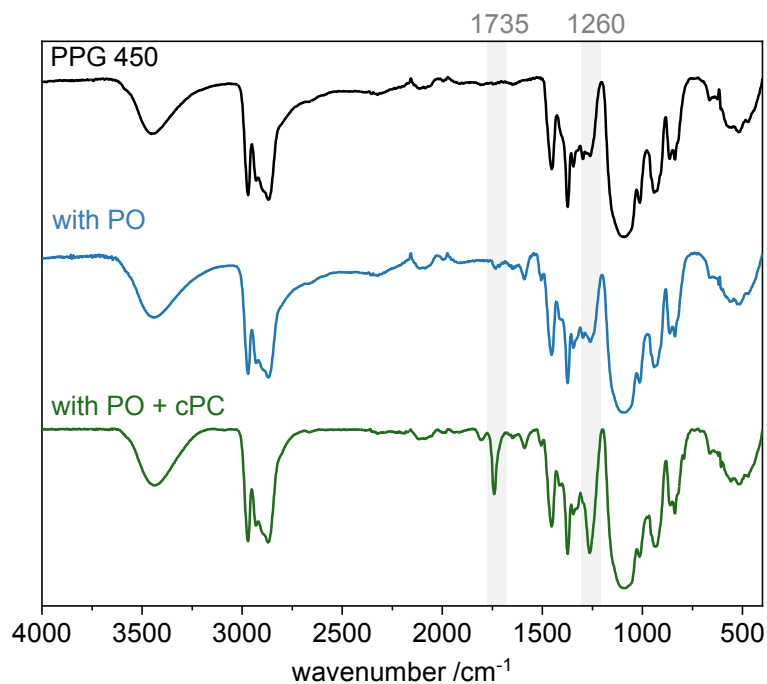


Figure 14. FTIR spectra of PPG450 (black) and of homopolymer obtained as byproduct from oxypropylation of OSL with PO (blue) and PO + cPC (green).

Next, various amounts of PO were replaced by cPC in attempts to oxypropylate lignin. Reactions with 5 %, 10 % and 15 % cPC were carried out, corresponding to a molar ratio of cPC to total OH groups in lignin of 0.3:1, 0.7:1 and 1:1, respectively. All reactions led to dark brown, liquid products.

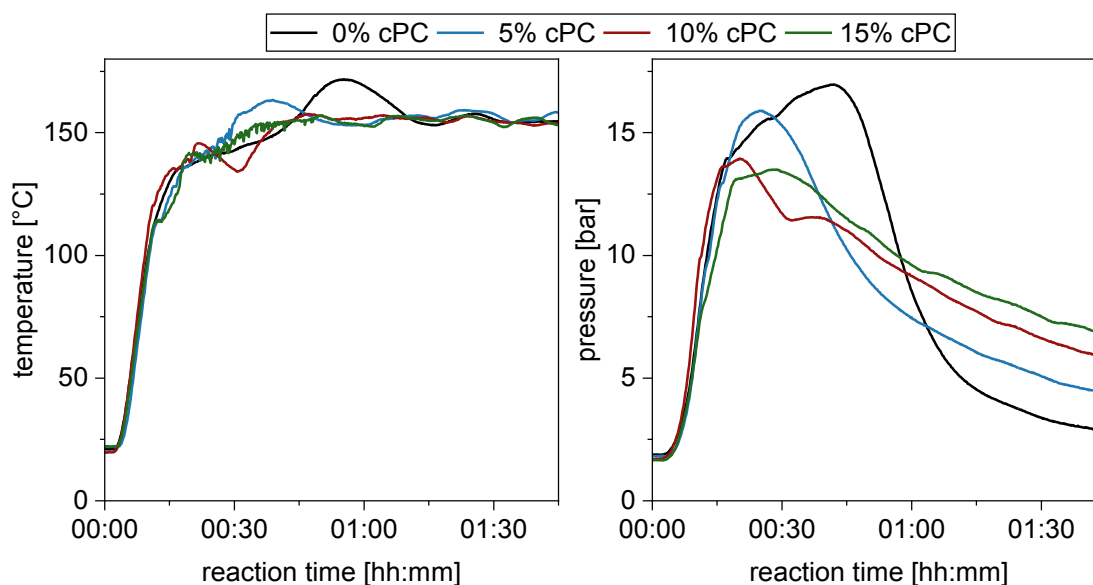


Figure 15. Temperature profile (left) and pressure profile (right) during oxypropylation with 0 % (black) 5 % (blue) and 10 % (red) and 15 % (green) cPC.

Table 4. Start time and T_{\max} for oxypropylation with different cPC contents.

cPC content	start time	T_{\max}
/%	/min	/°C
0	35	172
5	22	163
10	19	-
15	18	-

Reaction with higher concentrations of cPC started earlier but consumption of PO indicated by decreasing pressure was slower (Figure 15 and Table 4). Start time was reduced from 33 minutes without cPC to around 18 minutes for 15 % cPC. Start time is less accurate for higher cPC content because the reaction started already before the set temperature of 150 °C was reached. T_{\max} is not meaningful when using 10 % cPC and 15 % cPC: the exotherm increase occurred at lower temperature and the overall value is therefore not comparable. The approximate ΔT between the start of the exothermic reaction and the highest temperature reached decrease with increasing cPC content, supporting the assumption of a slower reaction with higher amount of cPC. A possible explanation for the faster start is good solubility of lignin in cPC. Dissolved lignin has more accessible OH groups than solid lignin with a limited surface, and the oxypropylation is faster. Reaction times are hard to estimate from the reactor logs because of the lack of exothermal peak and because pressure did not decrease to the start value. Nonetheless it is evident from pressure profiles that consumption of PO was slower at a higher cPC content. Full conversion was reached without cPC after approximately two hours whereas pressure reached a constant value after four hours for 15 % cPC. This lower reaction rate indicates that monomer addition to the growing chain is slower in the presence of cPC.

cPC will add to most of the graft chains over the course of the reaction, resulting in carbonate intermediates as described above. Further addition of monomers is mostly reversible, and chain growth only becomes possible after addition of multiple PO molecules to one chain. This would explain the overall slower reaction. Increasing viscosity during the reaction may lower the reaction rate further.

The crude product contained residual cPC which could be removed by washing with water (Figure A16 and Figure A17, appendix). Homopolymer is also removed in this step. Extraction with *n*-hexane separated the lignin fraction from the homopolymer but left cPC in both fractions. Separating homopolymer and residual cPC was challenging and made determination of homopolymer content less accurate for reactions with cPC. The lignin fraction isolated from cPC was 65 wt % of the crude product, leaving back 35 wt% of a mixture consisting of homopolymer and cPC. This percentage indicated that reactions with cPC led to an overall lower homopolymer content. The lower homopolymer content is consistent with the observation that no homopolymer was formed during oxypropylation with only cPC and can be explained by stronger driving force for PO ring opening.^[106]

Both FTIR and ¹H NMR spectra are consistent with a dependence of amount of carbonate groups in the polymer chains of oxypropylated lignin on cPC amount used in the reaction. The dependence allows to tailor the number of this functional group in lignin polyols and therefore control the properties of resulting polyol mixtures.

Amount of carbonate linkages in the polymer chain was higher for higher cPC content in the reaction mixture. The higher amount resulted in an increase of characteristic FTIR bands at 1620 cm⁻¹ and 1740 cm⁻¹ (Figure 16). A quantification of the amount of carbonate groups is possible by comparing the integral of the band at 1760 cm⁻¹ to that of the band at 1590 cm⁻¹ (Figure 17). The latter belongs to vibration of aromatic ring in lignin and can be assumed to be constant in all samples.^[107] A linear trend can be observed for the increase of C=O stretching with increasing cPC content (Figure 17).

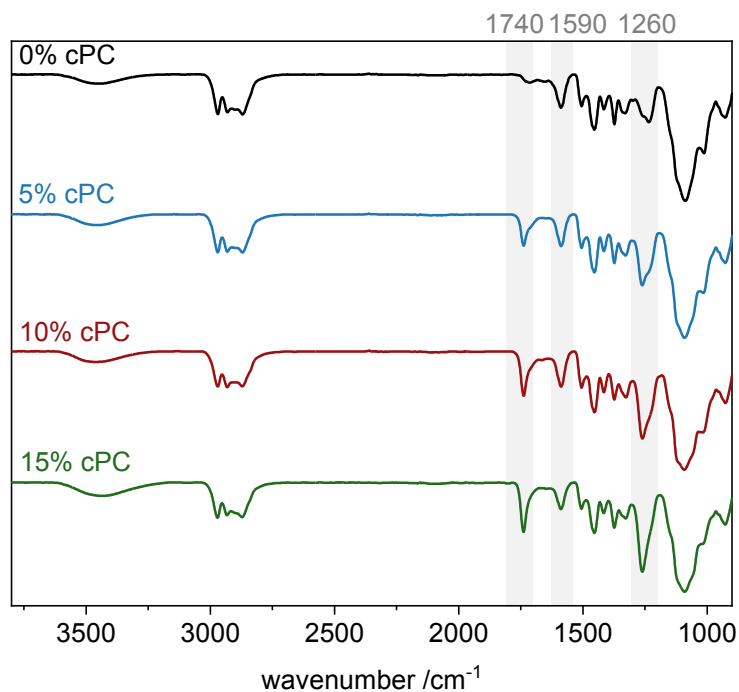


Figure 16. FTIR spectra of oxypropylated lignin with 0 % cPC (black), 5 % cPC (blue), 10 % cPC (red) and 15 % cPC (green).

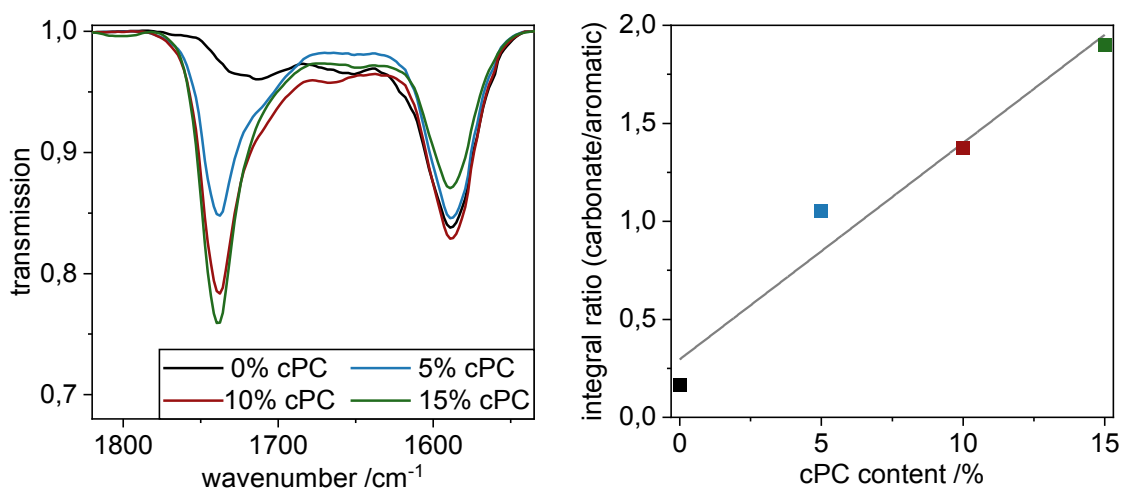


Figure 17. FTIR spectra of oxypropylated lignin with 0 % cPC (black), 5 % cPC (blue), 10 % cPC (red) and 15 % cPC (green) (left) and integral ration of carbonate band to aromatic band derived from those spectra (right).

The presence of carbonate groups at the polymer backbone could also be deduced from an ^1H NMR spectrum (Figure 18). The signal at 4.9 ppm corresponds to the proton of a CH group next to a carbonate group.^[106,108] ^1H NMR spectra with internal standard were

recorded to compare this signal for the reaction products with different cPC content (Figure A6, Figure A18, Figure A19 and Figure A20, appendix). The integral value was normalized considering the sample weight. An increase of this normalized integral value for 1 mg of sample confirmed higher amount of carbonate groups in modified lignin for higher cPC content (Figure 19).

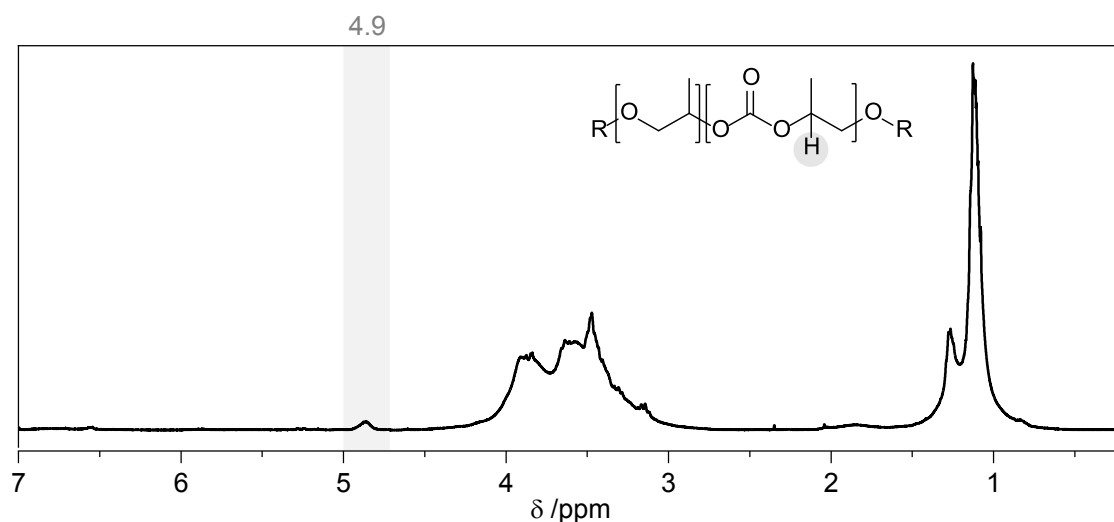


Figure 18. ^1H NMR spectrum of modified lignin oxypropylated with 15 % cPC.

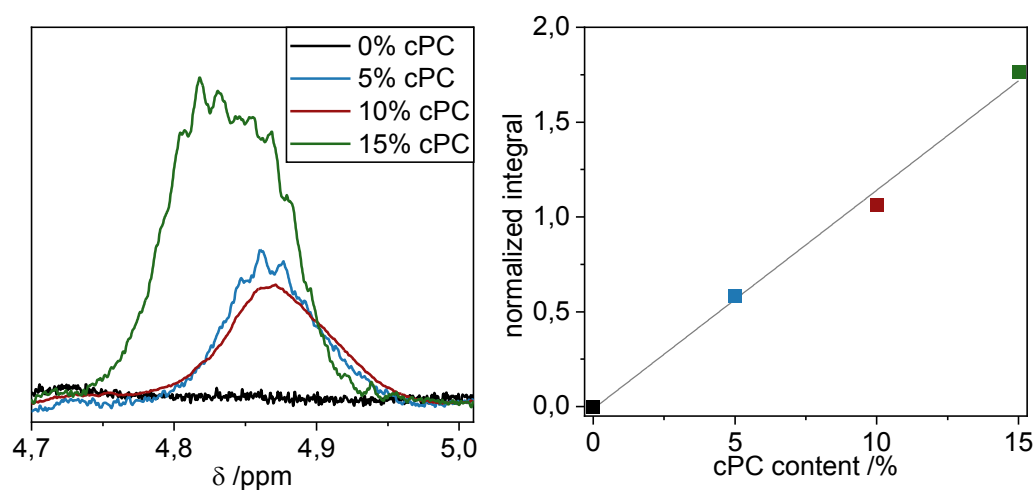


Figure 19. ^1H -NMR spectra of oxypropylated lignin with 0 % cPC (black), 5 % cPC (blue), 10 % cPC (red) and 15 % cPC (green) (left) and normalized integral value of signal.

3.4 Summary

Catalysts differing in basicity were used in the oxypropylation of lignin. Use of K₂OtBu led to a reduction of homopolymer content of 5 – 10 % over KOH, but the reaction time was up to twice as long and higher molecular weight lignin products were obtained. Use of DBU enabled oxypropylation with homopolymer content < 5 % but also reduced the conversion to 25 % after 24 h. All results indicate a preference for lignin modification over homopolymerization for catalysts with lower basicity and lower nucleophilicity. The choice of catalysts enables control over the homopolymer content and thus allows to tailor polyol properties like viscosity and OH number.

Oxypropylation of OS₂, KL and SL catalyzed by 5 wt% K₂OtBu resulted in liquid polyols. All products had a PPG homopolymer content of 42-43 %. K₂OtBu as alternative catalyst is thus suitable for different lignin types without further adjustment of the reaction conditions.

Substitution of PO by cPC is only partly suitable for the production of polyols for PU foams with high lignin content. Low number of only 1 – 2 repeating units led to solid oxypropylated lignin when using only cPC for the oxypropylation. The product has a low compatibility with commercial polyols and therefore limits the utilization. Partial substitution of PC by cPC led to liquid lignin polyols with carbonate linkages in the grafted chains. The amount of these linkages is proportional to the amount of cPC used in the feed. Higher cPC concentration also led to lower reaction rate because of lower reactivity of chains after addition of one cPC unit. Carbonate groups in the polyols are another parameter to tune polyol properties and thus present a versatile additional factor in the synthesis of tailor-made building blocks.

Oxypropylation is a robust process with promising perspective for scale-up. The obtained results demonstrate that variation of catalyst type and choice of monomers offer further possibilities to tune the polyol properties. These additional variables broaden the manifold possibility of oxypropylation to obtain lignin-based materials.

Therefore, this method represents a promising step towards sustainable polymer synthesis based on renewable resources.

4 Lignin-based Aerogels

4.1 Background

A gel is a colloidal or polymeric network whose pores are completely filled by a fluid. Once the fluid is removed and replaced by air, the gel is called aerogel. Aerogels are a class of solids with unique properties.^[109–111] These materials consist up to 95 % of air which results in an extremely low density. Their porous nature leads to high specific surface area and low thermal conductivity. Certain aerogels also have a high transparency similar to that of glass. These properties can only be obtained if the gel structure remains unchanged during the removal of the fluid. Change of shape, the so-called shrinkage, can be avoided by supercritical drying. The need for this complex method results in high costs for aerogel production.^[112]

The first aerogel used silica as starting material.^[113] Synthesis of aerogels from other inorganic materials like metal oxides followed.^[110,112] In the 1980s the first synthesis of aerogels from organic polymers was reported.^[114] This group of aerogels displayed better mechanical properties but at the expense of lower surface area and higher thermal conductivity.^[115]

Aerogel is defined by IUPAC as a “gel comprised of a microporous solid in which the dispersed phase is a gas”. A *xerogel* is an “open network formed by the removal of all swelling agents from a gel”.^[116] There is no clear differentiation between those definitions. However, the term *xerogel* was introduced first by H. Freundlich regarding shrinkage of gels upon drying^[117], while Kistler did not observe shrinkage in his supercritically dried *aerogels*.^[113] Therefore, a gel undergoing significant shrinkage is commonly referred to as a *xerogel* in literature.

Aerogels are of interest in various fields, including thermal insulation^[118,119], biomedical applications^[120], drug delivery^[121], use as sensors^[122] or catalytic materials^[123], for environmental remediation^[124] and in carbonized form as energy storage and

supercapacitor materials.^[125,126] Different aerogel products are available commercially, mostly for thermal insulation.^[112] Examples are a monolithic aerogel panels called *Airloy* by Aerogel Technologies or a flexible aerogel blanket called *Spaceloft* by Aspen Aerogels.^[127,128] Cabot Corporation commercialized a silica-based aerogel in granular form which can be used for various applications like building insulation, outdoor gear and personal care products.^[129]

The change from fossil to renewable feedstock is also relevant for the production of aerogels. The interest in bio-based aerogels has therefore grown in recent years.^[115,130] Biopolymers like cellulose^[131,132] and polysaccharides^[133,134] have been used for the production of aerogels.

4.1.1 Aerogels – Preparation and Theoretical Models

Aerogels are commonly synthesized in a sol-gel process.^[110–112] The character of the resulting gel depends strongly on the conditions during the synthesis. Understanding the sol-gel process is thus important to control the material properties.

The sol-gel process is a “process through which a network is formed from solution by a progressive change of liquid precursor”.^[135] The general process can be described as follows: Monomers in a liquid phase react to clusters and form a sol. Further reaction leads to the formation of an interconnected network, the gel. A sol is a stable suspension of colloidal particles in a liquid phase.^[136] The particle size should be approximately between 1 nm and 1 μ m to obtain a stable suspension.^[116] The transition from a sol to a gel is called the gel point. Here a sudden change occurs from a viscous liquid state to a gel which behaves like a single solid monolith.^[137]

One possibility to describe the gelation process is the theory developed by Flory and Stockmeyer. This theory is often called “classical” theory.^[138] It was first established to describe bond formation in a polymer network. A gel is considered an indefinitely continued polymer and is formed when a certain fraction p_c of all possible bonds is

formed. Certain assumptions are made which limit the accuracy of this model, e.g. that the formed polymer does not contain any closed loops.

Another possible theory to describe gelation is that of percolation. It was first established by Hammersley.^[139] *Bond percolation* is a suitable model to estimate the gelation process. The monomers in the sol can be visualized as sites on a grid. Then bonds are formed one after another between two sites at random. A gel is formed once the fraction p of bonds already filled in reaches a certain limit, the percolation threshold p_c . Above this threshold a spanning cluster reaching across the complete grid is formed, the equivalent to a gel. A dilute system can be described more accurately by *site-bond percolation*. In this model the sites are randomly filled with both monomer and solvent.^[140]

Classical and percolation theory describe equilibrium states and not the kinetics of gelation. Near the gel point larger clusters are present. Their reduced mobility is likely to prevent the system from reaching equilibrium and therefore alter the cluster growth. Also, the concentration of bonds in the clusters is not represented in the percolation theory, where they are uniformly distributed on the grid. The bond correlation present in real systems can be accounted for by kinetic models or growth models.^[137,141] Here, a gel is formed in an aggregation process, e.g. successive addition of particles from the sol to an initial particle. The focus is not on describing the macroscopic properties of the complete sample but on the study of just one aggregate.

Various types of aggregation can be considered in growth models.^[137,141] Monomers can be added to clusters (*monomer-cluster aggregation*) or two clusters can collide and aggregate (*cluster-cluster aggregation*). In *diffusion-limited aggregation* the colliding units always stick together, and the rate of aggregation is determined by transport kinetics. If many collisions occur before a link between two units is formed the process is called *reaction-limited aggregation*. The latter leads to more compact particles because there is more time for the clusters to interpenetrate. Experimental results suggest that growth mostly occurs by reaction-limited cluster-cluster aggregation or, if no repulsive barrier between clusters exists, by diffusion limited cluster-cluster aggregation.

Kinetic growth models appear to be more accurate for the cluster formation in the sol while percolation describes the later gel formation by linking of the clusters.^[137,141] The reason for this is that kinetic models are defined for diluted systems. Growing clusters cause a decrease of free solvent, making this assumption no longer applicable. Once the clusters have grown to be space-filling their mobility is reduced drastically. After this point the clusters link together in a percolation process.

4.1.2 Resorcinol-Formaldehyde Aerogels

Resorcinol and formaldehyde can form aerogels in a sol-gel process. The first synthesis of resorcinol formaldehyde (RF) aerogels was in an aqueous polycondensation reaction. Sodium carbonate, a weak base, was used as catalysts and the mechanism was described to be like that in inorganic aerogel synthesis.^[114] These first RF aerogels exhibited high porosities > 80 %, low densities around $0.03 \text{ g}\cdot\text{cm}^{-3}$, high surface areas of $400\text{--}900 \text{ cm}^2\cdot\text{g}^{-1}$ and small pore sizes < 50 nm.^[142–144] The reaction pathway leading to formation of RF gels is the polycondensation of resorcinol and formaldehyde to a phenolic resin. The monomers react in a sol-gel process to give a crosslinked gel (Figure 20).

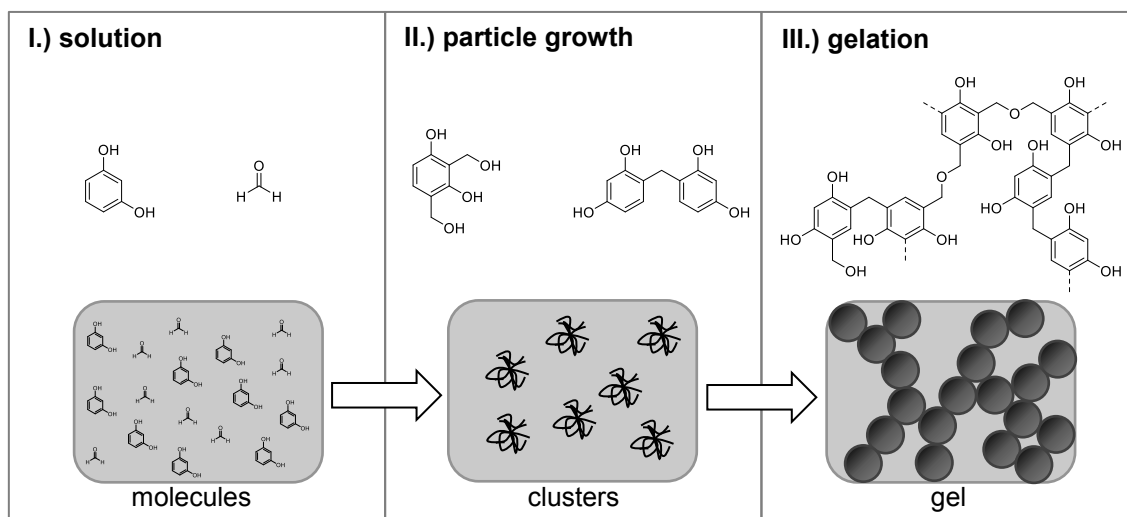


Figure 20. Sol-gel process of resorcinol and formaldehyde to a crosslinked gel.

Hydroxymethylated resorcinol is formed in a first step which then condenses to form clusters. These clusters can be described as “crosslinked colloidal-like particles”.^[145]

Further reaction leads to crosslinking between different clusters followed by aggregation and finally the formation of a gel.^[114,142] A later study verified that aggregation does not occur in the beginning but only in a later phase of the reaction.^[146]

RF aerogels are specifiable by e.g. their gelation time, particle size and morphology, density, pore size and volume, mechanical and thermal behavior. All these properties are mainly determined by the conditions during the sol-gel process.^[112] Common variables to describe the synthesis conditions are the molar ratio of resorcinol to formaldehyde R/F, the molar ratio of resorcinol to catalyst R/C and the solid or reactive content. The latter describes the weight fraction of reactive components like resorcinol, formaldehyde and catalyst relative to the amount of solvent used. Detailed studies describing the effect of catalyst type and amount, reaction time and temperature have been published and reviewed.^[147–149] The impact of aging the gels in an additional step has been investigated as well.^[150,151] The influence of the drying on the final gel structure has also been a topic of research.^[148,152]

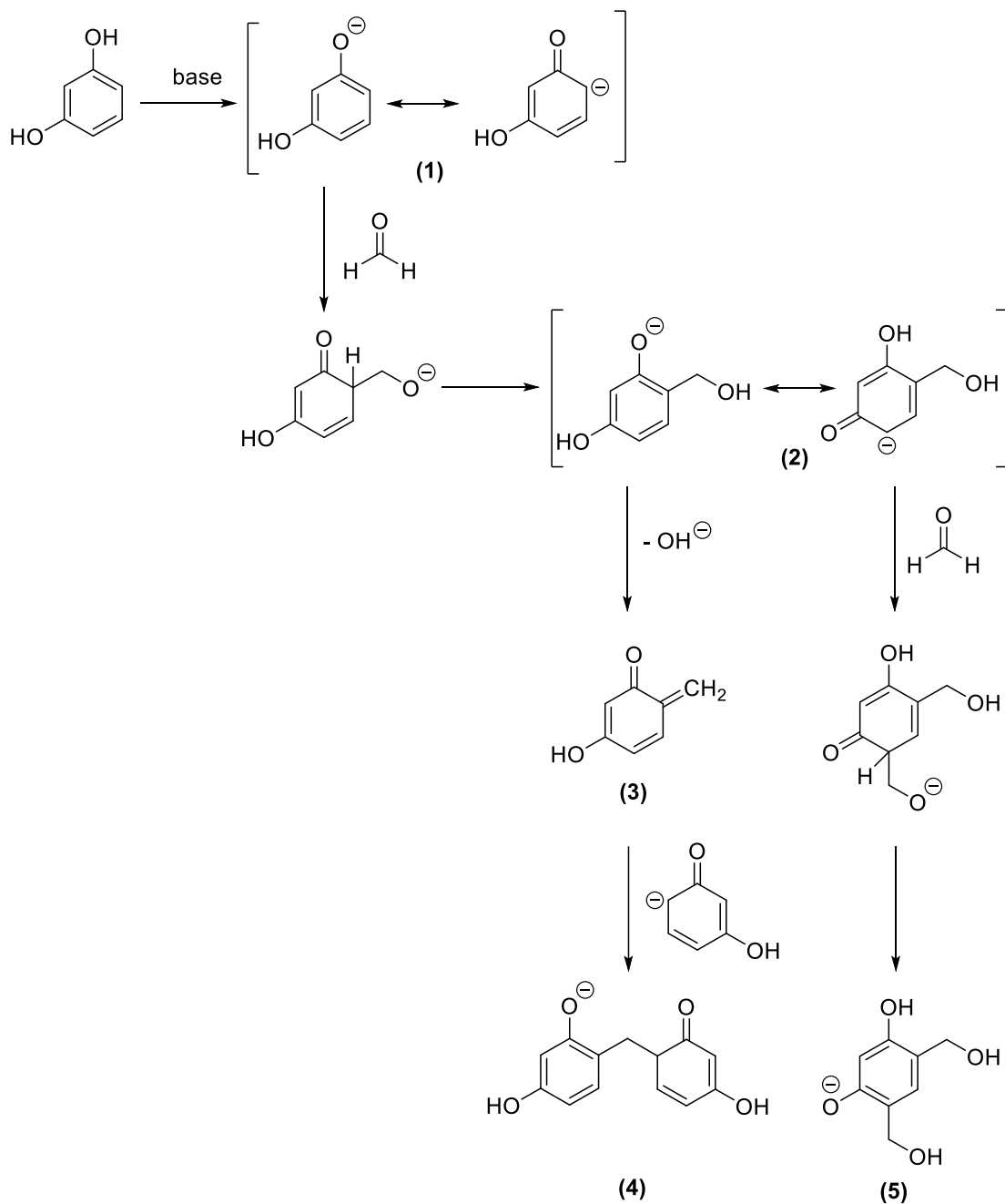
Understanding the relationship between synthesis conditions and resulting structure yields the possibility to obtain materials tailored to fit a given application. Very small variations of one parameter can result in drastic changes of properties. A thorough understanding of the effects of different conditions is therefore needed to achieve satisfying results. The mechanism of formation of RF aerogels has been explained by microphase separation^[153] or colloidal aggregation.^[154] More recent investigations indicate that implementation of both models eventually leads to the same structure.^[155] The circular shape of an individual aggregate can be explained by a layer-by-layer addition of monomers.^[156]

Influence of catalyst type on gelation mechanism and gel properties

The preparation of RF aerogels with alkaline catalysis has been studied extensively.^[142–145,157–159] Recently, the focus is more directed to acid catalysis, mostly because of shorter reaction times, the formation of larger beads and higher mechanical stability of the resulting gels.^[160,161] Acids like HCl^[162,163], HClO₄^[164,165], HNO₃^[166] and citric acid^[167] have been used. The term “catalyst” is somewhat misleading in the formation of resorcinol-

formaldehyde resins. Base and acid are partly consumed during the reaction and therefore do not fit the definition of a catalyst. The word is nonetheless still used in literature.

Combined approaches i.e. using acid and base catalysis have been published as well.^[168–171] The reaction is started in the presence of a base catalyst and an acid is added later. The different properties caused by the change of catalyst type can be explained by considering the respective reaction pathways. The base-catalyzed pathway yields intermediates that are activated towards further electrophilic aromatic substitution on account of the increased electron donating ability of the aromatic ring (Scheme 14).

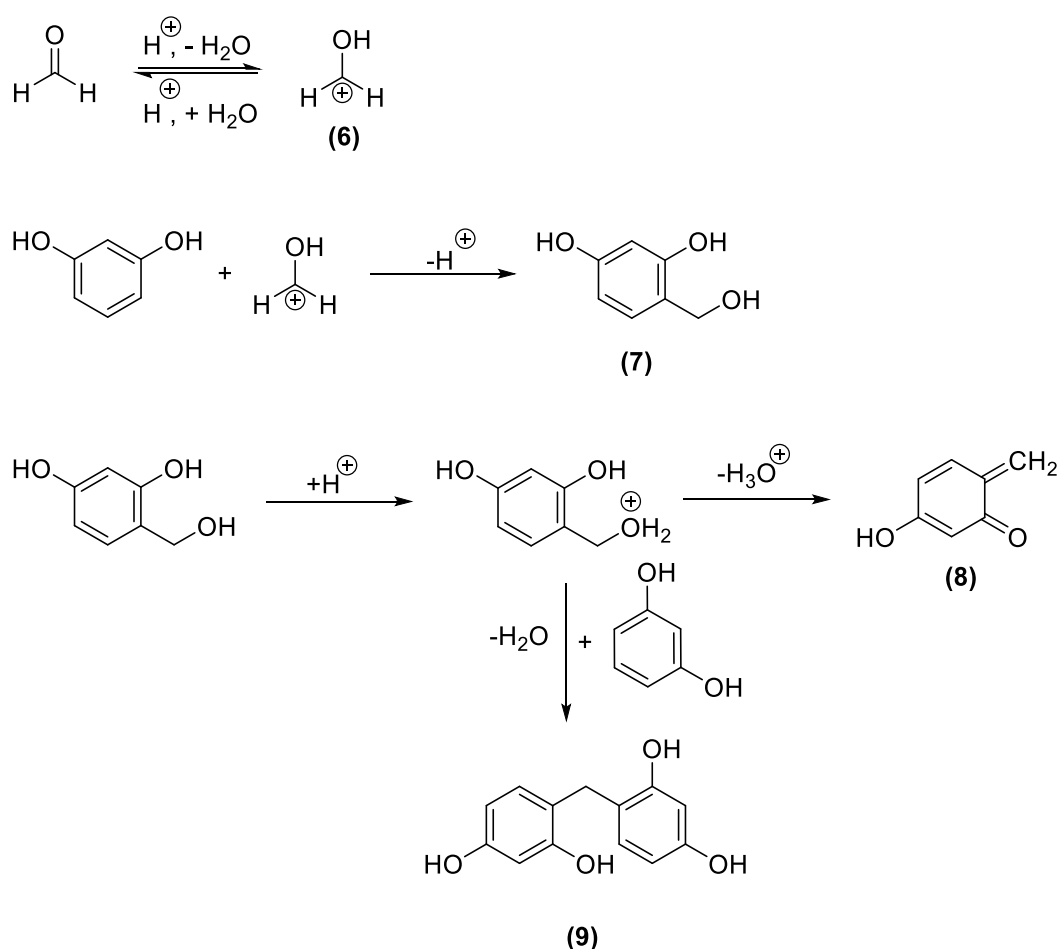


Scheme 14. Base-catalyzed condensation of resorcinol and formaldehyde.

The basic medium leads to deprotonation of resorcinol (1). The electron density is increased at position 4 of the aromatic ring leading the addition of formaldehyde and formation of deprotonated hydroxymethylated resorcinol (2). Elimination of OH forms the reactive *o*-quinone methide (3). This intermediate reacts with a resorcinol anion under formation of a stable methylene linkage (4). An increased electron density after hydroxymethylation furthermore activates the aromatic ring at position 6 and another

addition of formaldehyde takes place (5). The product has a novolak structure consisting of mostly methylene bridges. Formaldehyde addition dominates over condensation at basic conditions, leading to particle formation by nucleation and weaker structures.^[146] A very high pH value leads to unstable gels because condensation is suppressed.^[172]

The acid-catalyzed reaction pathway is based on an increase of electrophilicity of formaldehyde (Scheme 15).



Scheme 15. Acid-catalyzed pathway of resorcinol and formaldehyde.

The acid protonates the oxygen atom in the formaldehyde (6). Hydroxymethylation of resorcinol occurs after a nucleophilic attack of the aromatic entity (7). Protonation of the intermediate hydroxymethylated resorcinol gives an $-\text{OH}_2^+$ as a good leaving group and leads to the formation of a reactive o -quinone methide (8). Another likely reaction is the addition of another resorcinol molecule under formation of a methylene linkage (9). This

condensation reaction prevails under acidic conditions, the network formation is faster and larger particles with more crosslinks are formed.^[173] Percolation is dominant.^[165]

Wet gels prepared in base were also subjected to an aging cycle in acidic environment with the objective to increase the mechanical strength. It was assumed that the then dominant condensation of hydroxymethyl groups would lead to a higher crosslinking level and therefore higher mechanical stability.^[145]

The gelation time, meaning the time until a solid gel is formed out of the liquid sol, depends on the pH of the initial solution. Gelation time is overall longer for base catalysis than for acid catalysis.^[162] The slower gelation is a possible explanation for the different bead sizes observed in gels with different catalysts. Slow polycondensation leads to small structures while fast condensation results in coarse structures.^[174] Shrinkage, i.e. the change of shape during the drying is lower for lower pH, possibly because larger beads and thus larger pores sizes are more stable against capillary forces during the drying.^[160,172]

Viscosity measurements of base catalyzed condensation mixtures indicate that particle growth takes place predominantly in the first hour of reaction. Particles agglomerate in a second step occurring many hours later to form the final gel.^[175] The two regimes were correlated with a change in pH value which influences the dominant reaction mechanism.^[176] Almost complete consumption of formaldehyde and resorcinol takes place during the first part of the reaction and a decreasing pH value is measured.^[143] A shift from base catalyzed methylene linkage of two substituted resorcinol molecules to the acid-catalyzed formation of methylene-ether linkages between particles takes place at lowering the pH value. This description is supported by an experiment wherein acid was added after one hour, which indeed gave a fast gelation.

Influence of catalyst concentration on gelation mechanism and gel properties

Gelation and gel morphology are not only influenced by catalyst type but also by catalyst concentration as explained above. The amount of catalyst is mostly given by the molar ratio of resorcinol to catalyst, R/C. Higher values of R/C indicate lower catalyst concentration. Indication of catalyst concentration using the pH value is not reasonable

because of changing pH during the course of the reaction.^[177] Gelation times are shorter with more base catalyst.^[146,178] A higher number of clusters formed in the beginning of the reaction leads to an overall shorter time until they have grown enough to occupy the a critical volume needed for gel formation.^[146]

The initial pH value of the sol has a strong influence on the resulting gel properties.^[172,179] “Polymeric” aerogels have particles with large necks resulting in a “fibrous appearance”. These structures are obtained when high amounts of base catalyst are used.^[142,158] “Colloidal” aerogels have a “string of pearls” structure with smaller necks. They can be synthesized with a low amount of base catalyst.^[157,166] Polymeric aerogels show stronger shrinkage than colloidal ones.^[142] However, the larger necks give a higher mechanical strength.^[112,157,180,181] Larger pores lead to reduced shrinkage because of reduced capillary stress.^[182–184]

A higher pH value (or better: using more base catalyst) results in a higher shrinkage and smaller pores in the final resin.^[173] The particle size is smaller with a relative high amount of catalyst: more clusters are formed and each one grows less by the limitation of the available monomer.^[145] More catalyst also results in higher branching within the clusters because more resorcinol anions are formed.^[177] Particles with higher branching coalesce earlier during the gelation process. Therefore, smaller particles with stronger interconnection are formed which results in a decreasing mesopore volume.^[158] A pH value < 5.5 causes formation of a gel with micro- and macropores and low mechanical strength. A pH value > 6.3 produces a gel with only micropores. A non-porous material is obtained after further increase of the pH value.^[177] At very high pH values gelation is hindered.^[172]

Most studies conclude that the base only influences the reaction by defining the pH value of the initial solution. However, the counter ion of inorganic bases can influence the pore structure to some extent, probably by stabilizing the colloidal suspension.^[146] Charge and concentration of the cation (metal ions) are important, the ion size does not have a detectable influence.^[185]

The acid catalysis in the RF polycondensation shows opposing correlations - a higher amount of catalyst results in a lower pH value. Again, smaller particles are formed when more catalyst is used because of the increasing number of clusters formed early in the reaction.^[164] The dependence of particle and pore size on catalyst concentration is weaker than with a base catalyst.^[167] Acid catalysis leads to the formation of overall larger beads and a shorter gelation time over base catalysis because condensation is favored.^[164,166] Gel density is higher when acid catalysis is used, indicating more crosslinking.^[161]

Influence of other reaction parameters on gelation mechanism and gel properties

The concentration of resorcinol and formaldehyde in the solvent determines the density of the resulting gel. Higher dilution of the reactants results in a lower density.^[186] Actual densities may be slightly higher than the theoretical ones because of shrinkage during the drying process.^[176,179] Higher dilution leads to longer gelation times.^[145] The particle and pore size increases with higher dilution because there is a larger distance between reactive clusters in the early reaction stage in the sol and each individual bead can grow longer until a space-filling network is formed.^[147,161] A higher dilution also results in a higher surface area.^[161,179] It has been reported that a certain mass ratio is necessary for the formation of homogeneous gels, the exact range being depended on the other synthesis conditions.^[167]

Formaldehyde content is described by molar ratio of resorcinol to formaldehyde, R/F. Higher amount of formaldehyde leads to higher average functionality of hydroxymethylated resorcinol. This should lead to a higher crosslink density.^[176] Larger amount of formaldehyde relative to resorcinol in the feed leads to larger clusters.^[186]

Changing the solvent has been reported to influence gelation time and particle morphology.^[187] A small change in solvent composition, e.g. a variation in the residual methanol content of commercial formaldehyde, can result in structural variations.^[188,189]

Lignin contains aromatic rings and hydroxy groups and thus shows high structural similarity to resorcinol. Various evaluations of the suitability of lignin as replacement for resorcinol in phenolic resins have been published.^[190,191] The synthesis of organic

resorcinol-lignin-formaldehyde (RLF) aerogels is reported with the substitution of up to 50 % of resorcinol with a lignin of non-specified origin.^[192,193] Sodium hydroxide was used as catalyst in water, the reaction was performed at 85 °C. A longer gelation time and a higher density with lower surface area product is obtained the higher the lignin content is in the feed. High shrinkage of 20 - 60 % was observed despite supercritical drying. A similar approach also with NaOH as catalyst has been patented in 2018.^[194] Subcritical drying improved the mechanical properties of RLF aerogels and reduced shrinkage < 5 %.^[195] SL was used with water as solvent and sodium hydroxide as catalyst in the study. The approach was limited to a maximum lignin content < 30 %. High lignin contents of 75 % were reported for aerogels with 5-methylresorcinol and formaldehyde.^[196] OLS from different plant sources was used and NaOH as catalyst.

A synthesis of gels comprised only of lignin and formaldehyde was described too.^[197] A solid content of 20 *wt%* was used with water as solvent and sodium hydroxide as catalyst. Kraft and Organosolv lignin were used. The findings conflict with a study reporting that no gelation was possible only from KL and formaldehyde with sodium hydroxide.^[198]

The only report of acid catalysis for lignin-containing RF gels concerns xerogels prepared from sulfated lignin and formaldehyde with hydrochloric acid as catalyst.^[199] The beads size of a few μm was significantly larger than that of base-catalyst gels. The obtained gels were mechanically not stable.

The studies carried out so far suggest that partial replacement of resorcinol by lignin is a promising perspective for sustainable material synthesis. However, the knowledge about RLF gels is very limited. Low lignin content and low stability are remaining challenges.

The influence of reaction parameters on the gel properties has not been addressed in detail. The example of RF aerogels without lignin shows that in-depth research resulted in understanding the relationship between synthesis conditions and gel structure and made it possible to vary material properties over a wide range. Further research is needed to close the knowledge gap for RLF gels in order to achieve a similar versatility.

Few studies exist about the application of lignin in RF aerogels. Expensive synthesis routes and unfavorable mechanical properties still limit the use of RF aerogels on an industrial scale. Investigation of lignin-containing gels provides room for further optimization with regard to these factors. This would lead to a promising and sustainable material class.

4.2 Scope of this work

The possibility of preparing RLF gels from different lignin types will be explored in this work. The influence of synthesis parameters on material properties like lignin content, formaldehyde concentration and reactive content have not been investigated yet for RLF gels. This work will address the effect of these parameters on the resulting gel properties. The gained insights for lignin-based gels will be related to the knowledge obtained for RF gels.

Several drawbacks remain impeding aerogel production on a larger scale. Base-catalyzed gels need days or weeks for gelation, rendering this process unfeasible and economically unviable on industrial level. Acid-base catalysts promises gelation within minutes for RF gels but has not been successfully applied to stable lignin-containing gels. A systematic investigation of sulfuric acid as catalyst for the synthesis of lignin-containing aerogels will be carried out. Possible interaction with other reaction parameters will be determined.

Brittleness of organic aerogels is another challenge hindering their everyday application. High mechanical stability is necessary for utilization e.g. in the construction sector. A structure-property relationship will be established for lignin-containing aerogels to find suitable synthesis conditions for required material properties.

4.3 Results and Discussion

Lignin-containing resorcinol formaldehyde aerogels are hardly investigated and acid catalysis has not been applied for preparing these gels so far. The possibility to replace resorcinol by lignin in an acid-catalyzed gelation reaction was tested in a first step. The catalyst concentration will be referred to in terms of a molar ratio of monomer to catalyst (M/C), the formaldehyde concentration by the molar ratio of monomers to formaldehyde (M/F). The reactive content (RC) describes the ratio of reactive components to all components including solvent. The lignin content is defined as the mass fraction of resorcinol replaced by lignin.

All gels were synthesized in polypropylene containers with a lid. The samples were kept in a water bath at a set temperature until gelation occurred. The gels were then removed from the container and if necessary H₂O was removed by solvent exchange. Samples were dried by solvent evaporation at 60 °C if not indicated otherwise. OSL, the lignin type with good solubility in organic solvents was the source of lignin. Up to 50 wt% of resorcinol was replaced by OSL in earlier work.^[200] Sulfuric acid was used as catalyst in EtOH/H₂O (50/50, wt/wt) at 65 °C in the preparation. Stable gels were obtained with RC = 20 wt%, M/C = 4.5 and M/F = 0.8. This formulation was used as a starting point for the consecutive study.

Two gels, one with lignin and one without, were synthesized under identical reaction conditions as described above. The reaction mixture without lignin was initially colorless and transparent. Gelation occurred after five minutes. The sample solidified and remained colorless and transparent. The gel turned translucent after 10 minutes indicating further particle growth after gelation. A faint red appeared after 25 minutes. The appearance of this color can be explained by formation of *o* – quinone methide structures in the network.^[8] The analogous solution with OSL substituting 50 wt% of the resorcinol was dark brown. It was transparent in the beginning and turned opaque when gelation occurred after six minutes. The appearance of a red color was not obvious as the dark brown color of lignin dominated the appearance.

Unmodified OSL consists of ill-defined primary particles with a size of a few hundred nanometers and irregular surfaces. The RLF gel with 50 *wt%* OSL is made of spherical beads with a size around 2 μm (Figure 21). The beads have smooth surfaces and are interconnected by large necks. This “string of pearls” structure is similar to the one described in literature for gels without lignin.^[142,159] The SEM images indicate that OSL was homogeneously incorporated in the gel structure. No evidence for residual unmodified lignin was found.

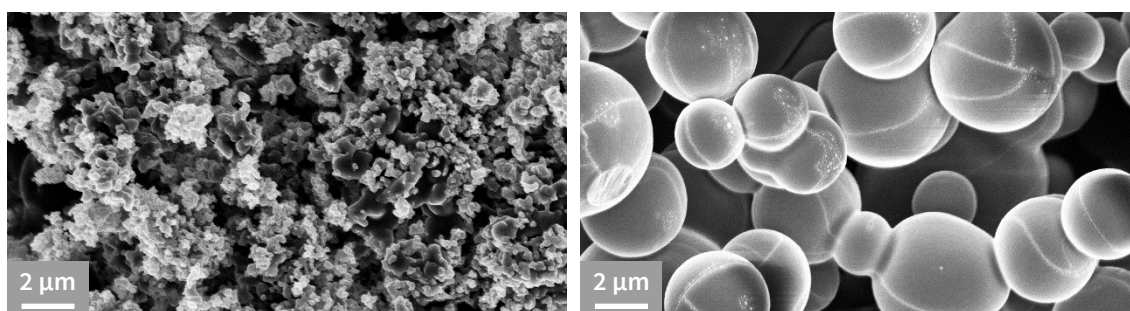


Figure 21. SEM images of unmodified OSL (left) and RLF gel with 50 *wt%* OSL (right).

4.3.1 Gels with various Lignin Contents

The appearance of the lignin containing gels after drying is markedly dependent on the lignin content, ranging from dark brown, shrunken samples over reddish to dark brown larger samples (Figure 22). All samples are shown at the same scale. Gels could be synthesized with a lignin percentage between 0 *wt%* and 50 *wt%*. Formulations with lignin contents higher than 50 *wt%* led to incomplete dissolution of lignin. Inhomogeneous products were then obtained which were friable. They break upon removal from the mold.

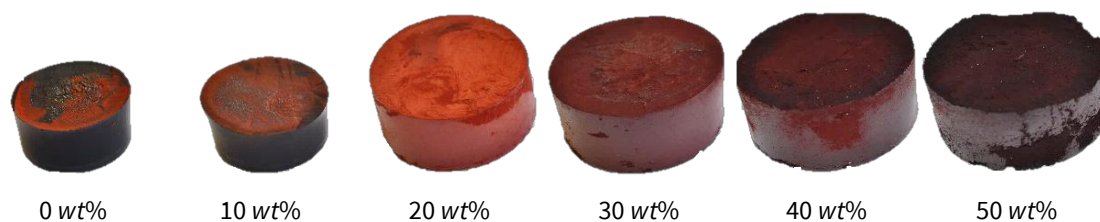


Figure 22. Gels with lignin content from 0 *wt%* to 50 *wt%* (M/C = 4.5, M/F = 0.8, RC = 20 *wt%*).

The samples with 0 *wt%* and 10 *wt%* OSL were dark brown with smooth surfaces. These gels with low lignin content appeared hard and dense with no visible pores. Gels with 20 *wt%* and 30 *wt%* OSL were orange and light brown. These gels with intermediate lignin content were porous yet stable against pressure. Samples with 40 *wt%* and 50 *wt%* OSL had a red-brown color similar to the color of OSL. Large pores were visible and gels were friable. The extent of shrinkage was smaller at higher lignin content (Figure 23). Shrinkage was measured using the gel diameter before and after solvent evaporation. Repetition of experiments indicated an error in the shrinkage of about 2 %.

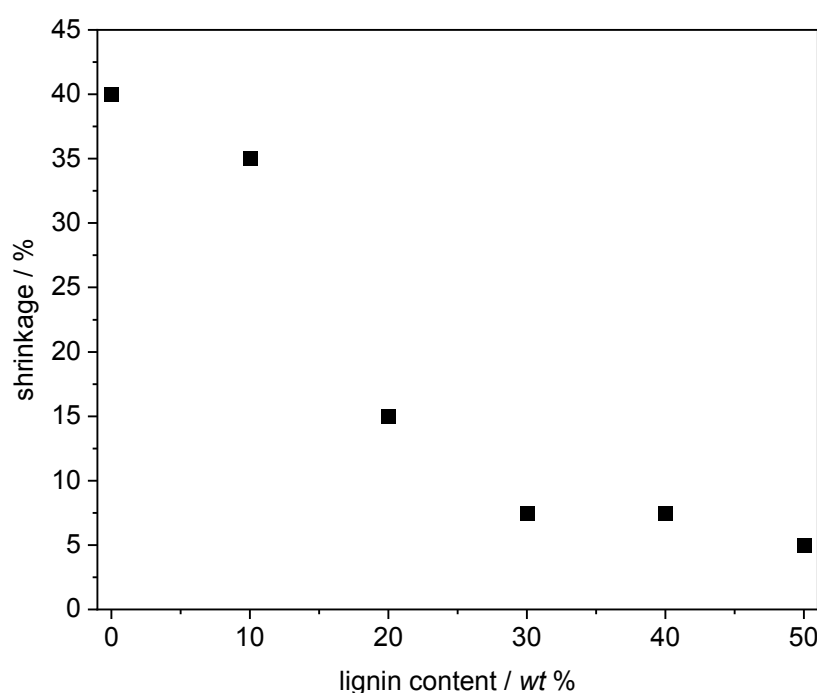


Figure 23. Shrinkage of gels in dependence of lignin content ($M/C = 4.5$, $M/F = 0.8$, $RC = 20$ *wt%*).

The largest shrinkage of 40 % was observed for the gel without lignin. The shrinkage is lower for higher OSL content, reaching 8 % for the gel with 30 *wt%* OSL. Shrinkage was on same low level for gels with 40 *wt%* and 50 *wt%* OSL. A low shrinkage appears to go along with the formation of large pores. This observation may be related to different capillary forces in the material during the drying process. Shrinkage occurs because capillary forces during evaporation of the solvent contract the gel. These forces are lower for larger pores.^[182–184]

Larger beads in gels with higher lignin content are obvious in the respective SEM images (Figure 24). Bead sizes were around 600-800 nm for 20 *wt%* and around 1-3 μm for 50 *wt%* OSL. Beads of gels with less lignin had a rougher surface and were less spherical. They appear to consist of smaller particles that agglomerated.

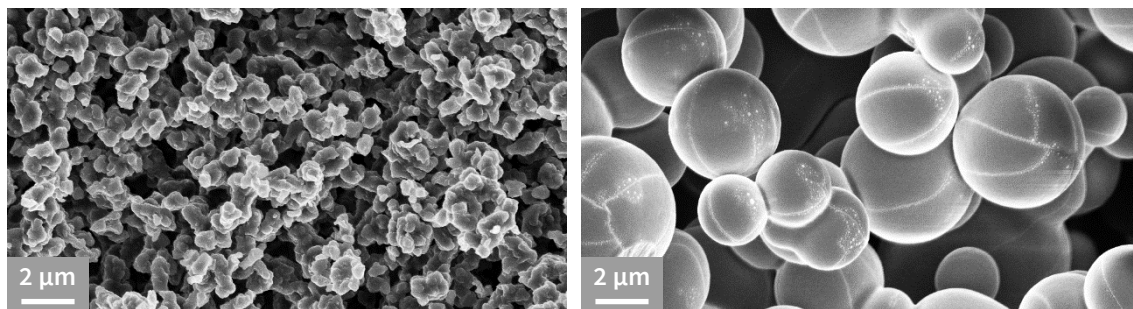


Figure 24. SEM images of RLF gels synthesized in EtOH/H₂O with 20 *wt%* OSL (left) and 50 *wt%* OSL (right) (M/C = 4.5, M/F = 0.8, RC = 20 *wt%*).

The final bead size and the overall morphology are reminiscent of the gelation process. Particle precipitation is caused by decreasing solubility of the intermediate formed polymer: Clusters will lose their solubility at a given point during the polyreaction and precipitate. This point is reached earlier for polymers with a lower solubility. Clusters keep growing after precipitation by aggregation until all monomers are consumed.

OSL has a lower solubility in EtOH/H₂O than resorcinol. Lignin-containing clusters therefore precipitate earlier and form a structure with larger beads with a lower surface area per volume. Having a small contact area is energetically favorable for two immiscible phases. The formation of a small number of large beads rather than a high number of small beads is thus a favorable pathway in the gelation process.

Gelation occurs after five minutes independent of lignin content. Gelation times were initially determined by tilting the container with the gel in regular time intervals. The loss of fluid-like behavior was taken as the gelation time. Differences in gelation time for gels with various lignin contents were too small to be determined visually by this method. Gelation time was therefore measured using rheology. Time sweep experiments were performed at constant oscillation frequency and constant strain. The measurement was started after addition of formaldehyde and was conducted at 40 °C. Gelation times

determined in that way differ from gelation times determined visually because they were measured at lower temperature. Low temperatures were necessary to reduce solvent evaporation during measurements. Mechanical stress caused by oscillation could also influence the gelation process.

Change of complex viscosity in time is similar to that described in literature for RF gels (Figure 25).^[175,178] The first, steep viscosity increase after 20 min is associated with the onset of gelation and cluster formation. Particle growth takes place in the next phase. Another change of slope after 50 min indicates particle agglomeration which ultimately leads to full curing. The time to the first distinct viscosity increase is defined here as gelation onset time and is used as a marker for the gelation rate.

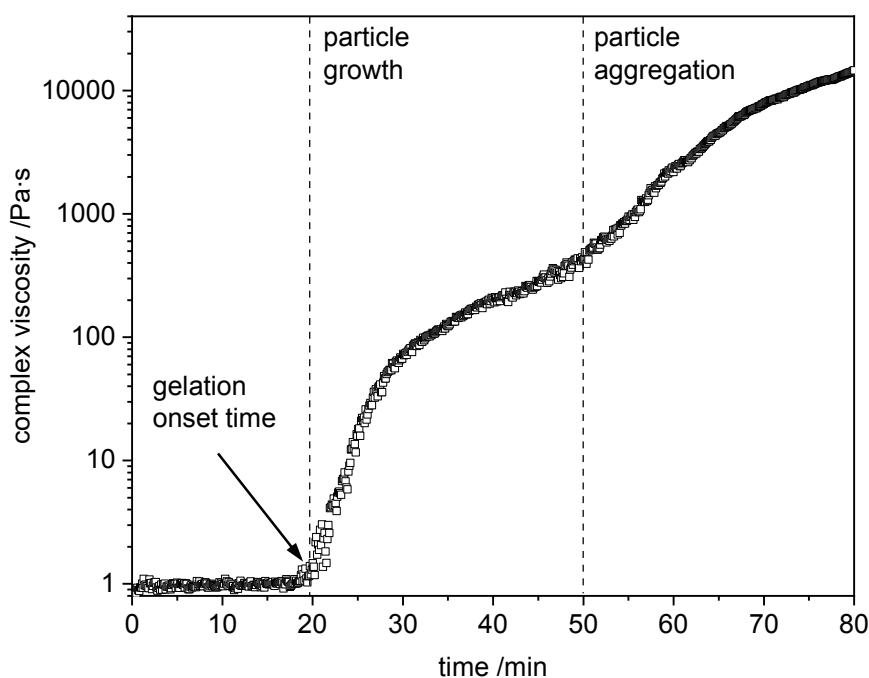


Figure 25. Time-dependent complex viscosity during gelation of a RLF gel (30 % OSL, M/C = 10, M/F = 0.8, RC = 20 wt%).

Scattering of data in early reaction phases occurred in some measurements, artefacts occurred repeatedly and randomly in multiple measurements (Figure 26). These issues could not be resolved by variation of measurement settings. They rather are a characteristic of the gelation. Gelation is an exothermic process. The thin film between the plates is not well-mixed and temporary variations in viscosity and removal of solvent

changes the total amount of the sample. Local high temperatures caused by inhomogeneous reactant distribution can e.g. lead to gas bubbles in the sample. The onset gelation time can nonetheless be used as a process characteristic. Interpretation of additional features like slope or plateau viscosity reached after gelation are however not reasonable.

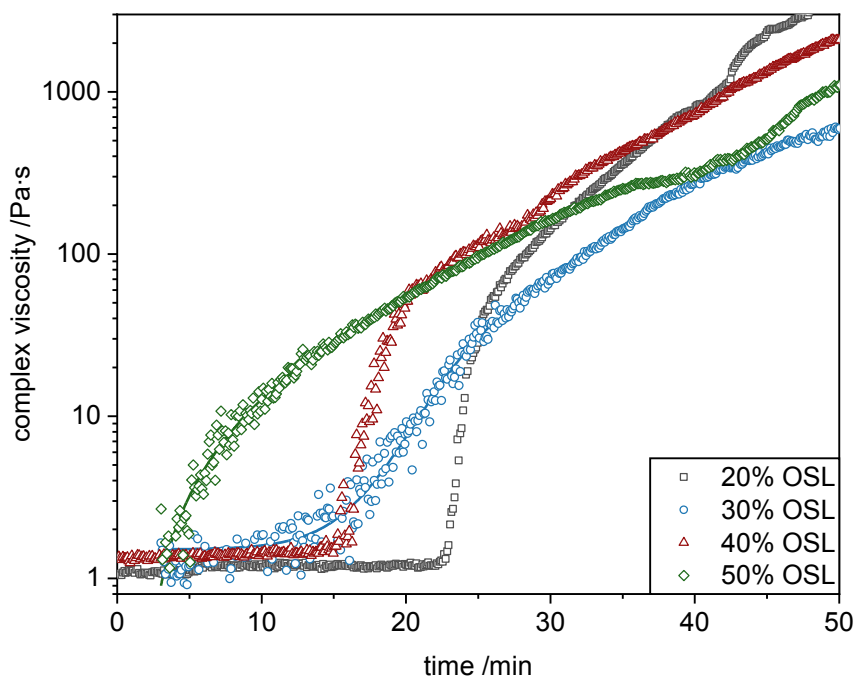


Figure 26. Time-dependent complex viscosity of samples with 20 % (black), 30 % (blue), 40 % (red) and 50 % OSL (green) ($M/C = 10$, $M/F = 0.8$, $RC = 20 \text{ wt\%}$). Lines were added for 30 % and 50 % OSL to guide the eye.

Gelation onset is faster for gels with higher lignin content (Figure 26) as expected, because lignin has a lower solubility in EtOH/H₂O than resorcinol. Gelation onset time was approximately 5 min shorter for any 10 wt% of lignin added. Lower solubility leads to earlier cluster precipitation and therefore an earlier viscosity increase. This observation is in agreement with literature describing longer gelation times for more stable sols.^[201]

4.3.2 Gels with Different RC

The first results are promising. The replacement of up to 50 % of resorcinol was possible with H_2SO_4 as catalyst. Gelation was fast and occurred within a few minutes. Supercritical drying was not necessary and low shrinkage was obtained after drying by solvent evaporation. Variation in the reactive content (RC), i.e. the ratio of reactive components to solvent determines the final gel density.^[186]

Experiments towards denser gels were conducted to find out that a higher RC resulted furthermore in shorter gelation time and lower shrinkage (Figure 27). Gelation time was reduced from 40 min for RC = 20 to 5 min for RC = 30. A higher reaction rate in more concentrated solution and a faster formation of the critical particle size needed for network formation is expected at higher reactant concentrations.^[176]

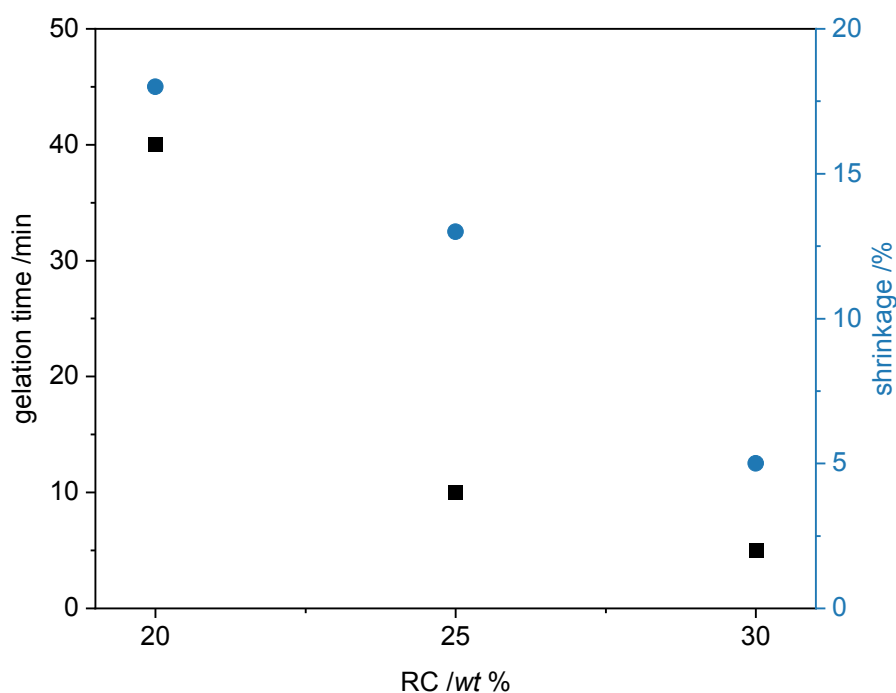


Figure 27. Gelation time (black) and shrinkage (blue) in dependence of RC (50 % OSL, M/C = 10, M/F = 0.8).

The shrinkage of the sample was 18 % for RC = 20 and only 5 % for RC = 30. The result is higher mechanical stability at a higher solid content. The earlier gelation further improves mechanical stability of gels. More monomer is left in the solution when

gelation occurs earlier. Addition of those monomers to the precipitated beads results in enhanced neck formation and thus higher strength of polymer network. However, a higher RC should also result in smaller beads. Clusters precipitate in closer proximity to each other and are therefore expected to grow less before gelation occurs. Smaller beads lead to smaller pores and thus higher capillary forces during drying. The result is a larger shrinkage. Here, the stabilizing effect of a higher density and extensive neck formation appears to outweigh the destabilizing effect of smaller pores.

4.3.3 Gels with Different M/F

Larger amounts of formaldehyde (i.e. a lower M/F value) in the formulation lead to a faster gelation and lower shrinkage (Figure 28). Gelation time changes from 15 min for $M/F = 0.5$ to 45 min for $M/F = 0.9$. Higher formaldehyde concentration leads to a faster formation of reactive hydroxy methylene intermediates and consequently of gelation. Shrinkage was 13 % for $M/F = 0.5$ and 20 % for $M/F = 0.9$. More formaldehyde leads to higher crosslinking density because more methylene bridges are formed between the aromatic rings. The formed network is stronger and withstands capillary forces better during drying.

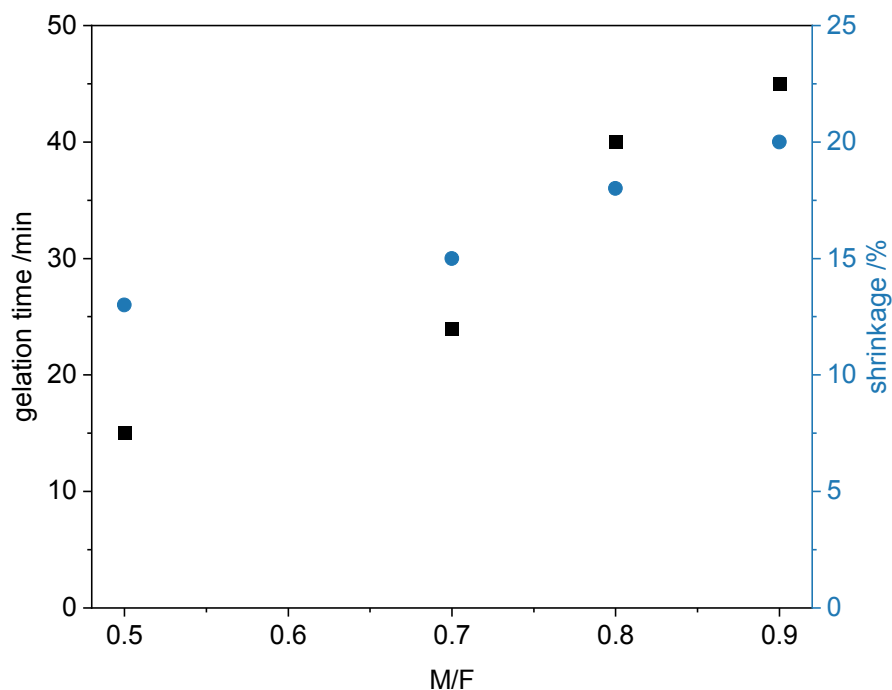


Figure 28. Gelation time (black) and shrinkage (blue) in dependence of M/F (50 % OSL, M/C = 10, RC = 20 wt%).

4.3.4 Gels with Different M/C

Larger amount of acid catalyst in the formulation results in a faster gelation and gives a gel which has undergone a lower shrinkage (Figure 29). Gelation time rose from 5 min for M/C = 5 to 120 min for M/C = 20. Shrinkage rose from 8 % for M/C = 5 to 18 % for M/C = 20. Gelation onset time derived from complex viscosity increase confirmed the findings. Lower M/C values led to shorter gelation onset time (Figure 30). These results are in accordance with observations made for gels without lignin.^[176]

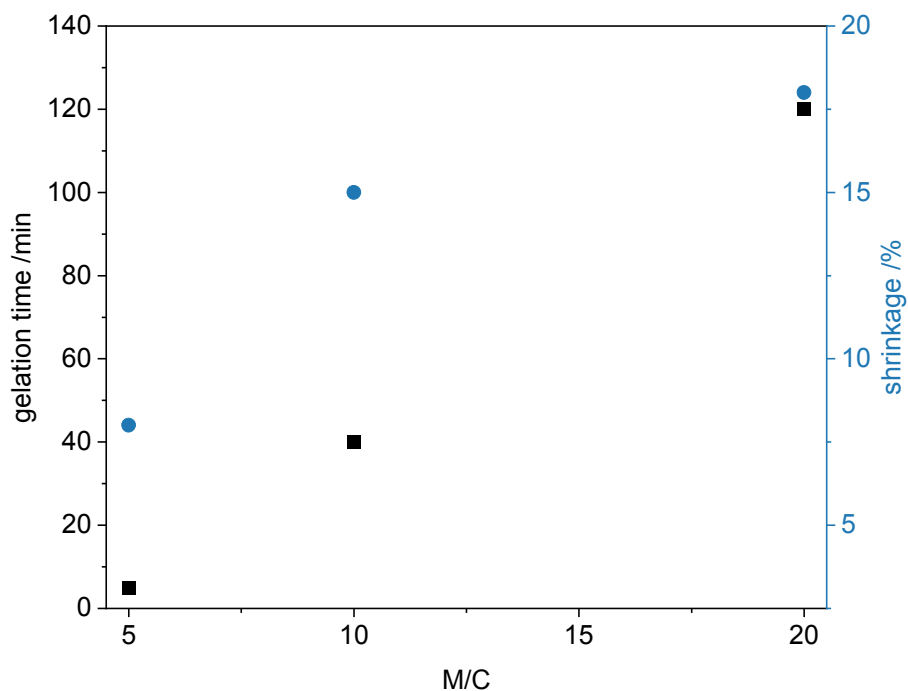


Figure 29. Gelation time (black) and shrinkage (blue) in dependence of M/C (50 % OSL, M/F= 0.8, RC = 20 wt%).

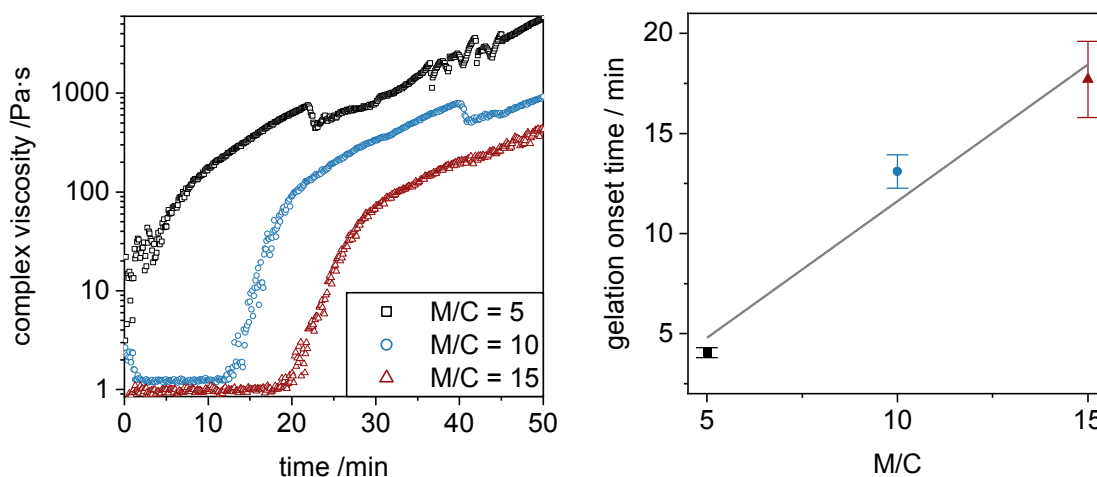


Figure 30. Complex viscosity of samples with M/C = 5 (black), M/C = 10 (blue) and M/C = 15 (red) (left) and gelation onset times (right) (50 % OSL, M/F = 0.8, SC = 20 wt%).

Larger amount of acid catalyst (i.e. a lower M/C value) leads as expected to the smaller bead sizes (Figure 31) as explained in the introductory part of this chapter. More catalyst causes more activated formaldehyde molecules and therefore a transient higher number of reactive clusters in the reaction mixture. This leads to many small initial clusters that agglomerate in due course. These findings are again consistent with results for gels without lignin.^[145]

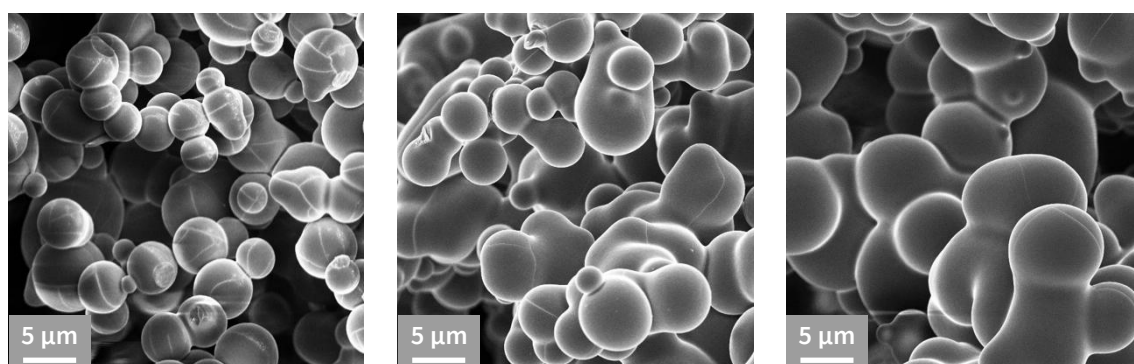


Figure 31. SEM images of RLF gels with M/C = 5 (left), M/C = 10 (middle) and M/C = 15 (right) (50 % OSL, M/F = 0.8, RC = 20 wt%).

Larger beads found in formulations with a higher M/C seem inconsistent with observed larger shrinkage. A smaller of shrinkage is expected for larger beads because of lower capillary forces during drying. Bead morphology in the respective SEM images also shows no reason for an overall weaker network at higher M/C. However, longer gelation times for $M/C \geq 10$ led to sedimentation of polymer particles before full gelation occurred. Resulting inhomogeneous density might have caused higher shrinkage.

Synthesis of homogeneous monolithic gels was not possible for $M/C > 20$. Beads agglomerated and sedimentation occurred before gelation was complete. A solvent system optimization is needed to stabilize growing beads, prevent agglomeration and sedimentation and allow to prepare homogeneous gels.

4.3.5 Gels Synthesized in various Solvent Systems

RF gels without lignin are mostly synthesized in H₂O. However, OSL is only soluble in H₂O under basic conditions. Formulations with acids as catalysts mostly contained precipitated OSL. Addition of EtOH, a good solvent for OSL, was effective for obtaining homogeneous conditions. The application of water-soluble organic solvents like ethanol or acetone in lignin formulations may be a method for obtaining superior gels.

The solubility of OSL in mixtures of EtOH/H₂O and acetone/H₂O has limits which dependent on the solvent ratio (Figure 32), a high content of organic solvents gives a higher solubility of OSL. A highly viscous slurry with a solid and liquid phase (not trivial to separate) was formed with more than 60 % H₂O in ethanol. Complete dissolution of lignin was observed for all samples with less than 40 % H₂O. An overall better solubility was achieved with acetone/H₂O. Almost complete OSL dissolution (96 %) was observed in this solvent mixture at a ratio of 50/50. Only 53 % OSL could be dissolved in EtOH/H₂O with this ratio. These insights were elaborated using an amount of lignin corresponding to an RC of 20 *wt%* which was placed in the solvent mixtures and the solubility was determined by gravimetrical analysis of the solid residue. The formation of gels in both mixtures proceeded with an RC of 20 *wt%* with comparable morphologies (Figure 33).

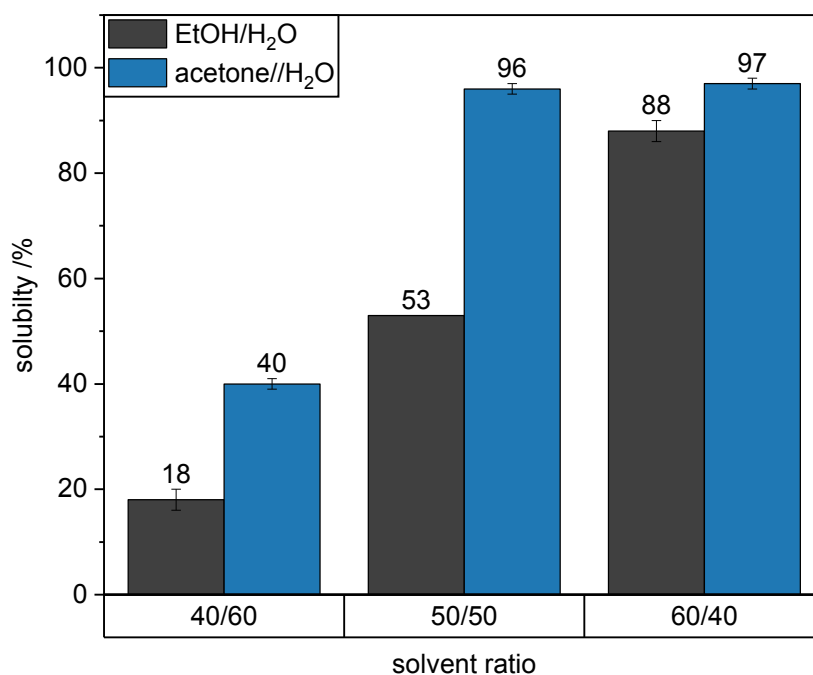


Figure 32. Solubility of OSL in mixtures of EtOH/H₂O (dark grey) and acetone/H₂O (grey) with ratios of 40/60, 50/50 and 60/40.

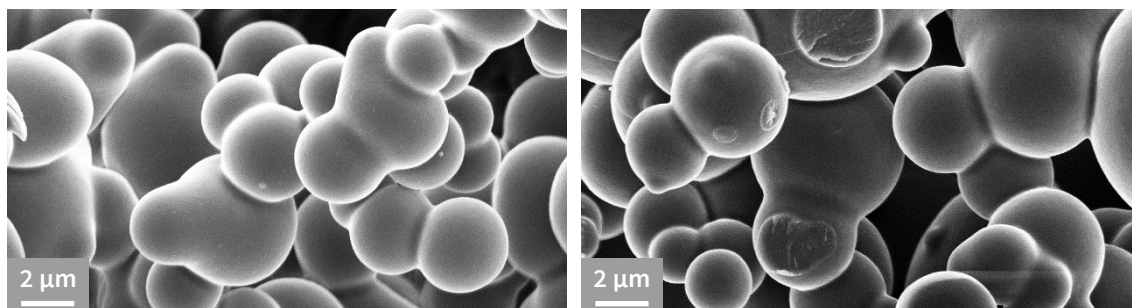


Figure 33. SEM images of RLF gels synthesized in EtOH/H₂O (left) and acetone/H₂O (right) (M/C = 10, M/F = 0.8, RC = 20 wt%).

Reduction of catalyst amount to $M/C > 20$ in the formulation prevented the formation of a gel, regardless of the solvent system. However, substituting up to 70 wt% resorcinol with OSL was possible in acetone/H₂O. The bead size was larger the higher the lignin content (Figure 34). This increase in bead size is similar to observations made for gels synthesized in EtOH/H₂O. Beads are larger for a given lignin content when acetone/H₂O is used. This observation may indicate that the solubility of the formed polymer is lower

in acetone than in EtOH: Larger beads result from earlier cluster precipitation in the gelling process.

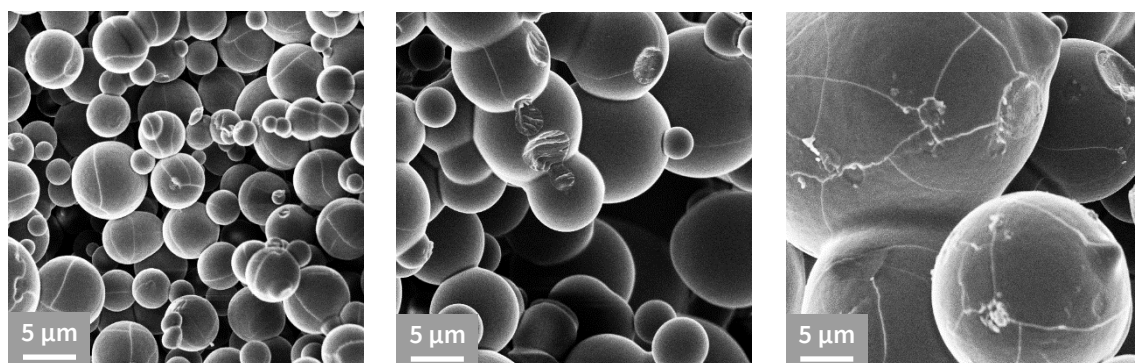


Figure 34. SEM images of RLF gels synthesized in acetone/H₂O with 20 % OSL (left), 50 % OSL (middle) and 70 % OSL (right) ($M/C = 5$, $M/F = 0.8$, $SC = 20 \text{ wt\%}$).

Gels with very small beads around 100 nm were obtained with only EtOH as solvent (Figure 35). The resulting gel had a black color and was brittle. Shrinkage was higher than 50 % and the sample was no longer porous after ambient drying.

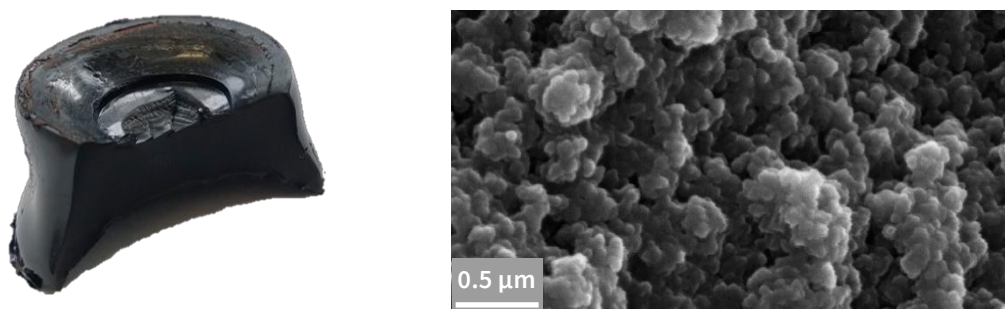


Figure 35. Images of an RLF gel synthesized in EtOH (50 wt% OSL, $M/C = 10$, $M/F = 0.8$, $RC = 20 \text{ wt\%}$).

All these experiments indicate that solvent choice is a most relevant parameter to control bead size and morphology. A mixture of a solvent and a non-solvent for lignin leads to interconnected beads with strong necks, low shrinkage and high mechanical stability. The solvent is needed to dissolve or swell lignin sufficiently to yield enough accessible groups for crosslinking. The non-solvent is needed to cause cluster precipitation in an early stage of conversion, which finally leads to large particles with low surface area.

4.3.6 RLF Aerogels from Non-Soluble Lignin

OSL showed good results as replacement for resorcinol in organic aerogels. However, this lignin type is not available on an industrial scale. High price, small batch sizes and variable properties limit use of lignin as replacement for petrol-based chemicals. HL was tested as a more viable alternative to OSL. HL is not soluble in aqueous acidic environment, most organic solvents and mixtures of both. The low solubility is of course a major factor in the sol-gel process. The starting point of the gelation using HL was a suspension rather than a solution. The result is a more complex reaction system.

HL consists of ill-defined particles with different sizes. This rough surface is transformed to a smooth one after gelation and spherical structures are formed (Figure 36). SEM images of unmodified HL and a sample after gelation indicate that HL is incorporated into the polymer network. Functionalization has presumably started on the surface of the dispersed lignin agglomerates. The formed polymer network gives a coating around the agglomerates and connects them. Stable monolithic RLF gels with up to 70 *wt%* HL were synthesized in acetone/H₂O.

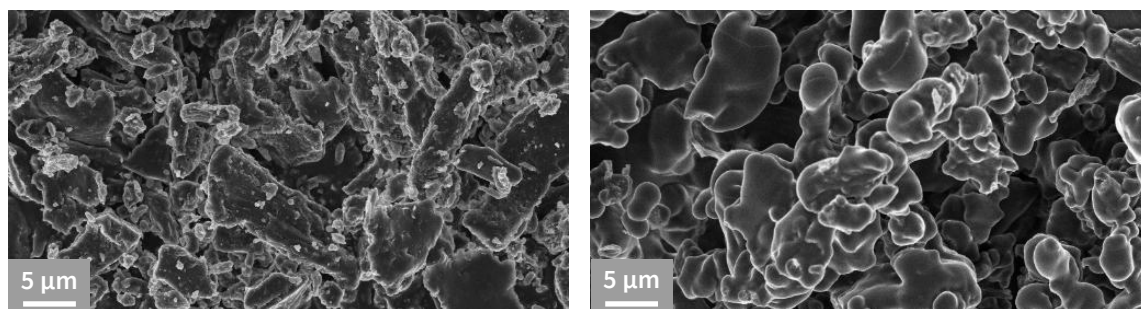


Figure 36. SEM images of HL before (left) and after gelation with resorcinol and formaldehyde (60 *wt%* HL, M/C = 8, M/F = 0.8, RC = 23 *wt%*) (right).

The resulting gels had a brown color and could be dried under ambient conditions. The extent of shrinkage was between 10 – 20 %. Overall stability was lower than for gels with OSL and samples could be crushed into powder easily. This observation and the SEM images indicate a weaker interconnection between individual beads. An enhanced lignin solubility could improve the incorporation of lignin into the polymer network.

4.3.7 Acetone/H₂O as Solvent System

Variation of solvent ratio by a few percent resulted in significant change of bead size for RLF gels with OSL. The same behavior was observed for gels with HL. Changing the ratio between acetone and H₂O changed the optical appearance and particle morphology of resulting RLF gels (Figure 37; images have the same scale).

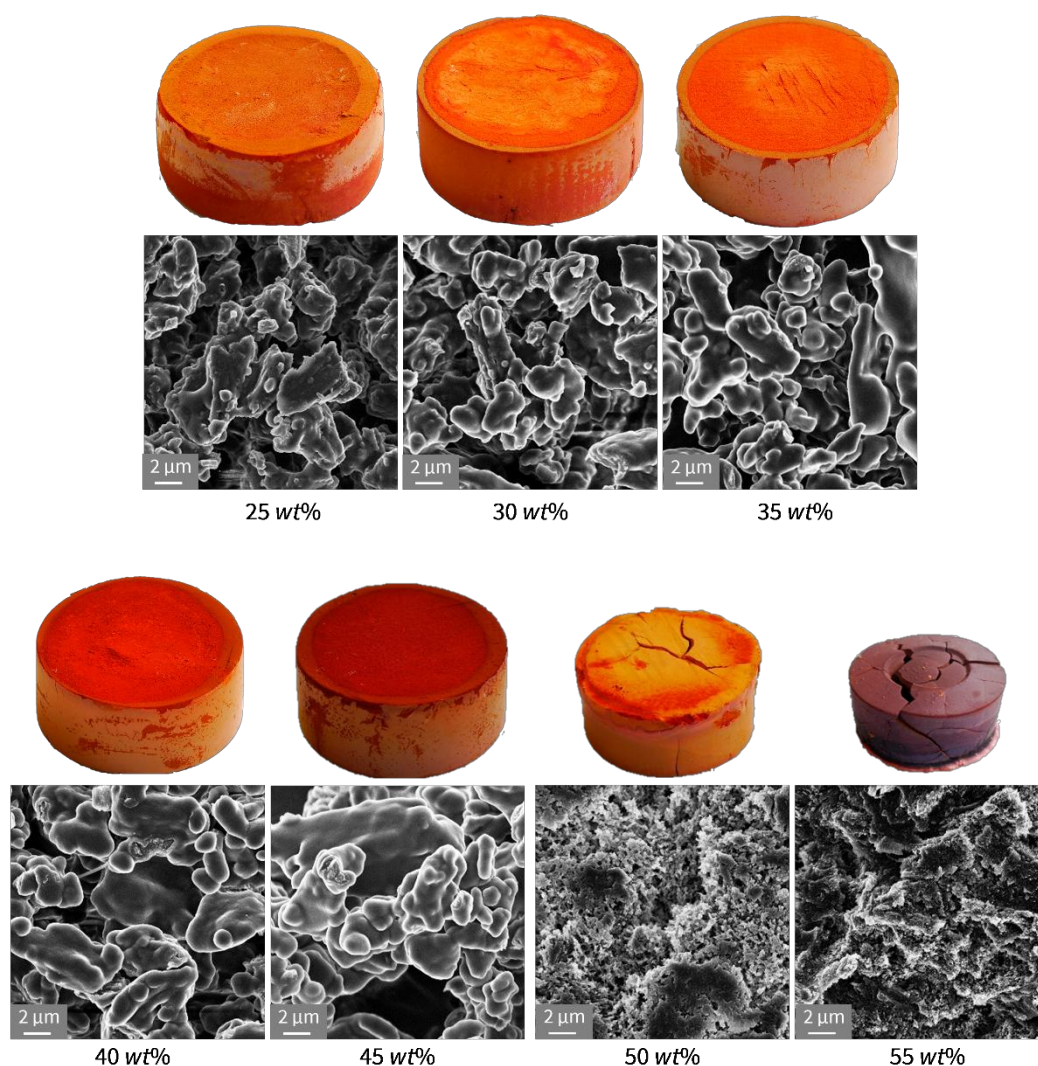


Figure 37. Images of RLF gels with acetone content ranging from 25 wt% to 55 wt% (60% HL, M/C = 20, M/F = 0.8, RC = 20 wt%).

Acetone contents between 25 wt% to 35 wt% lead to friable gels with an orange color. Red gels which are relatively stable against pressure are obtained using acetone/water

mixtures between 40 *wt%* and 45 *wt%*. A gel with 50 *wt%* of acetone was orange and cracks appeared during drying. A purple gel with large cracks was obtained with 55 *wt%* of acetone. The impression of color might result from different pore sizes as has been reported already for RF gels.^[112]

The observed change in appearance and mechanical stability is correlated with bead size. Higher acetone content led to smaller beads with sizes changing from 200 nm to around 2 μm . Lignin agglomerates were detected in gels from formulations with acetone contents up to 45 *wt%*. Coating of the agglomerates was more distinct in formulations with a higher acetone content. Low acetone content means little swelling and thus few lignin OH groups are accessible, resulting in minor incorporation of HL in to the polymer network. Acetone contents of 50 *wt%* and more in the formulation apparently breaks some agglomerates apart as deduced from the SEM images.

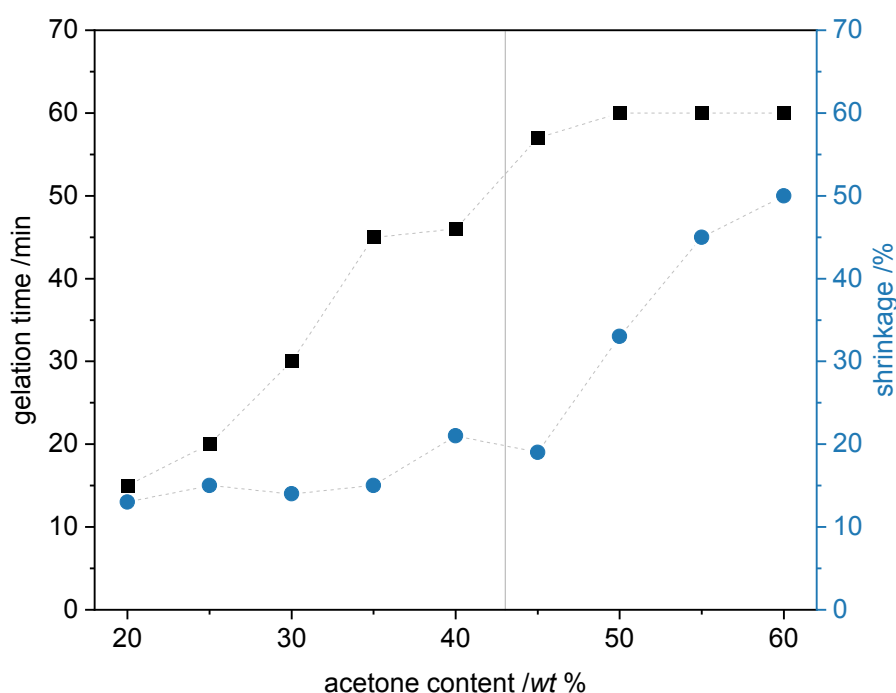


Figure 38. Gelation time and shrinkage in dependence of acetone content (60 % HL, M/C = 20, M/F = 0.8, RC = 20 *wt%*). Lines are added to guide the eye.

Increasing acetone content results in longer gelation times and higher shrinkage (Figure 38). Gelation time increased from 15 minutes for 20 *wt%* acetone to 55 minutes for 45 *wt%* acetone in the gel formulation. Acetone contents higher than 45 *wt%* had a constant

gelation time of around 60 minutes. This observation implies a change in the gelation process between 40 *wt%* and 50 *wt%* acetone. Lignin agglomerates $> 2\ \mu\text{m}$ are present already before the gelation reaction when a low solvent percentage is used. Less time is needed until sufficient polymer is formed to connect them to a space-filling network. Lignin agglomerates are dissolved once a sufficient solvent amount is present and reaction is no longer limited to the agglomerate surface. Higher solvent amount may lead to higher accessibility of reactive OH groups and therefore a faster reaction rate of formaldehyde with lignin, enhancing the solubility further and slowing down the network formation. The more or less constant gelation time above a certain threshold may be the result of two or more opposing effects of enhancing solubility and increasing reaction rates.

The extent of shrinkage of the gels can also be divided into two regimes. Shrinkage remained almost constant from 20 *wt%* to 45 *wt%* followed by a steep shrinkage increase from 45 *wt%* to 60 *wt%*. This observation is in accordance with changing appearance and bead size between the two regimes. Virgin HL agglomerates are in the range of 1-5 μm . The presence of agglomerates leads to pores at the same order of magnitude, which will undergo only a low shrinkage. Absence of agglomerates and clearly smaller beads size for acetone contents of 50 *wt%* and higher resulted in smaller pores and explain the higher shrinkage.

These results for a non-soluble lignin show that the ratio of solvent to non-solvent is also the most influential parameter for bead morphology in such a system. A high non-solvent percentage leaves larger lignin agglomerates intact. These agglomerates are covered during polycondensation resulting in corresponding large beads. Fast gelation occurs because large agglomerates are already present in the beginning and a space-filling network is formed after short reaction times. The material is friable because inter-bead connectivity is weak. A high organic solvent part in the formulation causes dissolution of lignin agglomerates and leads to a (much more) homogeneous reaction system. Only small particles remain in the starting solution resulting in overall smaller beads. Gelation is slower because smaller beads need to grow longer until they touch

each other but eventually gelation time remains constant because of an increasing reaction rate. The resulting small pores cause higher shrinkage.

4.3.8 DMSO/H₂O as Solvent System

Acetone/H₂O as solvent system for gel formulations led either to large remaining aggregates or to very small particles. An intermediate bead size in between is expected to be ideal for synthesis of gels with low shrinkage and high mechanical stability. Dimethyl Sulfoxide (DMSO)/H₂O was chosen as solvent system to evaluate this hypothesis. The mixture gives homogeneous suspensions of HL. Formulations with DMSO content between 0 *wt%* and 50 *wt%* gave gels which varied in optical appearance and particle morphology after drying (Figure 39; images at the same magnitude of enlargement).

Gels prepared without DMSO were friable and broke upon removal from the mold. SEM images showed lignin agglomerates next to polymer beads. Lignin particles are dispersed but not dissolved or swollen in pure H₂O. Only few OH groups on the particle surface are accessible for reaction. Lignin agglomerates and polymer are barely connected via covalent bonds and only a weak network is formed.

Porous yet stable gels were obtained with DMSO content between 25 *wt%* and 35 *wt%*. Lignin particles are swollen to some extent and a higher percentage of the lignin polymer reacts. A stronger network is formed and an even coating of remaining agglomerates is indicated.

Higher DMSO amount resulted in hard and dense gels. DMSO contents of 45 *wt%* and 50 *wt%* led to dissolution of lignin agglomerates as well as a higher solubility of the intermediates. Bead sizes in those gels are significantly smaller, decreasing to around 200 nm in formulations with 50 *wt%* of DMSO. The sample with 40 *wt%* DMSO gives beads in the μm range but with a rougher surface than for lower DMSO contents. The presence of agglomerates is less pronounced. This amount of DMSO presumably causes sufficient swelling of lignin and additional OH groups inside the agglomerates become

accessible. Polycondensation does not only take place on the surface, leaving less monomer to form a coat around the beads.

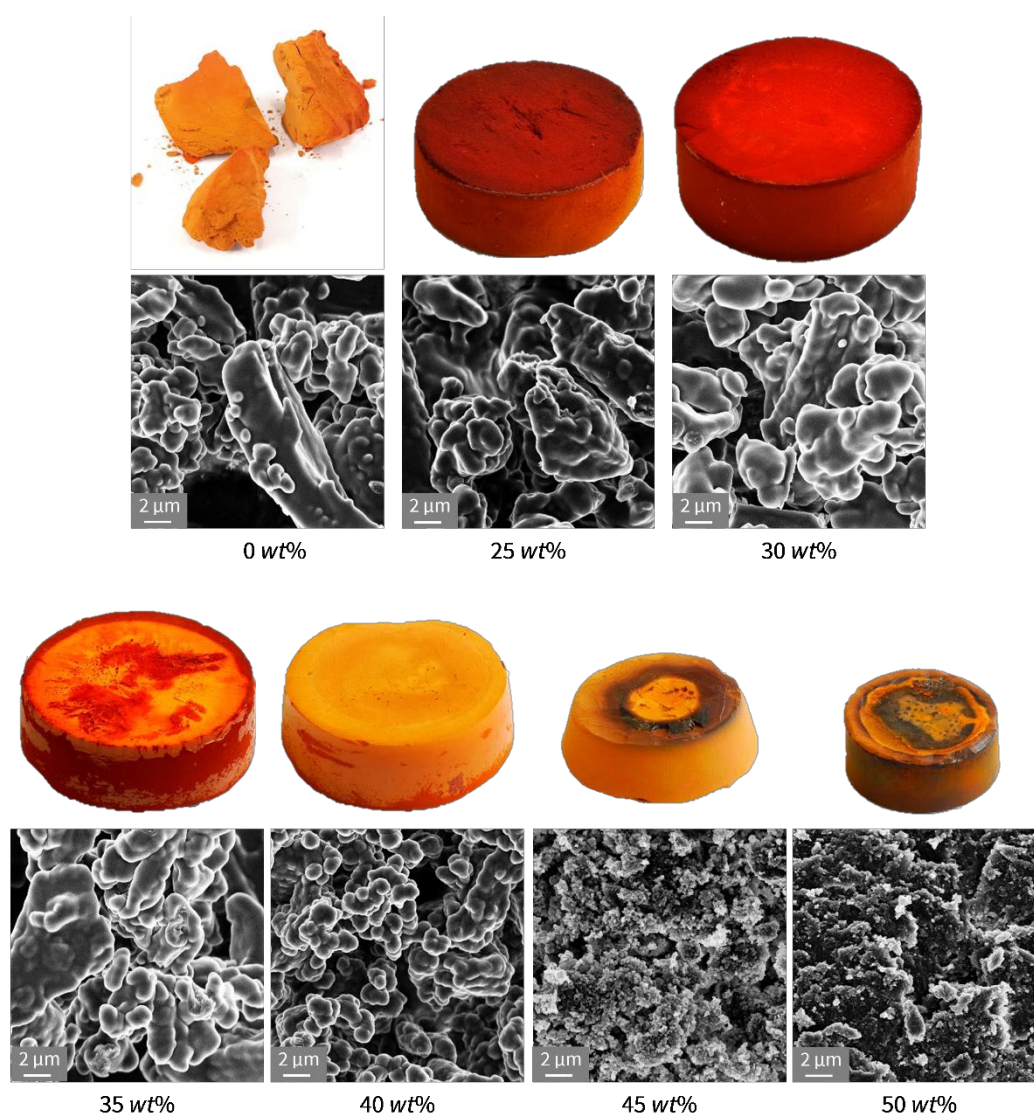


Figure 39. Images of RLF gels with DMSO content ranging from 0 *wt%* to 50 *wt%* (50 % HL, M/C = 50, M/F = 0.8, RC = 20 *wt%*).

Gelation time was longer for higher DMSO content. A minimal shrinkage was observed for intermediate DMSO content (Figure 40). Shrinkage could not be evaluated for DMSO contents lower than 25 *wt%* because resulting gels were very friable and monoliths broke apart after removal from the mold.

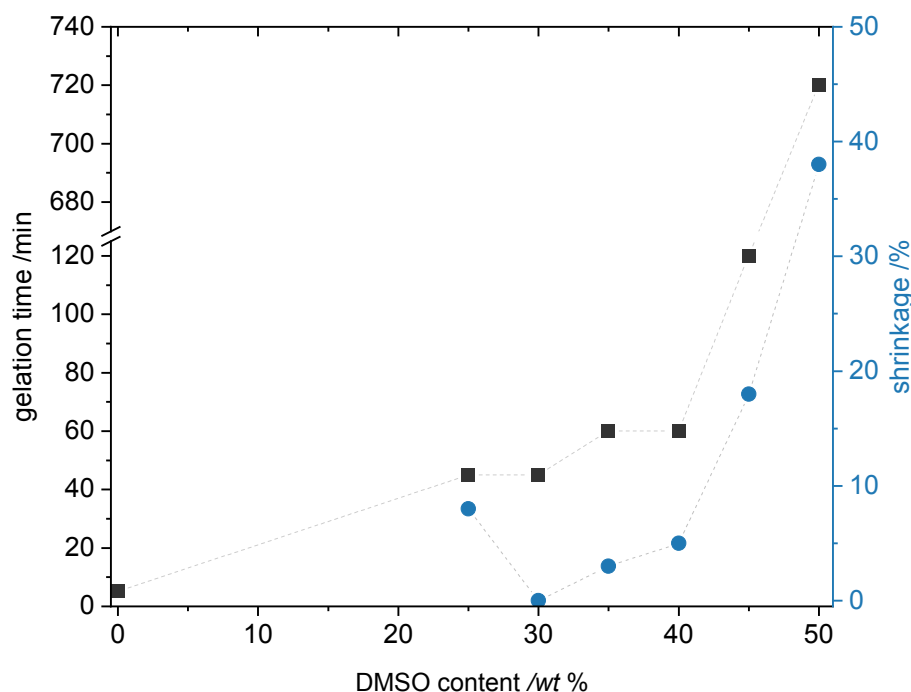


Figure 40. Gelation time and shrinkage in dependence of DMSO content (60 % HL, M/C = 20, M/F = 0.8, RC = 20 wt%). Lines are added to guide the eye.

Short gelation times for low DMSO content are interpreted like before: the presence of large lignin agglomerates filling a significant space already before the reaction. Longer gelation times results from higher solubility of the formed polymer. Less DMSO causes earlier cluster precipitation and formation of large beads to minimize the surface area. Gelation time is significantly longer for DMSO contents higher than 40 wt% because lignin agglomerates are dissolved and the network has to grow longer to be space-filling. In addition, polymer clusters stay soluble over a longer time, resulting in formation of small beads.

Low mechanical strength of the gel results from lignin agglomerates that are barely incorporated in the polymer network by covalent bonds, typical from formulations with low DMSO contents. The weak interconnection yields a very friable gel. Shrinkage showed a minimum for 30 wt% DMSO where the gel did not shrink noticeably. This minimum results from optimal lignin incorporation by sufficient covalent bonds and a smooth coating of agglomerate as well as a large pore sizes causing low capillary forces during drying. Lower DMSO content led to higher shrinkage because of less crosslinks

and weaker interparticle connection. Higher DMSO content caused higher shrinkage because of smaller pores and resulting higher capillary forces during drying.

DMSO/H₂O is a promising solvent system for the synthesis of stable RLF gels with high lignin content. Shrinkage was overall lower when DMSO was used instead of acetone in the formulation. Lower shrinkage in DMSO may result from a higher mechanical stability of the gel, which effectively is caused by the better solubility of HL. Complete dissolution of lignin agglomerates is not favorable, but a certain DMSO amount leads to sufficient accessibility of OH groups to allow for the formation of a strong network.

4.3.9 Solid Content Reduction using a higher Viscosity of the Formulation

Lower solid content of the gel forming formulation results in materials with lower density. This is favorable for some applications, e.g. usage as thermal insulation material. A solid content ≤ 15 wt% did not lead to stable gels with HL because sedimentation occurred during the synthesis and resulting samples were not homogeneous. One possibility to reduce sedimentation rate is using formulations with a higher viscosity. Higher viscosity was achieved by using an aqueous 0.2 wt% solution of agar in H₂O.

An agar solution for gel synthesis with 15 wt% solid content indeed show a lower sedimentation rate and led to gels with a lower density. Higher viscosity of the formulation comes along with an uneven reactant and possibly catalyst distribution in the solution. SEM images of the gel sample shows bead sizes in a broad range from nm to μ m and various particle morphologies (Figure 41). The sample was notably inhomogeneous in the inside. The overall process of bead formation, agglomeration and functionalization of HL is non-uniform, with a range of local conditions. Diffusion barriers appear, making the process complex and the outcome hard to control. Although a gel with lower RC could be reached, large efforts need to be undertaken to find conditions that allow a reproducible preparation. Prolonged stirring or shaking would be an option to obtain a homogeneous gel, possibly the presence of some organic solvent is useful but all of this adds complexity to the system. Therefore, this approach was not pursued further.

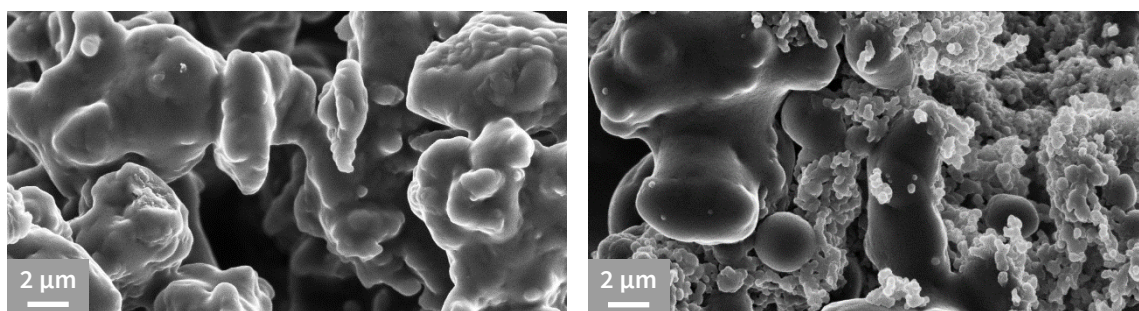


Figure 41. SEM images of RLF gel without agar (left) and with 0.2 *wt%* solution of agar in H₂O (right) (50 % L; DMSO/H₂O 5:95; M/C=25, M/F=0.5).

4.3.10 Combination of Base and Acid as Catalyst for RLF Gels

A combination of base and acid catalysis has been used to obtain RF gels with both small bead sizes and good mechanical stability.^[168,202] Final gel properties depended on the amount of catalysts and on the addition point in time of the acid. This combined approach was adapted for lignin-containing gels. Na₂CO₃ was used as base catalyst in a first reaction step and H₂SO₄ as acid catalyst was added at different times.

First experiments were carried out with HL in H₂O to determine suitable amounts of base and acid, respectively described by the ratios M/C_b and M/C_a. Brittle gels with high shrinkage form at higher base concentration, whereas a low amount resulted in gels that already crumbled on touch. A larger amount of acid will cause instant gelation at the addition spot and thus inhomogeneous gels. Long gelation times arise when only small amounts of acid were added.

An appropriate range for the base catalyst was $100 < M/C_b < 250$ and for the acid catalyst $5 < M/C_a < 50$. A M/C_b ratio at the high end leads to gels with larger beads with smoother surface (Figure 42). The corresponding low amount of base catalyst will result in the formation of less active clusters in the beginning of the reaction. This results in larger bead sizes. The shorter gelation time for low amount of base is in contrast to a slower reaction expected for the use of less catalyst. Early gelation is caused by earlier cluster precipitation during the gelling process. These findings imply an impact of base not only as catalyst but also by changing educt and product solubility. Lignin solubility is lower

for lower pH, i.e. lower amount of base. This results in larger agglomerates in the initial solution and possibly also in earlier precipitation of the formed polymer.

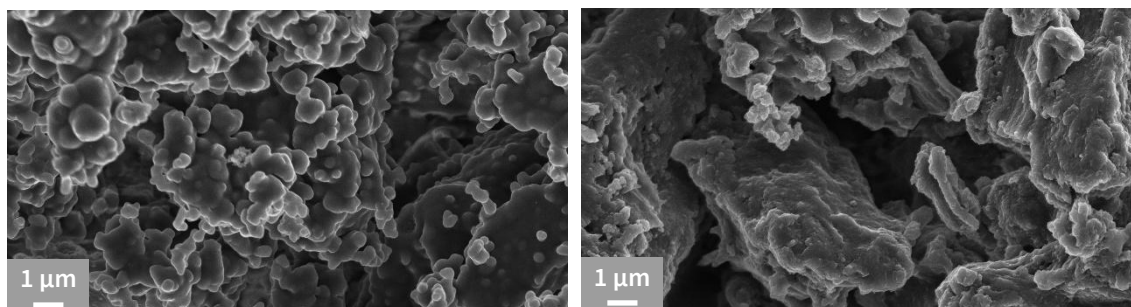


Figure 42. SEM images of RLF gels prepared with (left) $M/C_b = 100$, $M/C_a = 5$ and (right) $M/C_b = 250$, $M/C_a = 10$ and addition after 150 minutes.

The addition after 90 min of any amount of acid in the M/C_a range mentioned above does not change the gel structure (Figure 43, A and B), the base catalyzed reactions had not progressed to a determining extent and the acid catalyzed step controls the final gel properties. The addition after 150 minutes leads to gels with smaller bead sizes from μm range to nm range for $M/C_a = 30$ (Figure 43, A and C). Base catalysis favors monomer addition leading to spherical particles while acid catalysis favors condensation promoting particle neck formation.^[202] Acid addition induced a change in the reaction mechanism: a fast condensation of the previously formed particles with the remaining monomers takes place. A large amount of remaining monomer in the solution before acid addition leads to the formation of a layer covering the previously formed structures.^[168] A longer phase of base catalysis means more time for spherical particles to grow and those particles quickly form a network after acid addition. Less monomer remains in the solution, resulting in the formation of only a thin layer. Larger beads for higher M/C_a ratios, i.e. at a lower acid concentration are observed for late addition of acid (Figure 43, C and D). Less acid results in slower gelation, generating time for the remaining monomers to form a smoother layer. The later addition of small amounts of acid (higher M/C_a ratio) resulted in even smaller bead sizes, but the change was less pronounced (Figure 43, B and D). The longer the base-catalyzed reaction phase, the longer the spherical particle growth. Less monomer was left when acid was added, leaving less possibility to form necks or smooth surfaces.

SEM images all show lignin agglomerates (Figure 43). Friable gels were obtained as a result. Solvent change from H₂O to a mixture of EtOH/H₂O dissolved agglomerates and allowed for gel structures with beads in the range of a few hundred nm. Amount of acid and base were adjusted to achieve stable gels with short gelation time. The reaction was started with $M/C_b = 35$. A given acid amount corresponding to $M/C_a = 5$ was added after 90, 120, 150 and 180 minutes.

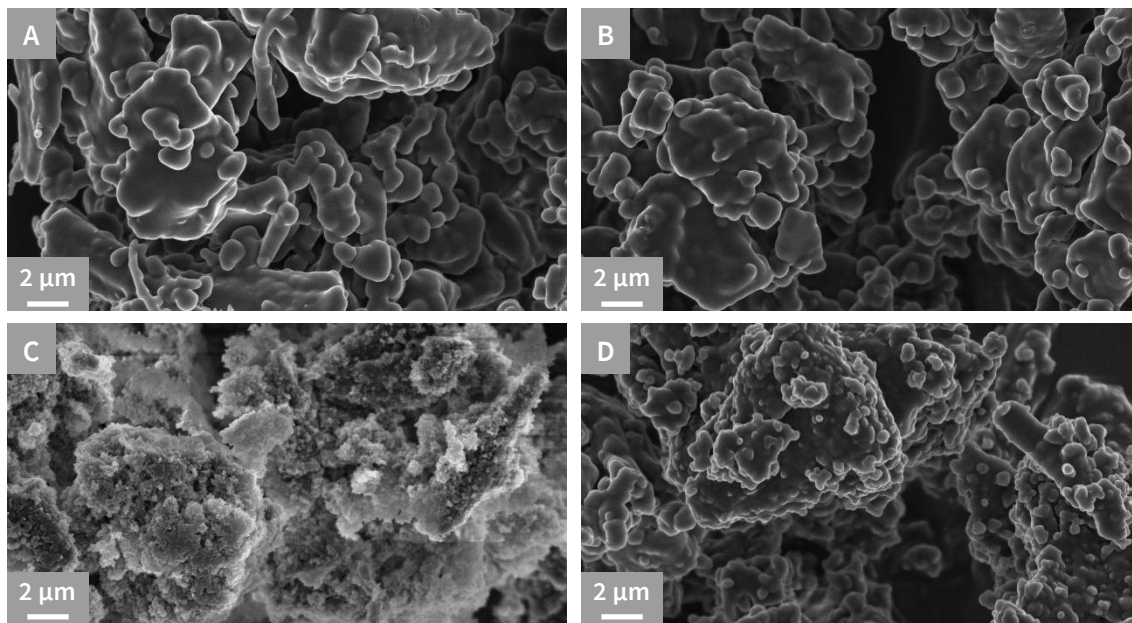


Figure 43. SEM images of RLF gels prepared with (A) $M/C_b = 250$, $M/C_a = 30$, 90 minutes (B) $M/C_b = 250$, $M/C_a = 50$, 90 minutes, (C) $M/C_b = 250$, $M/C_a = 30$, 150 minutes (D) $M/C_b = 250$, $M/C_a = 50$, 150 minutes.

The SEM images now show a change from colloidal to polymeric morphologies (Figure 44). Bead sizes were in the range of 300 nm for all gels. The sample with acid addition after 90 minutes appeared denser, with few pores and agglomerated beads forming a rough surface. The sample with acid addition after 180 minutes showed a fibril-like structure. Pores are visible between fibrils. The gels resulting from acid addition after 120 minutes and 150 minutes are intermediate between the two, showing that the process is quite robust (except that mixing is crucial, vide infra). This structural change

aligns with reports describing a pearl necklace structure for acid catalysis and a fibril-like structure for base catalysis.^[202]

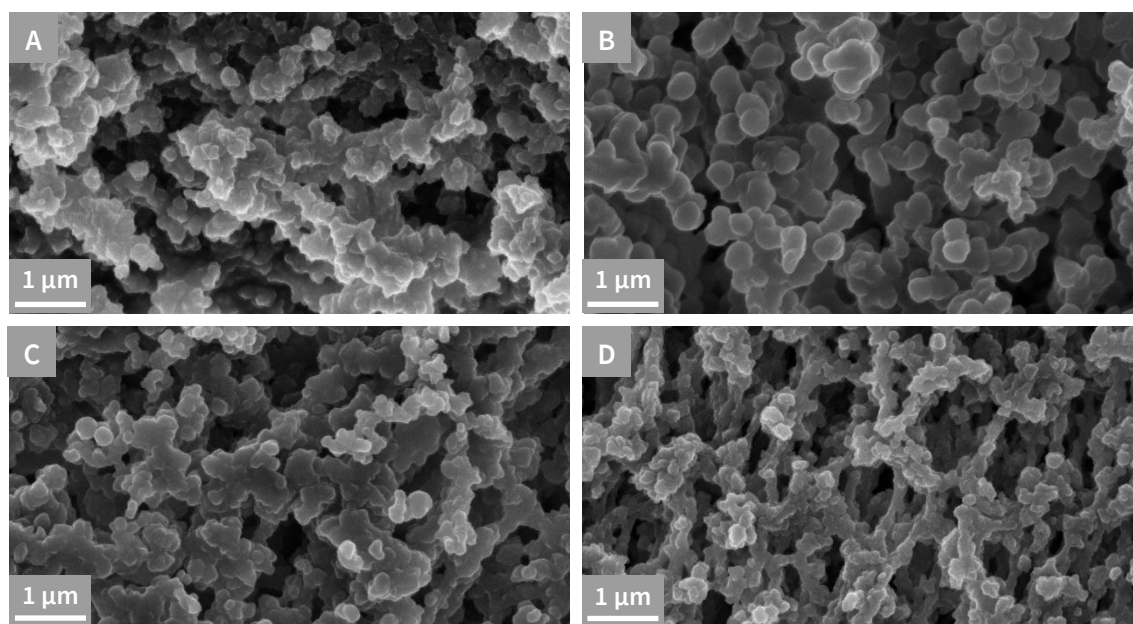


Figure 44. SEM images of RLF gels prepared with $M/C_b = 35$, $M/C_a = 5$ and acid addition after (A) 90 minutes, (B) 120 minutes, (C) 150 minutes and (D) 180 minutes.

The gels with fibril-like structures show a descent mechanical stability despite the small pore sizes and therefore have some promise as thermal insulation materials. Unfortunately, reproducible material synthesis was difficult because fast gelation occurring at the spot of acid addition, resulting in inhomogeneities in the products, in particular when performed on a larger scale. Various approaches including methods for homogenization during acid addition and addition of diluted acid did not improve the results. Therefore, the combined approach of base and acid catalysis is rather limited to lab scale and was not pursued further.

4.3.11 Property Optimization by Design of Experiments

The results of this study indicate a strong influence of solvent system on particle morphology. Other influential parameters, also described in literature, are M/C and M/F , which appear also essential in the preparations with lignin monomer. Design of Experiments (DoE) was used to establish the interdependency of the various synthesis

parameters on the final gel. This experimental design used diverse statistical methods to determine the influence of multiple input factors on responses. Interactions between different input factors could also be elucidated.^[203]

Influence of DMSO content (0 *wt%* - 50 *wt%*), M/C (25 – 100) and M/F (0.5 – 0.9) was studied using a response surface methodology (Table A2, appendix). Measured responses were gelation time, shrinkage and overall gel quality (Table A3, appendix). All gels were prepared with HL and RC = 20 *wt%*. Images of dried gels can be found in the appendix (Figure A 21).

Gelation time was longer for higher DMSO content. It was also longer for higher M/F and higher M/C values. The effect is expected: Higher DMSO content increases gelation time because less lignin agglomerates are present in the beginning. Higher M/F value means lower formaldehyde concentration and results in slower reaction. Lower catalyst concentration indicated by higher M/C value leads to a slower reaction. The contour plots show interdependence between all factors (Figure 45). For low R/C values (high amount of acid) gelation is fast for any amount of formaldehyde. For high R/C values (low amount of acid) the concentration of formaldehyde apparently becomes more relevant for the reaction rate. Effects caused by changing M/F and M/C are less pronounced at low DMSO content. Presence of large lignin agglomerates at low DMSO content apparently suppresses all other effects. This assumption is supported by the analysis of the coded factors obtained from the model equation (Table A4, appendix). Higher factors mean higher relative impact, implying that the DMSO content has the highest relative impact on the gelation time, followed by M/C. M/F has the lowest relative impact. The coded factors for the combined terms estimate the relative impact of the factors to be $(M/C \cdot \text{DMSO content}) > (M/C \cdot M/F) > (M/F \cdot \text{DMSO content})$.

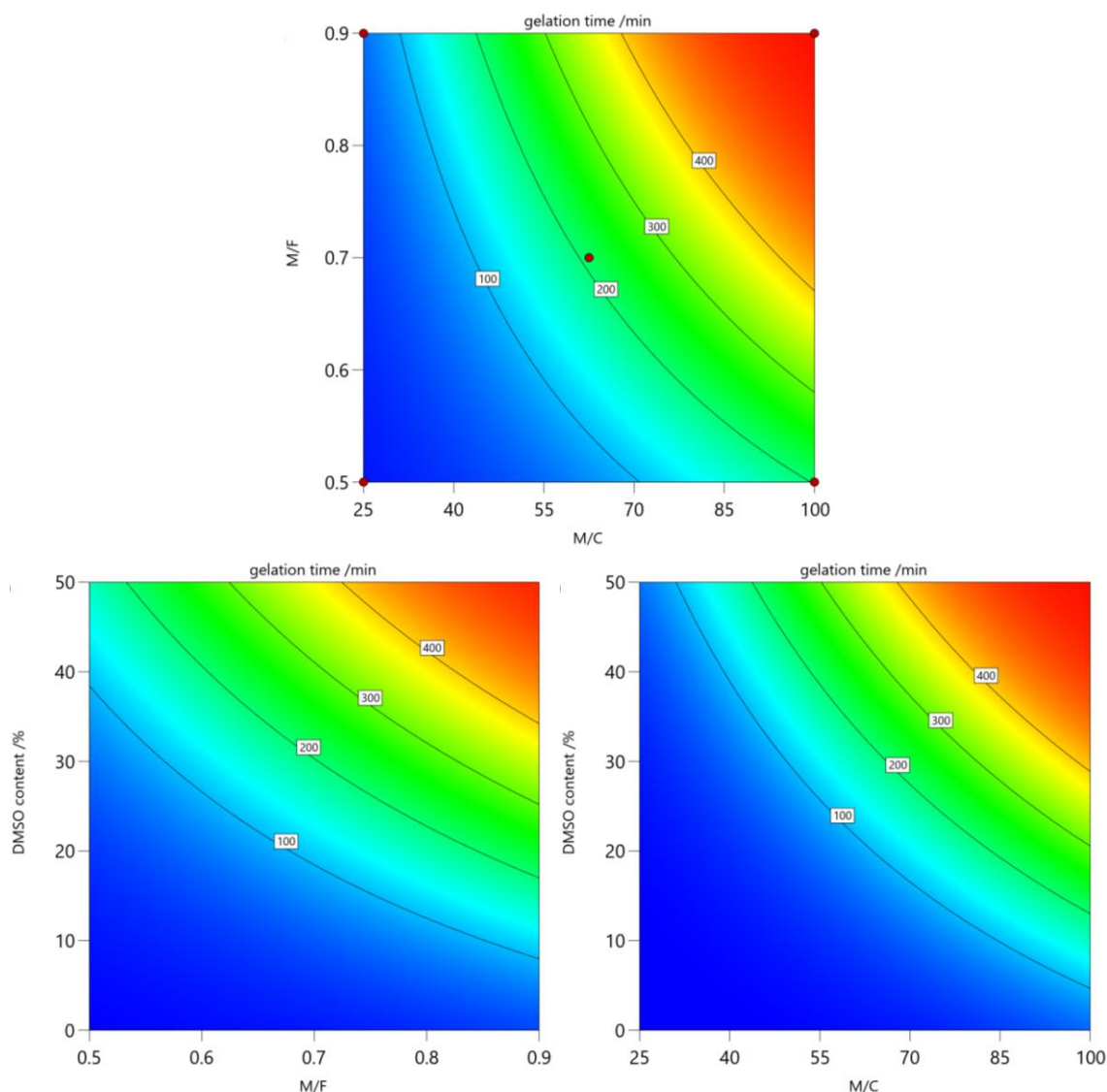


Figure 45. Contour plots of the interdependence of gelation time on M/F and M/C (top), DMSO content and M/F (bottom left) and DMSO content and M/C (bottom right).

The obtained model describing gelation time represents a general trend rather than a prediction of actual values. Gelation time measured by optical inspection results in a significant error. A statistical model based on this data set has the same error. Nonetheless the contour plots represent overall dependencies.

Shrinkage is predominantly dependent on DMSO fraction and not so much on the M/F or M/C value (Figure 46). The explanation follows as above: High DMSO contents give a more extensive lignin dissolution, and the gelation is faster giving smaller beads and pores and therefore a higher shrinkage. Shrinkage is barely influenced by M/F and M/C.

A small effect is only visibly for high DMSO close to 50 *wt%*, where shrinkage appears to be minimal for $M/F = 0.7$ and $M/C < 80$. Again, presence of lignin agglomerates has the strongest influence on the network morphology and therefore other effects are only apparent when they are broken apart by high DMSO content.

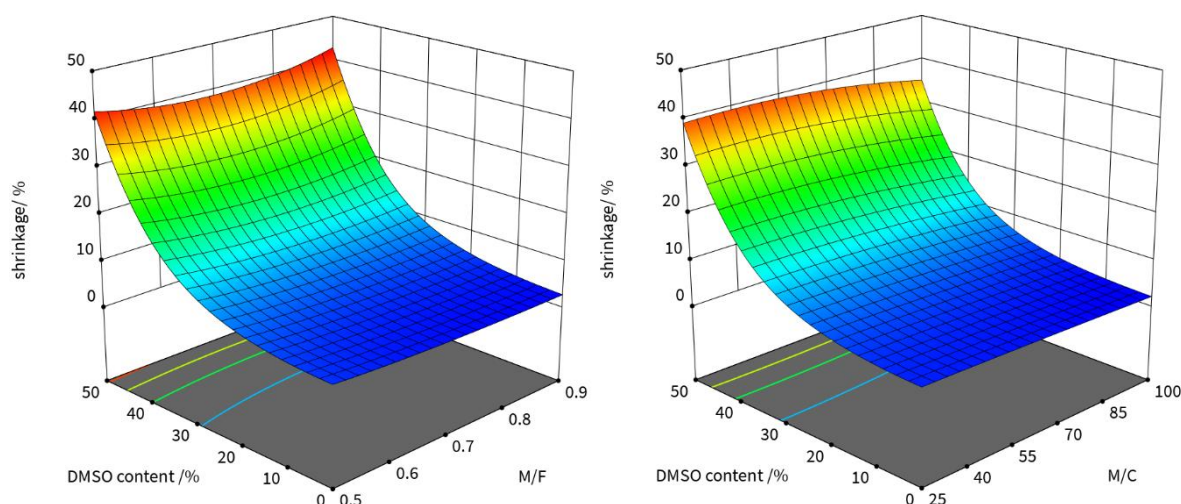


Figure 46. Response surface describing the interdependence of gel shrinkage on DMSO fraction and M/F value (left) and M/C value (right).

Overall gel quality was rated from on a scale from 1 (poor) to 5 (excellent) considering shrinkage and mechanical stability. Gels with excellent overall quality did not shrink and had high compression strength. Overall quality depends mostly on DMSO fraction and not on M/F and M/C values (Figure 47).

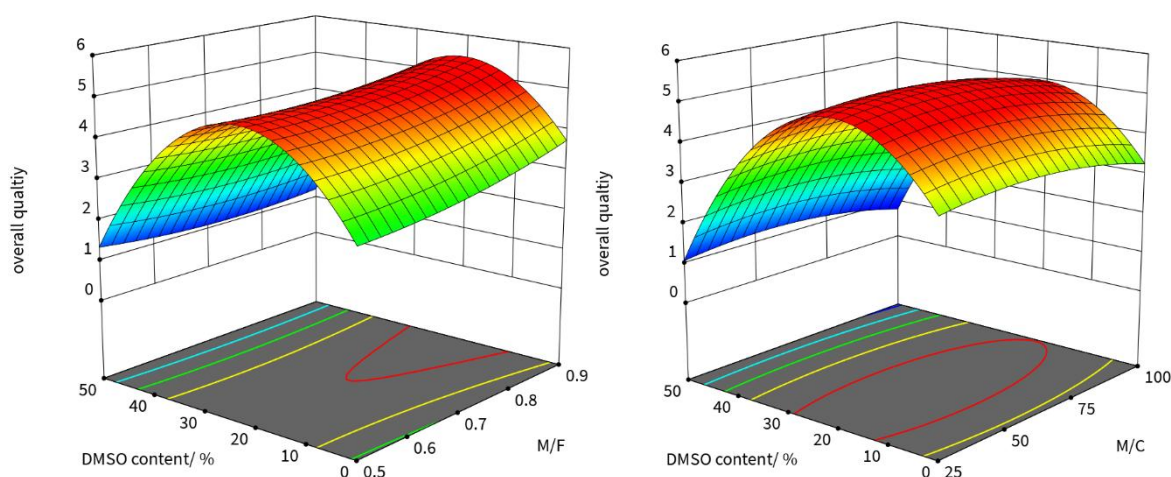


Figure 47. Response surface describing dependence of overall gel quality on DMSO fraction and M/F value (left) as well as M/C value (right).

There is a maximum of overall quality between 15 *wt%* and 30 *wt%* DMSO. Quality fell from 5 to 3 for low DMSO content because the gels were friable but did not shrink. Overall quality dropped to 1 for higher DMSO fractions because high shrinkage occurred and the gels were brittle.

Minimal influence of M/F and M/C on the quality is predicted for low and high DMSO content. Absence of lignin agglomerates is again presumably the explanation for this behavior at high DMSO content. M/F and M/C could gain importance at low DMSO content because agglomerates are only superficially covered, leading to a higher impact of crosslinking density for overall mechanical stability, and solubility of lignin may increase in the course of gelation by the progressing hydroxy methylation.

The obtained results from the DoE allow to propose an optimized formulation for RLF gels. Optimal gel stability with reduction of acid and formaldehyde content is obtained with a DMSO content of 20 %, M/F = 0.9 and M/C = 100. More catalyst and formaldehyde are only useful if a reduction of gelation time is desired.

4.3.12 Scale-Up of Promising Formulations

A detailed understanding of factors influencing the gel structure was obtained from the study above. The next step is a scale-up to validate a suitability for production on a larger scale. Samples with a maximum dimension of 15x15x3 cm were targeted. SEM images indicated no structural difference between gels of different sizes. Two formulations were chosen based on the obtained knowledge aiming for two samples with opposing material properties (Table 5). Approach A is directed to a material with large beads and approach B to a gel with a fine pore structure.

Table 5. Synthesis parameters and drying method of scale-up along approach A and B.

	A	B
lignin content /wt%	60	50
Solvent system	acetone/H ₂ O	EtOH/H ₂ O
ratio (wt/wt)	(40/60)	(50/50)
M/C	4	5
M/F	0.6	0.9
RC /wt%	15	20
drying	ambient	supercritical CO ₂

The M/C ratio was similar, the M/F ratio was lower in approach A. A higher amount of formaldehyde is expected to lead to a faster gelation and lower shrinkage because of higher crosslink density. The most significant difference is that of solvent system. Acetone/H₂O was used for A and EtOH/H₂O was used for B. A allowed for maximal lignin content of 60 wt% and a minimal RC of 15 wt%. B had a lignin content of 50 wt% and RC was 20 wt%. Different drying methods were applied. A was dried by solvent evaporation under ambient conditions. B was dried with supercritical CO₂. Drying

under ambient conditions was not possible with this formulation because large cracks appeared and no monolithic sample could be obtained.

Material A starts to form after a gelation time of around 5 minutes and resulted in a red-brown gel with an appearance similar to woodgrain (Figure 48). Pores were detected by eye. The gel was friable upon touch and was easily pulverized. Material B had a gelation time of around 10 minutes and led to a light brown gel. The sample appeared denser, less porous and quite stable upon touch. A shrinkage of 20 % occurred despite supercritical drying. It must be noted that optimization of supercritical drying conditions for a given material is a research topic itself. Optimization of drying conditions was not addressed in this work, but it has to be expected that lower shrinkage is possible for this approach

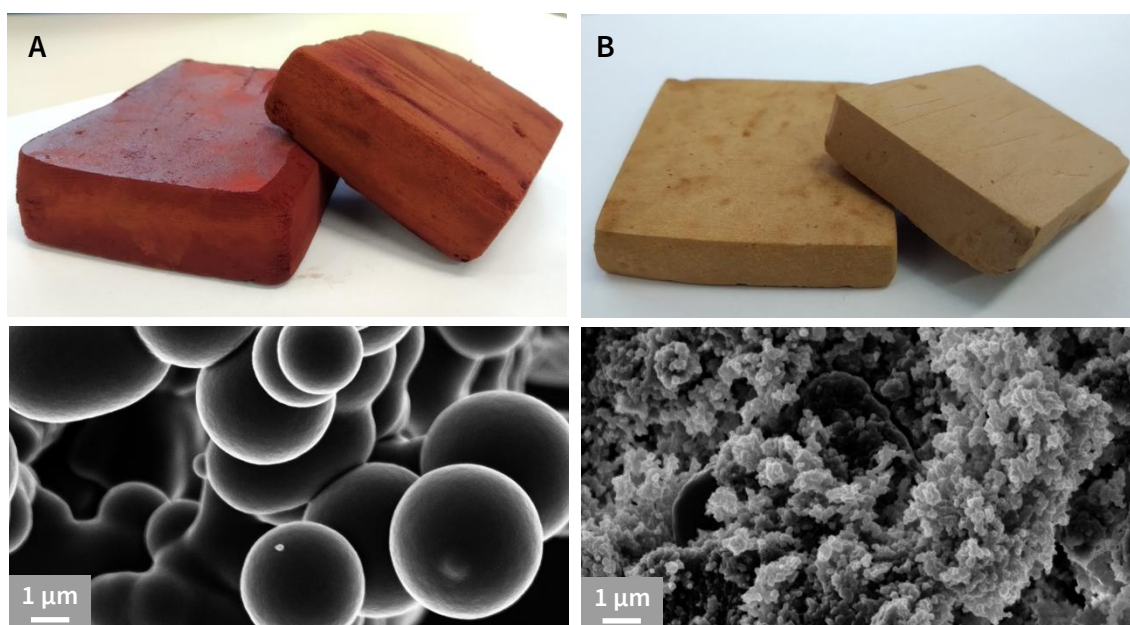


Figure 48. Images of gels from scale-up approach A and B.

SEM images showed large beads with a size of a few μm for material prepared in approach A. Beads had a smooth surface and large necks. The bead size of material along B was in the nm range and had a rougher surface (Table 6).

Table 6. Properties the materials prepared along the scale-up approach A and B.

	A	B
density / $\text{kg}\cdot\text{m}^{-3}$	250	460
porosity / %	82	68
Young's modulus / MPa	1.0 ± 0.3	8.5 ± 1.0
thermal conductivity / $\text{mW}\cdot\text{m}^{-1}\cdot\text{K}^{-1}$	67.6	110
BET surface area / $\text{m}^2\cdot\text{g}^{-1}$	26.1	77.6

Formulation A led to a gel with a density of $250 \text{ kg}\cdot\text{m}^{-3}$ and a porosity of 82 %. Formulation B resulted in a much denser gel after a substantial shrinkage. Density was $460 \text{ kg}\cdot\text{m}^{-3}$ with a porosity of 68 %. Gel A had a lower compression strength with a Young's Modulus of 1 MPa compared to B with a Young's modulus of 8.5 MPa. The lower mechanical stability of A results from its lower density.

The lower density is also the explanation for the lower thermal conductivity of gel A. Thermal conductivities were 67 and $110 \text{ mW}\cdot\text{m}^{-1}\cdot\text{K}^{-1}$ for A and B, respectively. The thermal conductivity of expanded styrene as benchmark is around partly in the same order of magnitude at $40 \text{ mW}\cdot\text{m}^{-1}\cdot\text{K}^{-1}$.^[204] Heat transfer in an aerogel will proceed by the polymer backbone, by gas molecules in the pores and by thermal radiation. Both thermal radiation and conductivity is lower at lower densities.^[112] Low gaseous thermal conductivity often described for aerogels results from the Knudsen effect observed for pore size in the nm range. Pore sizes for RLF aerogels are in the μm range, therefore this effect is not relevant.^[119]

Approach A and B represent two points in the broad spectrum of material properties attainable with RLF gels. Sufficient mechanical stability could be obtained for material A by formation of large beads, resulting in the possibility for ambient drying, preserving

the initial low density. Gels with finer pore sizes may undergo a high shrinkage, like is observed in material B. Material B has a higher inner surface area.

The interparticle connection in gels with large beads was better in materials from formulation on the basis of DMSO/H₂O. Therefore, this solvent system was also used for further larger scale preparation of gels. Results from DoE allowed to optimize formulations to obtain a material with low density. In addition, short gelation times were desired to facilitate the synthesis and formaldehyde content should be minimal. These criteria led to approach C and D (Table 7).

Table 7. Synthesis parameters and drying method of scale-up approach C and D.

	C	D
lignin content /wt%	50	50
solvent system	DMSO/H ₂ O	DMSO/H ₂ O
ratio (wt/wt)	(6/94)	(11/89)
M/C	50	25
M/F	0.9	0.9
RC /wt%	20	15
drying	ambient	ambient

The formulations in approach C and D both are based on a lignin content of 50 wt% and a M/F ratio of 0.9. M/C was 50 for C and 25 for D, the RC was 20 and 15, respectively. The ratio of DMSO to H₂O was 6/94 for C and 11/89 for D. Gelation time was 20 minutes. Ambient drying with minimal shrinkage was observed for the gel of both formulations: material C shrunk by 3 % and D by 6 %. The gels had a similar red-brown appearance (Figure 49), and pores were visible by eye. The gels are mechanically delicate and crumbled slightly upon touch but had overall higher resistance to pressure than the gel

from approach A. SEM images showed similar bead morphologies. Lignin agglomerates were present but coated by polymer. The slightly higher DMSO content for D did not influence bead morphology significantly: the amount used in both formulations is too low to substantially dissolve or even swell the HL.

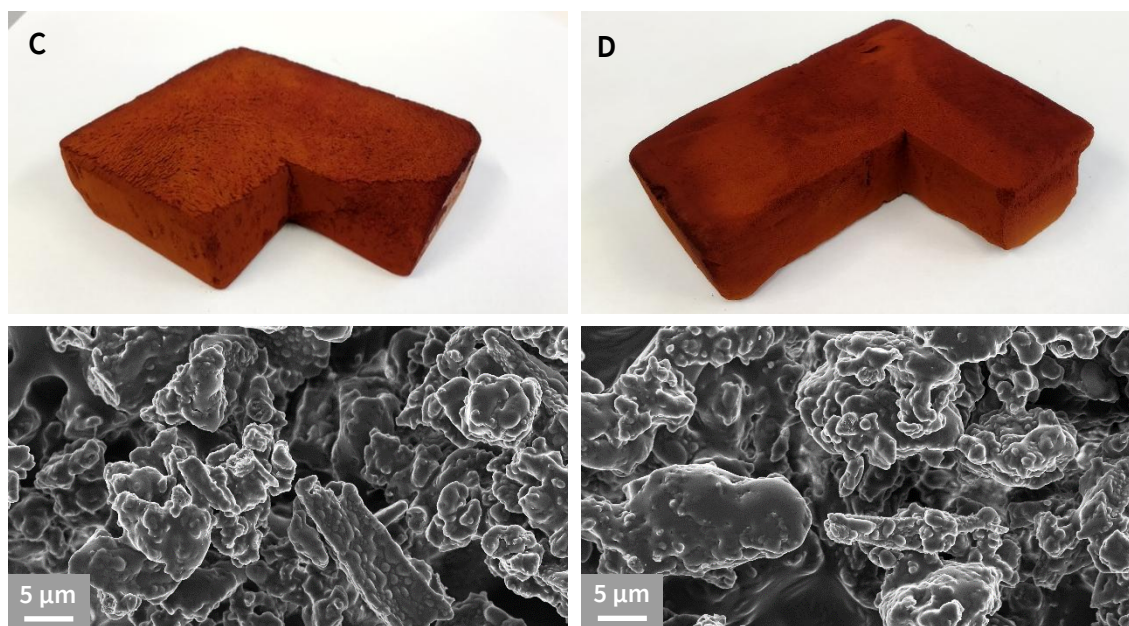


Figure 49. Images of gels from the scale-up approach C and D.

The density of gel D is lower than of C, despite their similar appearance (Table 8). A lower density is in accordance to the lower RC and also underlies a higher porosity (as shrinkage is low in both materials). The compressive strength is similar for both materials. Thermal conductivity is slightly lower for D also as a result of its lower density.

Table 8. Density, porosity, Young's modulus and thermal conductivity of Scale-up approaches C and D.

	C	D
density /$\text{kg}\cdot\text{m}^{-3}$	225	196
porosity /%	79	85
Young's modulus /MPa	1.6 ± 0.3	1.2 ± 0.2
thermal conductivity /$\text{mW}\cdot\text{m}^{-1}\cdot\text{K}^{-1}$	60.0	58.4

Scale-up of approach C and D shows the possibility to tailor RLF gel by variation of RC. Lowering RC reduces density, leading to a lower thermal conductivity but also lower mechanical stability. Reduced acid and formaldehyde concentration and ambient drying, thus making supercritical drying obsolete, are beneficial for the sustainability of the whole process. Using HL is especially promising because this lignin type is expected to become available in larger quantities in the future.

4.4 Summary

OSL can partly replace resorcinol in the acid-catalyzed synthesis of organic aerogels, at least up to a level of 50 % when formulation is in EtOH/H₂O or 70 % in acetone/H₂O mixtures. High mechanical stability obtained with specific solvent mixtures permits drying with low shrinkage by ambient solvent evaporation and not needing the much more elaborate supercritical drying.

Larger percentage of lignin in the formulation resulted in larger beads and shorter gelation time because of the lower solubility of the formed intermediate polymer. Higher formaldehyde content leads to a faster gelation. Higher catalyst concentration effected a faster gelation and smaller beads. The amount of acid catalyst could be reduced to a certain threshold below which no gelation occurs.

A denser crosslinking led to formation of a more stable network and resulted in lower shrinkage. A lower reactive content resulted in gels with lower density, below an RC of 15 *wt%* no coherent gels were formed, a higher dilution led to sedimentation and formation of inhomogeneous gels.

The choice of solvent proved to be the most influential factor for gelation process and for the resulting gel morphology. A mixture of solvent and non-solvent for lignin was found to be the best choice for homogenous gels. Solvent is needed for homogeneous distribution of lignin and high accessibility of OH groups. Non-solvent is needed to induce early gelation and formation of large particles with higher mechanical stability.

Synthesis of RLF gels was also successful with non-soluble HL. Agglomerates were incorporated into the polymer network. The role of the solvent system is even more relevant because presence and degree of swelling of agglomerates control mechanical properties of the resulting gels.

DMSO/H₂O proved to be the best solvent system for HL. A DoE study showed that lower acid and formaldehyde concentrations would not impact the gel to a larger extent. Obtained gels from formulations in DMSO/H₂O had low densities after ambient solvent evaporation and showed high compressive strength. Scale-Up allowed production of

monolithic gels with sizes of 15x15x3 cm. The chosen simple reaction setup is also promising for further scale-up. Acid catalysis in combination with suitable solvent system enables drying by solvent evaporation. This facilitates inexpensive production on a large scale.

A wide range of morphologies is accessible with RLF gels with lignin from diverse sources. This gives a variety of potential applications for these materials. High mechanical strength and fine pore structure are mutually exclusive to some extent. Nonetheless, detailed understanding of structure-properties relation for RLF gels allows for tailored properties. RLF gels therefore present a bio-based alternative for many materials and promote the shift from fossil to renewable resources.

5 Conclusions

The change from a fossil to a renewable feedstock is inevitable to prevent complete depletion of resources. This work has shown that lignin has the promise to make an important contribution to this change.

Oxypropylation is a very relevant modification for the valorization of lignin because its implementation into existing infrastructure is simple. The setup is very similar to the production of PPG, thus easy adaption of existing facilities would enable them to fit the needs of lignin modification.

Oxypropylation of lignin has been studied in detail in the past but determining factors for the success of the functionalization were not comprehensively understood. Multiple options for the catalyst as well as the combination of PO and cPC presented in this thesis expand the toolbox for oxypropylation. The versatility of this process is thereby amplified further. Amidine catalysts are a worthwhile topic for continuing research. Long reaction times may be less profitable, but resulting polyols with high lignin content raise the overall fraction of renewable resources in the product. Residual amidine in the polyol could also be suitable as catalyst for subsequent PU synthesis.

RLF aerogels were shown to be as versatile as their analogs made from fossil-based resources. The significance of this material is promoted by the fact that no chemical modification of lignin is necessary for this application.

The solvent in reactive formulations for gel preparation turned out to be the crucial factor for material properties. Analysis of solubility of a given lignin is a simple task compared to structural characterization on a molecular level. A small change in lignin properties could therefore be analyzed and compensated easily. This fact might help to produce lignin-based materials even while the production of lignin with unchanged properties is not yet possible on an industrial scale.

Formulations containing non-dissolved lignin can be used to generate gels, but size and morphology of the remaining agglomerates puts limits on the material properties. However, simple mechanical methods like sieving and milling of lignin could adjust lignin particles to a desired size. This approach would expand the fields of application without the need for extensive chemical modification.

Valorization of lignin has been a research topic for more than 50 years, yet no commercial product has been developed up to date. This fact could be interpreted as an indicator that it is not possible to obtain lignin-based materials in an economical way. However, growing knowledge and advancing technologies open up new pathways and help overcome existing obstacles. The growing need for a sustainable feedstock highlights once more the high potential of lignin as a resource. Only with continuing research the goal of lignin valorization in polymeric materials can be reached.

6 Experimental Details

6.1 Materials

Lignins

The lignins used in this work were provided and characterized as part of the research project POLIGOM (Porous Lignous Organic Materials - Hochporöse Ligninmaterialien).

The different lignins were extracted from different sources: OSL from hard wood, HL and KL from soft wood and SL from wheat straw. The molecular weight, ash content and OH group content is given in Table 9.

Table 9. Molecular weight, ash content and OH group content of different lignin used.

	OSL	HL	KL	SL
M_n [g·mol ⁻¹]	3200	3000	3300	2900
M_w [g·mol ⁻¹]	5700	5200	11700	8800
Ash content [%]	0.1	0.2	0.1	2.8
arom. OH [mmol·g ⁻¹]	3.3	2.8	2.5	1.2
total OH [mmol·g ⁻¹]	5	4.8	3.4	2.2

Other Chemicals

All chemicals were obtained from commercial sources and used without purification. Technical grade solvents were used.

6.2 Oxypropylation of Lignin

Oxypropylation of lignin with propylene oxide

Lignin was stored in an oven at 65° C overnight before use. It was placed in a 450 mL stainless steel autoclave (Parr Instrument GmbH, Moline, IL, USA, Figure 50).



Figure 50. Autoclave reactor used for oxypropylation of lignin.

A given amount of catalyst was added. The reactor was closed and the inside was purged with argon three times. After the third time a pressure of 1 bar was set. The desired amount of propylene oxide was added via a HPLC pump (Bischoff Chromatography, HPD Multitherm 200, Bischoff Chromatography, Leonberg, Germany) with a flow rate of 5 mL·min⁻¹. After stirring for 10 minutes the reactor was heated to 160° C. Pressure

and temperature were recorded via ProfiSignal 2.2 (Delphin Technology AG, Bergisch Gladbach, Germany). After completion of the reaction the heating source was removed, the reactor was cooled down to room temperature and the liquid product was removed.

Homopolymer Extraction

PPG homopolymer was removed from the crude reaction product by extraction. The crude reaction product was placed in a flask, a 10-fold amount of hexane was added and heated to 75 °C. After 15 minutes of stirring under reflux the hot hexane was decanted. The procedure was repeated three times. The solid lignin fraction was dried overnight in a vacuum oven at 40 °C. Hexane was removed from the liquid fraction by evaporation at reduced pressure, yielding the homopolymer as a viscous yellow liquid.

Characterization of lignin fraction

Grafting of PO on lignin was confirmed by FTIR analysis of isolated lignin fraction according to literature.^[61] Several changes were identified. Introduction of CH₃, CH₂ and CH groups caused an increase of the C-H stretching bands between 2800 – 3000 cm⁻¹. The C-O stretching at 1000 – 1100 cm⁻¹ can be explained by the introduction of ether groups and the band at 1371 cm⁻¹ corresponds to the added CH₃ groups.

Oxypropylation of lignin with propylene carbonate

Lignin and catalyst were dissolved in cPC in a round bottom flask. The reaction mixture was heated to 170 °C and stirred under reflux. After a given reaction time the mixture was cooled to room temperature and dispersed in diluted HCl with pH 4. The solid residue was filtered, redispersed in excess amount of H₂O and stirred overnight. After filtration the solid product was washed with H₂O and dried in a vacuum oven at 40 °C. If residual cPC was detected via FTIR the washing step was repeated.

Calculation of average degree of polymerization per OH group

The average number of repeating units per OH group was calculated based on ^1H NMR spectra of the oxypropylated lignins. An exemplary calculation is given for the oxypropylation product of OSL with 5 wt% KOtBu (Figure 51).

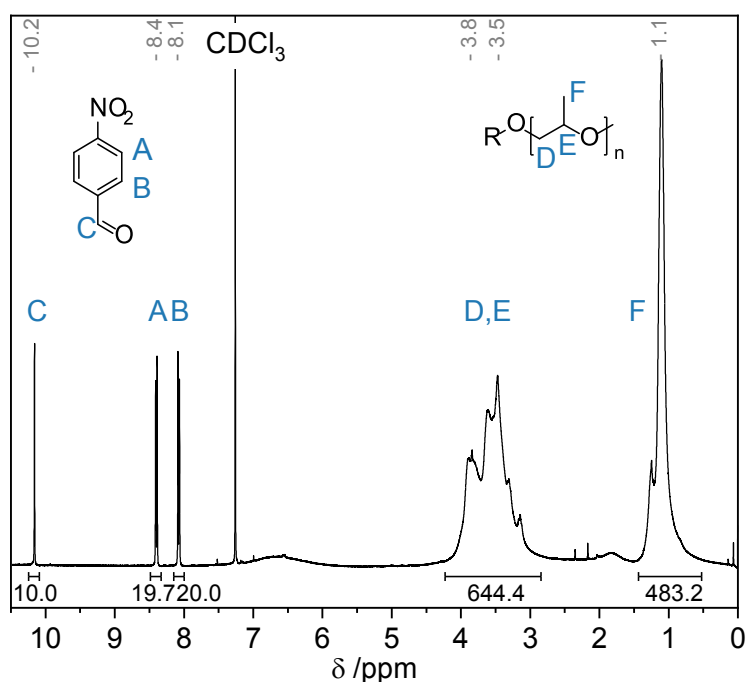


Figure 51. ^1H NMR spectrum of oxypropylated OSL with 4-Nitrobenzaldehyde as internal standard for the calculation of average DP per OH group.

$9.9 \cdot 10^{-3}$ mmol 4-Nitrobenzaldehyde were added as internal standard. The signal of the aldehyde proton (C) at 10.2 ppm was used as reference and set to an integral value of 10.

This allows to calculate the integral value $I_{1\text{mmol H}}$ of 1 mmol H:

$$I_{1\text{mmol H}} = \frac{I_{\text{Aldehyde}}}{n_{\text{Aldehyde}}} = \frac{10}{9.9 \cdot 10^{-3} \text{ mmol}} = 1010 \text{ mmol}^{-1}$$

The amount of substance of methyl groups n_{CH_3} in the sample can be calculated from the integral of the CH_3 group (F) at 1.1 ppm.

$$n_{\text{CH}_3} = \frac{1}{I_{1\text{mmol H}}} \cdot \left(\frac{I_{\text{CH}_3}}{3} \right) = \frac{1}{1010 \text{ mmol}^{-1}} \cdot \left(\frac{483.2}{3} \right) = 0.16 \text{ mmol}$$

Considering the sample weight and the amount of OH groups $n_{OH/mg}$ in OSL determined before as $5.1 \cdot 10^{-3} \text{ mmol} \cdot \text{mg}^{-1}$, the total amount of substance of OH groups in the sample can be calculated.

$$n_{OH} = n_{OH/mg} \cdot m_{sample} = 5.1 \cdot 10^{-3} \text{ mmol} \cdot \text{mg}^{-1} \cdot 10.2 \text{ mg} = 5.2 \cdot 10^{-2} \text{ mmol}$$

The amount of. This leads to the average DP per OH \overline{DP}_{OH} group to be calculated as

$$\overline{DP}_{OH} = \frac{n_{CH_3}}{n_{OH}} = \frac{0.16 \text{ mmol}}{5.2 \cdot 10^{-2} \text{ mmol}} = 3.1$$

6.3 Preparation of RLF Aerogels

General procedure

A given amount of resorcinol (R) and lignin (L) were placed in a 90 mL polypropylene sample tub with snap-on lid. Solvents and catalyst (C) were added, and the tub was placed on a shaker until a homogeneous mixture was obtained. Then the tub was placed in a H₂O bath for 30 minutes to heat the reaction mixture to the desired temperature. To start the reaction formaldehyde solution was added followed by thoroughly shaking the reaction mixture. The tub was kept in the H₂O bath until the gelation was complete.

The gelation was evaluated visually. The recorded gelation time was the time at which a gel could be gently tilted without causing a visible change to the meniscus.

If not indicated otherwise the total amount of resorcinol and lignin was 4.0 g. The lignin content described the amount of resorcinol in *wt%* that was replaced by lignin. Molar ratios of monomers to catalyst (M/C) and monomers to formaldehyde (M/F) were calculated assuming that only resorcinol was used.

The reactive content RC was calculated according to the following equation:

$$RC = \frac{m(R) + m(L) + m(F) + m(C)}{m(\text{solvents})}$$

Fully gelled gels in the closed tub where placed in an oven at 65° C overnight for aging. After cooling, the gels where rinsed 3 times with the solvents used and then removed from the tub.

Gel synthesis in solutions with increased viscosity

A solution with 0.2 wt% agar was prepared by dissolving a given amount of agar in demineralized water and boiling it for 5 minutes. It was cooled to room temperature before use.

The agar solution was used instead of H₂O in the preparation of RLF gels. The procedure was identical to the one described before.

Scale-Up

A given amount of lignin, resorcinol, catalyst and solvent were placed in a 1 L wide mouth bottle made from polypropylene. The bottle was placed on a shaker for homogenization. Then it was heated for 30 minutes in a H₂O bath. The reaction was started by addition of formaldehyde. The mixture was kept in the H₂O bath and stirred periodically. Five minutes before gelation (as determined in a previous experiment on a small scale) the reaction mixture was poured into a square box made from high density polyethylene with lid. The box was placed in an oven at 65 °C until full gelation occurred.

Solvent exchange and Drying

The gels were removed from the mold and washed with excess solvent. Then they were wrapped in filter paper and placed in a solvent bath overnight. The ratio of solvents in the bath was varied stepwise from the synthesis mixture to the pure solvent (EtOH or acetone).

Drying with supercritical CO₂ was carried out by the working group of Prof. Dr. I. Smirnova in the Institute for Thermal Separation Processes at Technical University Hamburg-Harburg. The procedure was adapted from previously published literature.^[205]

Solubility test

500 mg OSL were dissolved in 3.00 g of solvent. Mixtures of EtOH/H₂O and acetone/H₂O were used. The ratio of the two components was 40/60, 50/50 and 60/40 (*wt/wt*). Experiments were carried out in headspace crimp vials with septum. All samples were stored overnight on a shaker. After sedimentation of non-dissolved lignin, both fractions were separated by decantation. After complete removal of solvent at elevated temperature the amount of both fractions was determined gravimetrically. Each experiment was carried out three times.

Design of Experiments

Design of Experiments was performed following a Response Surface Model. Software DesignExpert12 was used to set up the experimental plan and evaluate the results. 2FI model with linear fit between 0 and 1500 min was used for gelation time. A quadratic model with linear fit between 0 % and 100 % was used for shrinkage. A quadratic model with linear fit between 0 and 6 was used for overall gel quality.

6.4 Sample Characterization

Scanning Electron Microscopy

Samples were coated with carbon using a Leica ACE600 prior to analysis with a LEO 1525 Gemini scanning electron microscope. Micrographs were recorded with an acceleration voltage of 5 kV.

¹H Nuclear Magnetic Resonance Spectroscopy

¹H NMR spectra were recorded using BRUKER spectrometers (Advance III 400 MHz, Advance I 500 MHz). For standard samples 16 scans and a delay time of 1 s was used, for polymer samples 64 scans and 3 s delay time. Sample concentrations were about 15mg mL⁻¹, CDCl₃ was used as solvent. The solvent signal was used as a reference.

Fourier-Transfer Infrared Spectroscopy

FT-IR spectra were recorded using a BRUKER Vertex-70 spectrometer. For each sample, 32 scans were performed in a range of 400 cm^{-1} to 4000 cm^{-1} .

Size Exclusion Chromatography

For the determination of the molecular weight distributions Size Exclusion Chromatography (SEC) measurements were performed. The equipment includes a RI 2012 RI detector (Schambeck) and a 1050 series UV detector (254 nm, HP), an AS1000 auto sampler (Thermo separation products), two pumps (AI-12 pump, FLOM and LC-10Atyp pump, Schimadzu) and a styrene-divinylbenzene GPC linear column with a particle size of 5 μm . The eluent THF was pumped at a flow rate of 1 mL/min. The samples were dissolved in THF at a concentration of approximately 1.5 mg/mL, of which 20 μL were injected. The temperature was room temperature. The software Chromatographica V1.0.25 was used for evaluation of the measurement data.

Viscosity Measurement

Viscosity measurements were conducted with Discovery Hybrid Rheometer DHR-2 (TA Instruments). A 60 mm steel cone with an angle of 2° and a steel Peltier plate were used as geometry and the gap was set to 50 μm . A sample volume of around 2 mL per measurement was used. Measurements were done at 25 $^\circ\text{C}$ and an oscillation frequency of 1 rad s^{-1} .

Rheological measurement of gelation onset time

Measurements of gelation onset time were conducted with Discovery Hybrid Rheometer DHR-2 (TA Instruments). A 25 mm parallel plate geometry made from aluminum was used. A Peltier plate was used to control the geometry temperature. The gap was set to 700 μm . A time sweep experiment was performed with an oscillation frequency of 6.2 rad s^{-1} and a strain of 0.2%.

Given amounts of lignin, resorcinol and catalyst were dissolved in 2 mL of a mixture of EtOH/H₂O and mixed on a shaker for 30 minutes. Formaldehyde was added to start the

reaction and the sample was placed on the geometry. Eight minutes after addition of formaldehyde the Peltier plate was heated to 40 °C and the measurement was started.

Compression test

Compression tests were performed with a Zwick Roell Z1.0 and evaluated with the software TestExpert. A pre-load of 2 kPa was used and the test speed was 10 mm/min.

Measurements performed by other working groups





Analysis of different lignins by ^{31}P NMR spectroscopy and determination of OH content was done by the working group of Prof. Dr. F. Liebner at Institute of Chemistry of Renewable Resources, University of Natural Resources and Life Sciences, Vienna.


















BET surface analysis and calculation of porosity as well as determination of thermal conductivity via the Hot Disk method were performed by the working group of Prof. Dr. I. Smirnova in the Institute for Thermal Separation Processes at Technical University Hamburg-Harburg.

Chemicals and Safety

The chemicals that were used in this work are listed in Table 10 together with their GHS-Pictograms, Hazard- and Precautionary-Statements and commercial source.

Table 10. Used chemicals, their Hazard- and Precautionary-Statements.

Substance	GHS-Pictograms	Hazard-Statements	Precautionary-Statements	Source
1,8-Diazabicyclo[5.4.0]undec-7-en		301, 314, 412, 290	273, 280, 201+310+330, 301+330+331, 303+351+338	TCI
Acetone		225, 319, 336	210, 240, 305+351+338, 403+233	VMP
Argon		280	403	99.999%, Praxair Deutschland GmbH
Citric Acid		319, 335	261, 264, 271, 280, 304+340+312, 305+351+338	Grüssing GmbH
Dimethylsulfoxid	Not classified as hazardous according to GHS			VWR / Grüssing GmbH

Substance	GHS-Pictograms	Hazard-Statements	Precautionary-Statements	Source
Ethanol	 	224, 319	210, 240, 305+351+338, 403+233	VMP
Formaldehyde (37% in H ₂ O)	  	301+311+331, 314, 317, 335, 341, 350, 370	201, 208, 301+330+331, 303+361+353, 304+340, 305+351+338, 308+310	Sigma Aldrich
Lupranol 1200	Not classified as hazardous according to GHS.			BASF SE
<i>n</i> -Hexane	   	225, 304, 315, 336, 361f, 373, 411	201, 210, 273, 301+330+331, 302+352, 308+313	Chemsolute
Potassium Hydroxide	 	290, 302, 314	234, 260, 280, 301+312, 303+361+353, 305+351+338	Merck KGaA
Potassium <i>tert</i> -Butoxide	 	228, 252, 314 EUH014	405	Acros Organics
Propylene Carbonate		319	305+351+338	Alfa Aesar
Propylene Oxide	  	224, 302, 311+331, 315, 319, 335, 340, 350	201, 210, 280, 302+352+312, 308+313, 403+233	99.9%, GHC Gerling, Holz & Co.




Substance	GHS-Pictograms	Hazard-Statements	Precautionary-Statements	Source
Resorcinol		302, 315, 317, 318, 370, 371, 410	273, 280, 301+312, 302+352, 305+351+338, 308+311	Sigma Aldrich
Sodium Carbonate		319	305+351+338	Merck KGaA
Sulfuric Acid 96%		290, 314	280, 301+330+331, 303+361+353, 305+351+338+310	VWR International GmbH

Table 11. Used carcinogenic and mutagenic substances and substances toxic for reproduction.

Substance	Hazard-Statements	CMR-Classification	Amount
Chloroform-D (solvent for NMR)	302, 315, 350, 373	1B (C)	100 x 0.7 mL
Formaldehyde (reactant)	301+311+331, 314, 317, 335, 341, 350, 370	1B (C)	500 x < 5 mL 50 x < 150 mL
Propylene Oxide (reactant)	24, 302, 311+331, 315, 319, 335, 340, 350	1B (M. C)	40 x < 45 mL

References

- [1] M. K. Hubbert, in *Am. Pet. Institute, Drill. Prod. Pract.*, San Antonio, **1956**, pp. 7–25.
- [2] U. Bardi, *Energy Res. Soc. Sci.* **2019**, *48*, 257–261.
- [3] A. J. Ragauskas, C. K. Williams, B. H. Davison, G. Britovsek, J. Cairney, C. A. Eckert, W. J. Frederick, J. P. Hallett, D. J. Leak, C. L. Liotta, J. R. Mielenz, R. Murphy, R. Templer, T. Tschaplinski, *Science* (80-.). **2006**, *311*, 484–489.
- [4] Y. Zhu, C. Romain, C. K. Williams, *Nature* **2016**, *540*, 354–362.
- [5] R. C. Thompson, C. J. Moore, F. S. vom Saal, S. H. Swan, *Philos. Trans. R. Soc. B Biol. Sci.* **2009**, *364*, 2153–2166.
- [6] D. K. Schneiderman, M. A. Hillmyer, *Macromolecules* **2017**, *50*, 3733–3749.
- [7] A. Gandini, T. M. Lacerda, *Prog. Polym. Sci.* **2015**, *48*, 1–39.
- [8] A. Gandini, *Macromolecules* **2008**, *41*, 9491–9504.
- [9] E. Commission, J. R. Centre, S. Nessi, T. Sinkko, C. Bulgheroni, P. Garcia-Gutierrez, J. Giuntoli, A. Konti, E. Sanye-Mengual, D. Tonini, R. Pant, L. Marelli, F. Ardente, *Life Cycle Assessment (LCA) of Alternative Feedstocks for Plastics Production. Part 1, the Plastics LCA Method*, Publications Office Of The European Union, **2021**.
- [10] Plastics Europe, “Plastics - the Facts 2022,” can be found under <https://plasticseurope.org/de/knowledge-hub/plastics-the-facts-2022/>, **2022**.
- [11] J. H. Lora, W. G. Glasser, *J. Polym. Environ.* **2002**, *10*, 39–48.
- [12] S. Laurichesse, L. Avérous, *Prog. Polym. Sci.* **2014**, *39*, 1266–1290.
- [13] E. Ten, W. Vermerris, *J. Appl. Polym. Sci.* **2015**, *132*, app.42069.
- [14] B. M. Upton, A. M. Kasko, *Chem. Rev.* **2016**, *116*, 2275–2306.
- [15] W. G. Glasser, *Front. Chem.* **2019**, *7*, DOI 10.3389/fchem.2019.00565.
- [16] M. S. Ganewatta, H. N. Lokupitiya, C. Tang, *Polymers (Basel)*. **2019**, *11*, 1176.
- [17] Z. Strassberger, S. Tanase, G. Rothenberg, *RSC Adv.* **2014**, *4*, 25310–25318.
- [18] P. C. A. Bruijninx, R. Rinaldi, B. M. Weckhuysen, *Green Chem.* **2015**, *17*, 4860–4861.
- [19] C. Li, X. Zhao, A. Wang, G. W. Huber, T. Zhang, *Chem. Rev.* **2015**, *115*, 11559–11624.
- [20] S. Fernando, S. Adhikari, C. Chandrapal, N. Murali, *Energy & Fuels* **2006**, *20*, 1727–1737.
- [21] J. E. Holladay, J. F. White, J. J. Bozell, D. Johnson, *Top Value-Added Chemicals from Biomass - Volume II—Results of Screening for Potential Candidates from Biorefinery Lignin*, Richland, WA (United States), **2007**.
- [22] A. J. Ragauskas, G. T. Beckham, M. J. Biddy, R. Chandra, F. Chen, M. F. Davis, B. H. Davison, R. A. Dixon, P. Gilna, M. Keller, P. Langan, A. K. Naskar, J. N. Saddler, T. J. Tschaplinski, G. A. Tuskan, C. E. Wyman, *Science* (80-.). **2014**, *344*, DOI 10.1126/science.1246843.
- [23] F. H. M. Graichen, W. J. Grigsby, S. J. Hill, L. G. Raymond, M. Sanglard, D. A. Smith, G. J. Thorlby, K. M. Torr, J. M. Warnes, *Ind. Crops Prod.* **2017**, *106*, 74–85.
- [24] A. Behr, T. Seidensticker, in *Einführung Die Chemie Nachwachsender Rohstoffe*, Springer Berlin Heidelberg, Berlin, Heidelberg, **2018**, pp. 201–216.
- [25] K. Freudenberg, A. Janson, E. Knopf, A. Haag, *Berichte der Dtsch. Chem. Gesellschaft (A B Ser.* **1936**, *69*, 1415–1425.
- [26] S. Sharma, A. Kumar, *Lignin*, Springer International Publishing, Cham, **2020**.
- [27] L. Serrano, R. Luque, B. F. Sels Editors, *Lignin Chemistry*, Springer International Publishing, Cham, **2020**.
- [28] C. F. Dahl, *Process of Manufacturing Cellulose from Wood*, **1884**, US296935A.
- [29] A. Behr, T. Seidensticker, in *Chem. Renewables*, Springer Berlin Heidelberg, Berlin, Heidelberg, **2020**, pp. 143–160.

- [30] A. Gandini, M. N. Belgacem, *Monomers, Polymers and Composites from Renewable Resources*, Elsevier, **2008**.
- [31] M. D. Kärkäs, B. S. Matsuura, T. M. Monos, G. Magallanes, C. R. J. Stephenson, *Org. Biomol. Chem.* **2016**, *14*, 1853–1914.
- [32] T. N. Kleinert, *Organosolv Pulping and Recovery Process*, **1971**, US3585104A.
- [33] H. Haridevan, D. A. C. Evans, A. J. Ragauskas, D. J. Martin, P. K. Annamalai, *Green Chem.* **2021**, *23*, 8725–8753.
- [34] A. Tribot, G. Amer, M. Abdou Alio, H. de Baynast, C. Delattre, A. Pons, J.-D. Mathias, J.-M. Callois, C. Vial, P. Michaud, C.-G. Dussap, *Eur. Polym. J.* **2019**, *112*, 228–240.
- [35] L. Dessbesell, M. Paleologou, M. Leitch, R. Pulkki, C. (Charles) Xu, *Renew. Sustain. Energy Rev.* **2020**, *123*, 109768.
- [36] M. Kienberger, S. Maitz, T. Pichler, P. Demmelmayr, *Processes* **2021**, *9*, 804.
- [37] M. Alinejad, C. Henry, S. Nikafshar, A. Gondaliya, S. Bagheri, N. Chen, S. K. Singh, D. B. Hodge, M. Nejad, *Polymers (Basel)*. **2019**, *11*, DOI 10.3390/polym11071202.
- [38] M. Witzler, A. Alzagameem, M. Bergs, B. El Khaldi-Hansen, S. E. Klein, D. Hielscher, B. Kamm, J. Kreyenschmidt, E. Tobiasch, M. Schulze, *Molecules* **2018**, *23*, 1885.
- [39] R. Liu, L. Dai, C. Xu, K. Wang, C. Zheng, C. Si, *ChemSusChem* **2020**, *13*, 4266–4283.
- [40] J. L. Espinoza-Acosta, P. I. Torres-Chávez, J. L. Olmedo-Martínez, A. Vega-Rios, S. Flores-Gallardo, E. A. Zaragoza-Contreras, *J. Energy Chem.* **2018**, *27*, 1422–1438.
- [41] H. Liu, T. Xu, K. Liu, M. Zhang, W. Liu, H. Li, H. Du, C. Si, *Ind. Crops Prod.* **2021**, *165*, 113425.
- [42] V. K. Thakur, M. K. Thakur, *Int. J. Biol. Macromol.* **2015**, *72*, 834–847.
- [43] A. Duval, M. Lawoko, *React. Funct. Polym.* **2014**, *85*, 78–96.
- [44] P. Jędrzejczak, M. N. Collins, T. Jesionowski, Ł. Klapiszewski, *Int. J. Biol. Macromol.* **2021**, *187*, 624–650.
- [45] J. Zakzeski, P. C. A. Bruijninx, A. L. Jongerius, B. M. Weckhuysen, *Chem. Rev.* **2010**, *110*, 3552–3599.
- [46] Z. Sun, B. Fridrich, A. de Santi, S. Elangovan, K. Barta, *Chem. Rev.* **2018**, *118*, 614–678.
- [47] M. P. Pandey, C. S. Kim, *Chem. Eng. Technol.* **2011**, *34*, 29–41.
- [48] V. K. Thakur, M. K. Thakur, P. Raghavan, M. R. Kessler, *ACS Sustain. Chem. Eng.* **2014**, *2*, 1072–1092.
- [49] S. Sen, S. Patil, D. S. Argyropoulos, *Green Chem.* **2015**, *17*, 4862–4887.
- [50] A. Eraghi Kazzaz, Z. Hosseinpour Feizi, P. Fatehi, *Green Chem.* **2019**, *21*, 5714–5752.
- [51] H. Liu, H. Chung, *J. Polym. Sci. Part A Polym. Chem.* **2017**, *55*, 3515–3528.
- [52] A. Vishtal, A. Kraslawski, *BioResources* **2011**, *6*, 3547–3568.
- [53] W. Glasser, R. Loos, B. Cox, N. Cao, *TAPPI J.* **2017**, *16*, 111–121.
- [54] J. Karthäuser, V. Biziks, C. Mai, H. Militz, *Molecules* **2021**, *26*, 2533.
- [55] Borregaard, “Lignin Products,” can be found under <https://www.borregaard.com/product-areas/lignin/>, **2023**.
- [56] UPM, “BioPiva,” can be found under <https://www.upmbiochemicals.com/lignin-solutions/products/UPM-BioPiva-product-family/>, **2023**.
- [57] R. V. Gadhave, P. A. Mahanwar, P. T. Gadekar, *Open J. Polym. Chem.* **2018**, *08*, 1–10.
- [58] X. Ma, J. Chen, J. Zhu, N. Yan, *Macromol. Rapid Commun.* **2021**, *42*, 2000492.
- [59] F. R. Vieira, S. Magina, D. V. Evtuguin, A. Barros-Timmons, *Materials (Basel)*. **2022**, *15*, 6182.
- [60] K. Kurple, *Lignin Based Polyols*, **1996**, US 602542A.
- [61] C. A. Cateto, M. F. Barreiro, A. E. Rodrigues, M. N. Belgacem, *Ind. Eng. Chem. Res.* **2009**, *48*, 2583–2589.
- [62] X. Pan, J. N. Saddler, *Biotechnol. Biofuels* **2013**, *6*, 1–10.
- [63] A. N. Hayati, D. A. C. Evans, B. Laycock, D. J. Martin, P. K. Annamalai, *Ind. Crops Prod.*

- 2018**, *117*, 149–158.
- [64] S. Luo, L. Gao, W. Guo, *J. Wood Sci.* **2020**, *66*, 23.
- [65] A. Gondaliya, M. Nejad, *Molecules* **2021**, *26*, 2302.
- [66] H. Haridevan, M. S. McLaggan, D. A. C. Evans, D. J. Martin, T. Seaby, Z. Zhang, P. K. Annamalai, *ACS Appl. Polym. Mater.* **2021**, *3*, 3528–3537.
- [67] C. A. Cateto, M. F. Barreiro, C. Ottati, M. Lopretti, A. E. Rodrigues, M. N. Belgacem, *J. Cell. Plast.* **2014**, *50*, 81–95.
- [68] P. Cinelli, I. Anguillesi, A. Lazzeri, *Eur. Polym. J.* **2013**, *49*, 1174–1184.
- [69] N. Mahmood, Z. Yuan, J. Schmidt, M. Tymchyshyn, C. Xu, *Green Chem.* **2016**, *18*, 2385–2398.
- [70] M. F. Sonnenschein, *Polyurethanes*, John Wiley & Sons, Inc, Hoboken, NJ, **2014**.
- [71] D. M. Simons, J. J. Verbanc, *J. Polym. Sci.* **1960**, *44*, 303–311.
- [72] E. C. Steiner, R. R. Pelletier, R. O. Trucks, *J. Am. Chem. Soc.* **1964**, *86*, 4678–4686.
- [73] J. Herzberger, K. Niederer, H. Pohlit, J. Seiwert, M. Worm, F. R. Wurm, H. Frey, *Chem. Rev.* **2016**, *116*, 2170–2243.
- [74] M. Ionescu, *Chemistry and Technology of Polyols for Polyurethanes*, Rapra Technology Limited, **2005**.
- [75] J. Milgrom, *Method of Making a Polyether Using a Double Metal Cyanide Complex Compound*, **1966**, US 3278457 A.
- [76] L.-K. Bi, *Polyether-Containing Double Metal Cyanide Catalysts*, **1997**, US 5637673 A.
- [77] I. Kim, J.-T. Ahn, C. S. Ha, C. S. Yang, I. Park, *Polymer (Guildf)*. **2003**, *44*, 3417–3428.
- [78] C. Pavier, A. Gandini, *Ind. Crops Prod.* **2000**, *12*, 1–8.
- [79] J. P. S. Aniceto, I. Portugal, C. M. Silva, *ChemSusChem* **2012**, *5*, 1358–1368.
- [80] B. Ahvazi, O. Wojciechowicz, T. M. Ton-That, J. Hawari, *J. Agric. Food Chem.* **2011**, *59*, 10505–10516.
- [81] L. C. -. Wu, W. G. Glasser, *J. Appl. Polym. Sci.* **1984**, *29*, 1111–1123.
- [82] H. Nadji, C. Bruzzè, M. N. Belgacem, A. Benaboura, A. Gandini, *Macromol. Mater. Eng.* **2005**, *290*, 1009–1016.
- [83] Y. Li, A. J. Ragauskas, *J. Wood Chem. Technol.* **2012**, *32*, 210–224.
- [84] C. Pavier, A. Gandini, *Carbohydr. Polym.* **2000**, *42*, 13–17.
- [85] R. G. Arnold, J. A. Nelson, J. J. Verbanc, *Chem. Rev.* **1957**, *57*, 47–76.
- [86] L. D. Antonino, J. R. Gouveia, R. R. de Sousa Júnior, G. E. S. Garcia, L. C. Gobbo, L. B. Tavares, D. J. dos Santos, *Molecules* **2021**, *26*, 2131.
- [87] W. G. Glasser, C. A. Barnett, T. G. Rials, V. P. Saraf, *J. Appl. Polym. Sci.* **1984**, *29*, 1815–1830.
- [88] J. A. Pinto, I. P. Fernandes, V. D. Pinto, E. Gomes, C. F. Oliveira, P. C. R. C. R. Pinto, L. M. R. Mesquita, P. A. G. Piloto, A. E. Rodrigues, M.-F. Barreiro, *Energies* **2021**, *14*, 3825.
- [89] M. Wu, J.-J. Peng, Y.-M. Dong, J.-H. Pang, X.-M. Zhang, *RSC Adv.* **2022**, *12*, 21736–21741.
- [90] A. Arshanitsa, A. Paberza, L. Vevere, U. Cabulis, G. Telysheva, *AIP Conf. Proc.* **2014**, *1593*, 388–391.
- [91] B. Berrima, G. Mortha, S. Boufi, E. El Aloui, M. Naceur Belgacem, *Cellul. Chem. Technol. Cellul. Chem. Technol* **2016**, *50*, 941–950.
- [92] M. Kurańska, J. A. Pinto, K. Salach, M. F. Barreiro, A. Prociak, *Ind. Crops Prod.* **2020**, *143*, 111882.
- [93] J. Perez-Arce, A. Centeno-Pedrazo, J. Labidi, J. R. Ochoa-Gómez, E. J. Garcia-Suarez, *Polym. Chem.* **2020**, *11*, 7362–7369.
- [94] J. Perez-Arce, A. Centeno-Pedrazo, J. Labidi, J. R. Ochoa-Gomez, E. J. Garcia-Suarez, *Polymers (Basel)*. **2021**, *13*, 651.
- [95] T. Sakakura, K. Kohno, *Chem. Commun.* **2009**, 1312.
- [96] B. Schäffner, F. Schäffner, S. P. Verevkin, A. Börner, *Chem. Rev.* **2010**, *110*, 4554–4581.

- [97] I. Kühnel, J. Podschun, B. Saake, R. Lehnen, *Holzforschung* **2015**, 69, 531–538.
- [98] I. Kühnel, B. Saake, R. Lehnen, *Ind. Crops Prod.* **2017**, 101, 75–83.
- [99] I. Kühnel, B. Saake, R. Lehnen, *React. Funct. Polym.* **2017**, 120, 83–91.
- [100] A. Duval, L. Avérous, *ACS Sustain. Chem. Eng.* **2017**, 5, 7334–7343.
- [101] F. R. Vieira, A. Barros-Timmons, D. V. Evtuguin, P. C. R. Pinto, *Holzforschung* **2020**, 74, 567–576.
- [102] F. R. Vieira, A. Barros-Timmons, D. V. Evtuguin, P. C. O. R. Pinto, *Materials (Basel)*. **2022**, 15, 1–17.
- [103] F. R. Vieira, N. V. Gama, D. V. Evtuguin, C. O. Amorim, V. S. Amaral, P. C. O. R. Pinto, A. Barros-Timmons, *Polymers (Basel)*. **2023**, 15, 1074.
- [104] D. E. Pearson, C. A. Buehler, *Chem. Rev.* **1974**, 74, 45–86.
- [105] F. R. Vieira, N. V. Gama, A. Barros-Timmons, D. V. Evtuguin, P. C. O. R. Pinto, *ChemEngineering* **2022**, 6, 95.
- [106] H. You, E. Wang, H. Cao, C. Zhuo, S. Liu, X. Wang, F. Wang, *Angew. Chemie Int. Ed.* **2022**, 61, DOI 10.1002/anie.202113152.
- [107] K. Schwetlick, *Organikum - Organisch-Chemisches Grundpraktikum*, Wiley-VCH Verlag, Weinheim, Germany, **2001**.
- [108] A. Duval, L. Avérous, *ACS Sustain. Chem. Eng.* **2016**, 4, 3103–3112.
- [109] J. Fricke, T. Tillotson, *Thin Solid Films* **1997**, 297, 212–223.
- [110] N. Hüsing, U. Schubert, *Angew. Chemie Int. Ed.* **1998**, 37, 22–45.
- [111] A. C. Pierre, G. M. Pajonk, *Chem. Rev.* **2002**, 102, 4243–4266.
- [112] M. Aegerter, N. Leventis, M. Koebel, *Aerogels Handbook*, Springer New York, New York, NY, **2011**.
- [113] S. S. Kistler, *Rubber Chem. Technol.* **1932**, 5, 600–603.
- [114] R. W. Pekala, *J. Mater. Sci.* **1989**, 24, 3221–3227.
- [115] S. Zhao, W. J. Malfait, N. Guerrero-Alburquerque, M. M. Koebel, G. Nyström, *Angew. Chemie Int. Ed.* **2018**, 57, 7580–7608.
- [116] J. V. Alemán, A. V. Chadwick, J. He, M. Hess, K. Horie, R. G. Jones, P. Kratochvíl, I. Meisel, I. Mita, G. Moad, S. Penczek, R. F. T. Stepto, *Pure Appl. Chem.* **2007**, 79, 1801–1829.
- [117] H. Freundlich, *Kapillarchemie : Eine Darstellung Der Chemie Der Kolloide Und Verwandter Gebiete*, Leipzig: Akad. Verlagsges., Leipzig, **1923**.
- [118] R. Baetens, B. P. Jelle, A. Gustavsen, *Energy Build.* **2011**, 43, 761–769.
- [119] P. C. Thapliyal, K. Singh, *J. Mater.* **2014**, 2014, 1–10.
- [120] J. Stergar, U. Maver, *J. Sol-Gel Sci. Technol.* **2016**, 77, 738–752.
- [121] Z. Ulker, C. Erkey, *J. Control. Release* **2014**, 177, 51–63.
- [122] A. Lukowiak, W. Strek, *J. Sol-Gel Sci. Technol.* **2009**, 50, 201–215.
- [123] C. Moreno-Castilla, F. J. Maldonado-Hódar, *Carbon N. Y.* **2005**, 43, 455–465.
- [124] H. Maleki, *Chem. Eng. J.* **2016**, 300, 98–118.
- [125] G. Gorgolis, C. Galiotis, *2D Mater.* **2017**, 4, 032001.
- [126] J.-H. Lee, S.-J. Park, *Carbon N. Y.* **2020**, 163, 1–18.
- [127] Aerogel Technologies, “Airloy Products,” can be found under <http://www.aerogeltechnologies.com/airloy/products/>, **2023**.
- [128] Aspen Aerogels, “Spaceloft,” can be found under <https://www.aerogel.com/product/spaceloft/>, **2023**.
- [129] Cabot, “Aerogel Products,” can be found under <https://www.cabotcorp.com/solutions/products-plus/aerogel>, **2023**.
- [130] R. J. White, N. Brun, V. L. Budarin, J. H. Clark, M.-M. Titirici, *ChemSusChem* **2014**, 7, 670–689.
- [131] L.-Y. Long, Y.-X. Weng, Y.-Z. Wang, *Polymers (Basel)*. **2018**, 10, 623.
- [132] K. J. De France, T. Hoare, E. D. Cranston, *Chem. Mater.* **2017**, 29, 4609–4631.

- [133] F. Zou, T. Budtova, *Carbohydr. Polym.* **2021**, 266, 118130.
- [134] C. A. García-González, M. Alnaief, I. Smirnova, *Carbohydr. Polym.* **2011**, 86, 1425–1438.
- [135] *The IUPAC Compendium of Chemical Terminology*, International Union Of Pure And Applied Chemistry (IUPAC), Research Triangle Park, NC, **2019**.
- [136] R. B. Perry, *J. Chem. Educ.* **1987**, 64, A328.
- [137] A. C. Pierre, *Introduction to Sol-Gel Processing*, Springer International Publishing, Cham, **2020**.
- [138] P. J. Flory, *J. Am. Chem. Soc.* **1941**, 63, 3083–3090.
- [139] J. M. Hammersley, *Math. Proc. Cambridge Philos. Soc.* **1957**, 53, 642–645.
- [140] A. Coniglio, H. E. Stanley, W. Klein, *Phys. Rev. Lett.* **1979**, 42, 518–522.
- [141] C. J. Brinker, G. W. Scherer, in *Sol-Gel Sci.*, Elsevier, **1990**, pp. 302–355.
- [142] R. W. Pekala, C. T. Alviso, F. M. Kong, S. S. Hulsey, *J. Non. Cryst. Solids* **1992**, 145, 90–98.
- [143] R. W. Pekala, F. M. Kong, *Le J. Phys. Colloq.* **1989**, 24, C4-33-C4-40.
- [144] R. W. Pekala, D. W. Schaefer, *Macromolecules* **1993**, 26, 5487–5493.
- [145] R. W. Pekala, C. T. Alviso, J. D. LeMay, *J. Non. Cryst. Solids* **1990**, 125, 67–75.
- [146] S. J. Taylor, M. D. Haw, J. Sefcik, A. J. Fletcher, *Langmuir* **2014**, 30, 10231–10240.
- [147] S. A. Al-Muhtaseb, J. A. Ritter, *Adv. Mater.* **2003**, 15, 101–114.
- [148] A. M. ElKhatat, S. A. Al-Muhtaseb, *Adv. Mater.* **2011**, 23, 2887–2903.
- [149] M. Prostředný, M. Abduljalil, P. Mulheran, A. Fletcher, *Gels* **2018**, 4, 36.
- [150] M. Wiener, G. Reichenauer, T. Scherb, J. Fricke, *J. Non. Cryst. Solids* **2004**, 350, 126–130.
- [151] F. Despetis, K. Barral, L. Kocon, J. Phalippou, *J. Sol-Gel Sci. Technol.* **2000**, 19, 829–831.
- [152] N. Job, A. Théry, R. Pirard, J. Marien, L. Kocon, J.-N. Rouzaud, F. Béguin, J.-P. Pirard, *Carbon N. Y.* **2005**, 43, 2481–2494.
- [153] D. W. Schaefer, R. Pekala, G. Beaucage, *J. Non. Cryst. Solids* **1995**, 186, 159–167.
- [154] T. Yamamoto, T. Nishimura, T. Suzuki, H. Tamon, *J. Non. Cryst. Solids* **2001**, 288, 46–55.
- [155] C. J. Gommès, A. P. Roberts, *Phys. Rev. E* **2008**, 77, 041409.
- [156] M. Prostředný, A. Fletcher, P. Mulheran, *RSC Adv.* **2019**, 9, 20065–20074.
- [157] X. Lu, M. C. Arduini-Schuster, J. Kuhn, O. Nilsson, J. Fricke, R. W. Pekala, *Science (80-.)*. **1992**, 255, 971–972.
- [158] X. Lu, R. Caps, J. Fricke, C. T. Alviso, R. W. Pekala, *J. Non. Cryst. Solids* **1995**, 188, 226–234.
- [159] G. C. Ruben, R. W. Pekala, T. M. Tillotson, L. W. Hrubesh, *J. Mater. Sci.* **1992**, 27, 4341–4349.
- [160] S.-W. Hwang, S.-H. Hyun, *J. Non. Cryst. Solids* **2004**, 347, 238–245.
- [161] D. Fairén-Jiménez, F. Carrasco-Marín, C. Moreno-Castilla, *Carbon N. Y.* **2006**, 44, 2301–2307.
- [162] S. Mulik, C. Sotiriou-Leventis, L. N. Leventis, *Chem. Mater.* **2007**, 19, 6138–6144.
- [163] M. Reuß, L. Ratke, *J. Sol-Gel Sci. Technol.* **2008**, 47, 74–80.
- [164] O. Barbieri, F. Ehrburger-Dolle, T. P. Rieker, G. M. Pajonk, N. Pinto, A. Venkateswara Rao, *J. Non. Cryst. Solids* **2001**, 285, 109–115.
- [165] S. Berthon, O. Barbieri, F. Ehrburger-Dolle, E. Geissler, P. Achard, F. Bley, A. M. Hecht, F. Livet, G. M. Pajonk, N. Pinto, A. Rigacci, C. Rochas, *J. Non. Cryst. Solids* **2001**, 285, 154–161.
- [166] C. I. Merzbacher, S. R. Meier, J. R. Pierce, M. L. Korwin, *J. Non. Cryst. Solids* **2001**, 285, 210–215.
- [167] R. Brandt, R. Petricevic, H. Pröbstle, J. Fricke, *J. Porous Mater.* **2003**, 10, 171–178.
- [168] J. Laskowski, B. Milow, L. Ratke, *Microporous Mesoporous Mater.* **2014**, 197, 308–315.
- [169] Z. Zhang, S. Zhao, G. Chen, J. Feng, J. Feng, Z. Yang, *Microporous Mesoporous Mater.* **2020**, 296, 109997.
- [170] M. Schwan, R. Tannert, L. Ratke, *J. Supercrit. Fluids* **2016**, 107, 201–208.

- [171] M. Schwan, M. Naikade, D. Raabe, L. Ratke, *J. Mater. Sci.* **2015**, *50*, 5482–5493.
- [172] C. Lin, J. A. Ritter, *Carbon N. Y.* **1997**, *35*, 1271–1278.
- [173] R. Tannert, M. Schwan, L. Ratke, *J. Supercrit. Fluids* **2015**, *106*, 57–61.
- [174] K. Barral, *J. Non. Cryst. Solids* **1998**, *225*, 46–50.
- [175] S. A. Letts, S. R. Buckley, F.-M. Kong, E. F. Lindsay, M. L. Sattler, *MRS Proc.* **1989**, *177*, 275.
- [176] S. M. Lambert, G. E. Overturf, G. Wilemski, S. A. Letts, D. Schroen-Carey, R. C. Cook, *J. Appl. Polym. Sci.* **1997**, *65*, 2111–2122.
- [177] N. Job, R. Pirard, J. Marien, J. P. Pirard, *Carbon N. Y.* **2004**, *42*, 619–628.
- [178] N. Job, F. Panariello, M. Crine, J. P. Pirard, A. Léonard, *Colloids Surfaces A Physicochem. Eng. Asp.* **2007**, *293*, 224–228.
- [179] E. J. Zanto, S. A. Al-Muhtaseb, J. A. Ritter, *Ind. Eng. Chem. Res.* **2002**, *41*, 3151–3162.
- [180] J. Wang, M. Glora, R. Petricevic, R. Saliger, H. Proebstle, J. Fricke, *J. Porous Mater.* **2001**, *8*, 159–165.
- [181] Z. Yang, J. Li, X. Xu, S. Pang, C. Hu, P. Guo, S. Tang, H.-M. M. Cheng, *J. Mater. Sci. Technol.* **2020**, *50*, 66–74.
- [182] R. Petričević, G. Reichenauer, V. Bock, A. Emmerling, J. Fricke, *J. Non. Cryst. Solids* **1998**, *225*, 41–45.
- [183] R. Saliger, V. Bock, R. Petricevic, T. Tillotson, S. Geis, J. Fricke, *J. Non. Cryst. Solids* **1997**, *221*, 144–150.
- [184] J. Feng, J. Feng, C. Zhang, *J. Sol-Gel Sci. Technol.* **2011**, *59*, 371–380.
- [185] N. Job, C. J. Gommers, R. Pirard, J. P. Pirard, *J. Non. Cryst. Solids* **2008**, *354*, 4698–4701.
- [186] R. Petričević, M. Glora, J. Fricke, *Carbon N. Y.* **2001**, *39*, 857–867.
- [187] D. Fairén-Jiménez, F. Carrasco-Marín, C. Moreno-Castilla, *Langmuir* **2008**, *24*, 2820–2825.
- [188] I. D. Alonso-Buenaposada, N. Rey-Raap, E. G. Calvo, J. Angel Menéndez, A. Arenillas, *J. Non. Cryst. Solids* **2015**, *426*, 13–18.
- [189] I. D. Alonso-Buenaposada, L. Garrido, M. A. Montes-Morán, J. A. Menéndez, A. Arenillas, *J. Sol-Gel Sci. Technol.* **2017**, *83*, 478–488.
- [190] Z. Gao, X. Lang, S. Chen, C. Zhao, *Energy & Fuels* **2021**, *35*, 18385–18395.
- [191] X. Gong, Y. Meng, J. Lu, Y. Tao, Y. Cheng, H. Wang, *Macromol. Chem. Phys.* **2022**, *223*, 2100434.
- [192] F. Chen, J. Li, *Adv. Mater. Res.* **2010**, *113–116*, 1837–1840.
- [193] F. Chen, M. Xu, L. Wang, J. Li, *BioResources* **2011**, *6*, 1262–1272.
- [194] *Production of Aerogels and Carbon Aerogels from Lignin*, **2018**, WO 2018/112092A.
- [195] C. D. Castro, G. C. Quintana, *Int. J. Polym. Sci.* **2015**, *2015*, 1–11.
- [196] P. Jöul, T. T. Ho, U. Kallavus, A. Konist, K. Leiman, O.-S. Salm, M. Kulp, M. Koel, T. Lukk, *Materials (Basel)*. **2022**, *15*, 2861.
- [197] B. S. Yang, K. Y. Kang, M. J. Jeong, *J. Korean Phys. Soc.* **2017**, *71*, 478–482.
- [198] L. I. Grishechko, G. Amaral-Labat, A. Szczurek, V. Fierro, B. N. Kuznetsov, A. Pizzi, A. Celzard, *Ind. Crops Prod.* **2013**, *41*, 347–355.
- [199] N. M. Mikova, V. A. Levdanskiy, Y. V. Mazurova, B. N. Kuznetsov, *Russ. J. Bioorganic Chem.* **2022**, *48*, 1506–1513.
- [200] I. Smirnova, et.al., “Abschlussbericht ‘Stoffliche Nutzung von Lignin: Nanoporöse Materialien,’” DOI 10.2314/GBV:1028935374can be found under <https://www.fnr.de/index.php?id=11150&fkz=22018312>, **2018**.
- [201] P. D. Brown, S. K. Gill, L. J. Hope-Weeks, *J. Mater. Chem.* **2011**, *21*, 4204.
- [202] M. Alshrah, M. P. Tran, P. Gong, H. E. Naguib, C. B. Park, *J. Colloid Interface Sci.* **2017**, *485*, 65–74.
- [203] M. J. Anderson, P. J. Whitcomb, *DOE Simplified*, Productivity Press, **2017**.
- [204] L. D. Hung Anh, Z. Pásztor, *J. Build. Eng.* **2021**, *44*, 102604.

- [205] C. A. García-González, M. C. Camino-Rey, M. Alnaief, C. Zetzl, I. Smirnova, *J. Supercrit. Fluids* **2012**, 66, 297–306.

Appendix

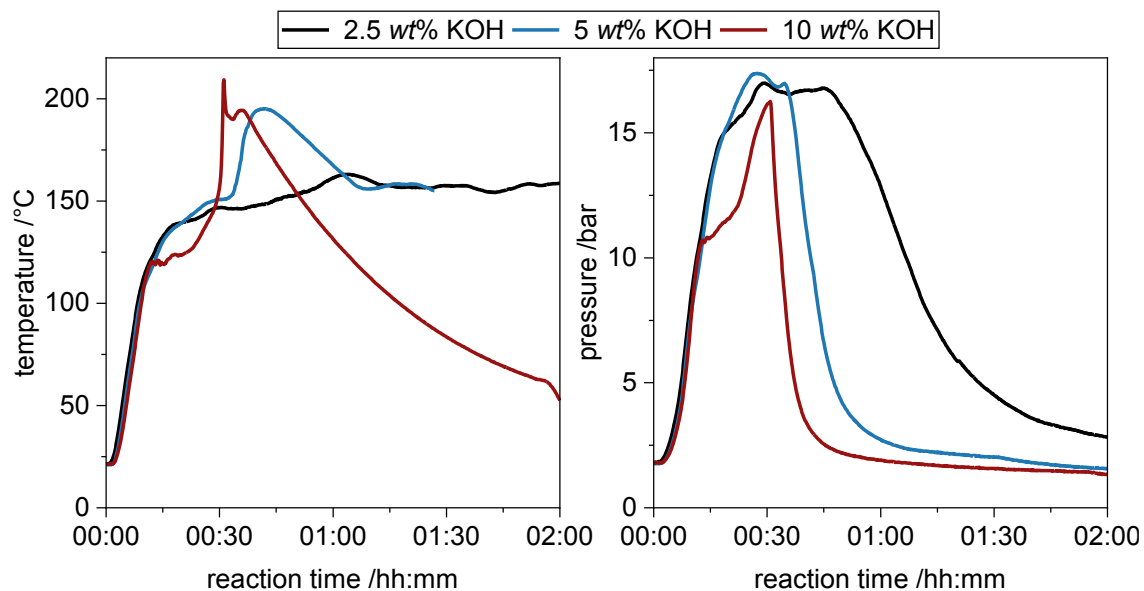


Figure A1. Temperature profile (left) and pressure profile (right) of oxypropylation with 2.5 wt% (black), 5 wt% (blue) and 10 wt% (red) KOH. For 10 wt% external heat source was removed after 30 minutes because of the high reaction temperature caused by the exothermic polymerization reaction.

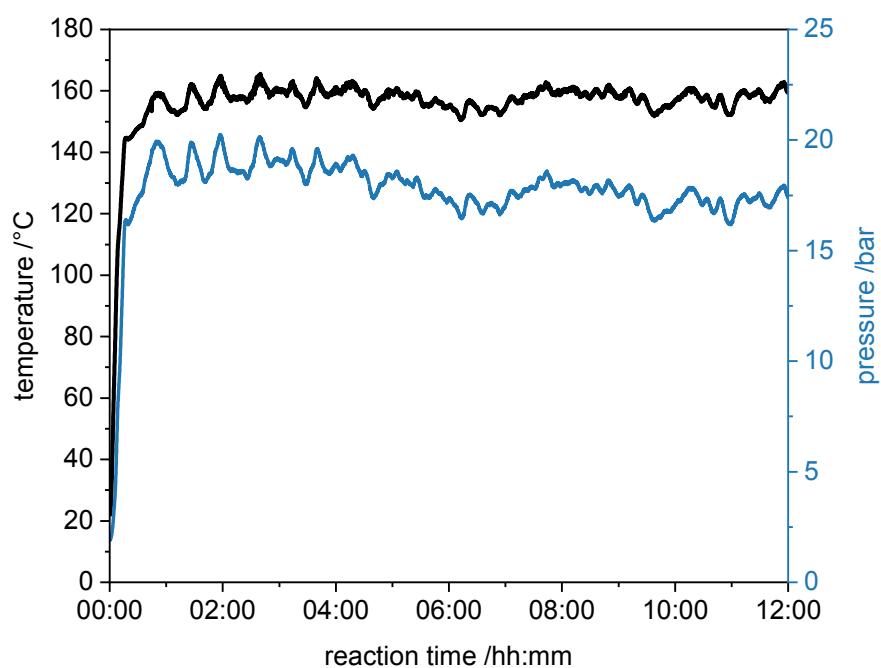


Figure A2. Temperature profile (black) and pressure profile (blue) of oxypropylation with 5 *wt%* DBU.

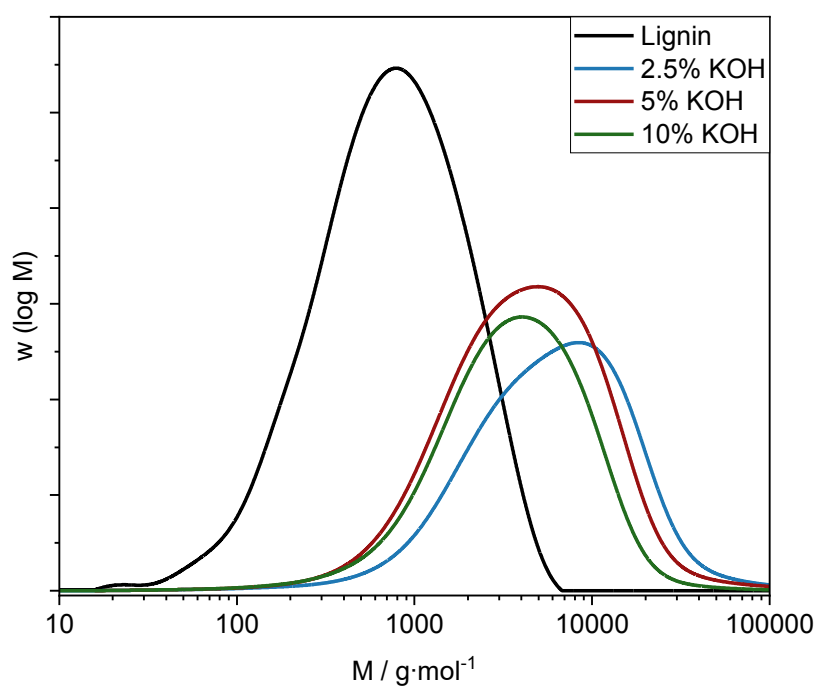


Figure A3. SEC chromatograms for unmodified lignin (black) and after oxypropylation with 2.5 *wt%* (blue), 5 *wt%* (red) and 10 *wt%* (green) KOH.

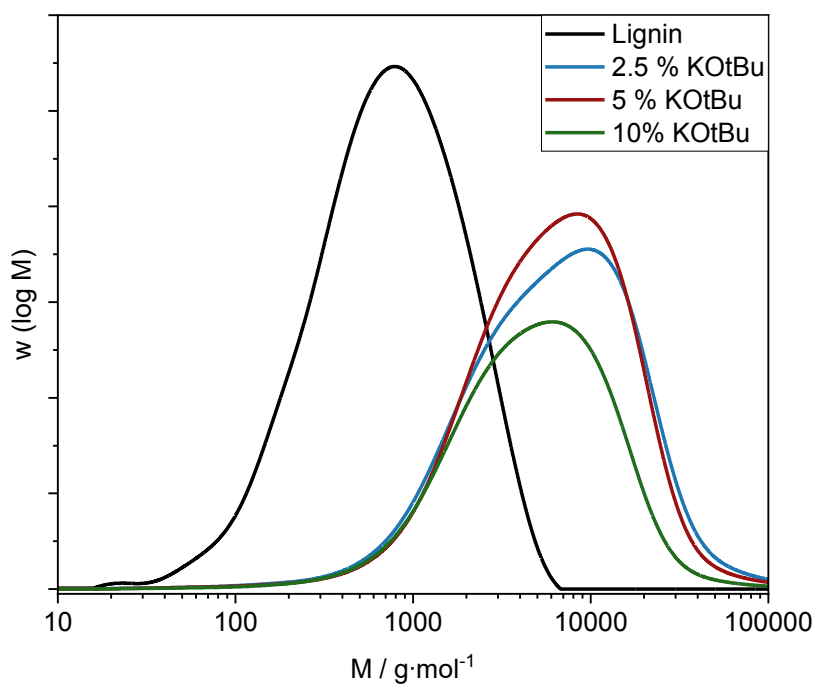


Figure A4. SEC chromatograms for unmodified lignin (black) and after oxypropylation with 2.5 wt% (blue), 5 wt% (red) and 10 wt% (green) KOtBu.

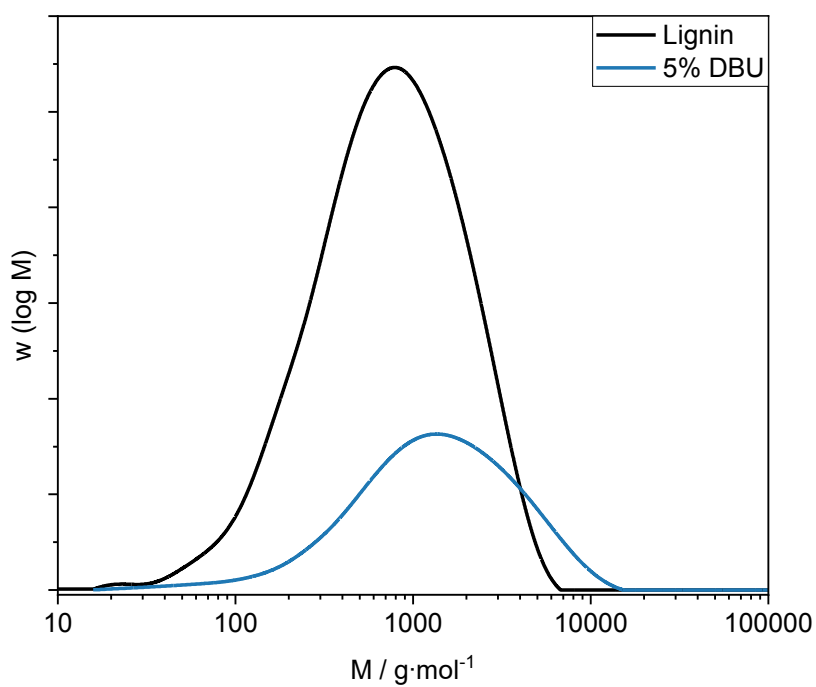


Figure A5. SEC chromatograms for unmodified lignin (black) and after oxypropylation with 5 wt% DBU (blue).

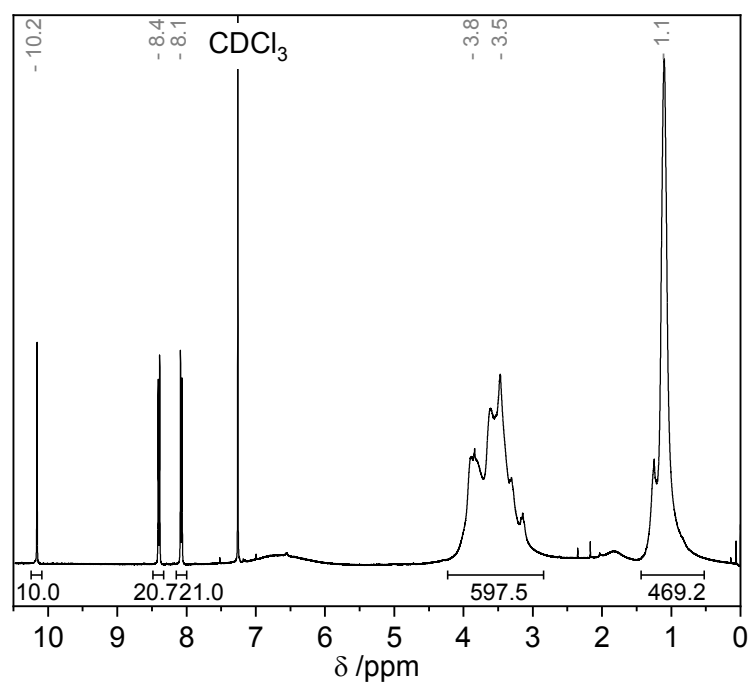


Figure A6. ^1H NMR spectrum of 10.2 mg modified OSL oxypropylated with 5 wt% KOtBu.

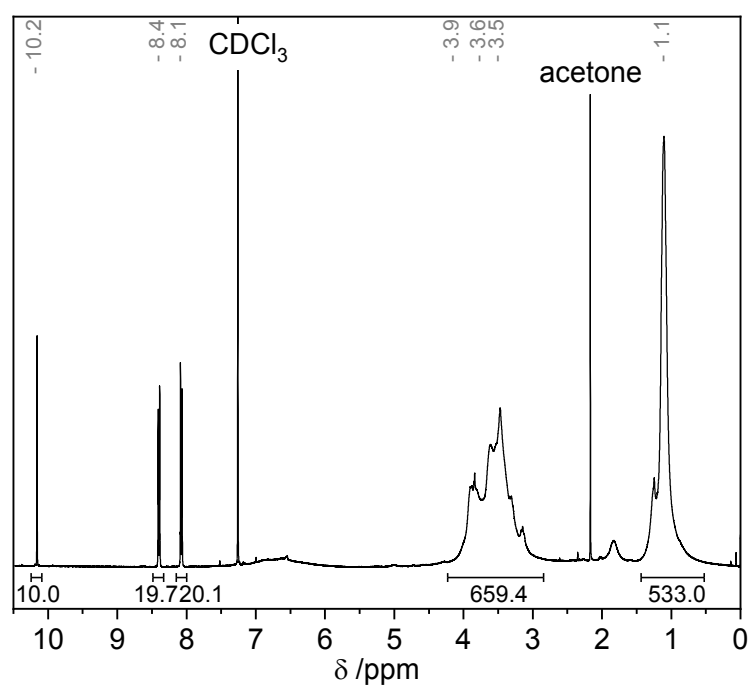


Figure A7. ^1H NMR spectrum of 10.8 mg modified KL oxypropylated with 5 wt% KOtBu.

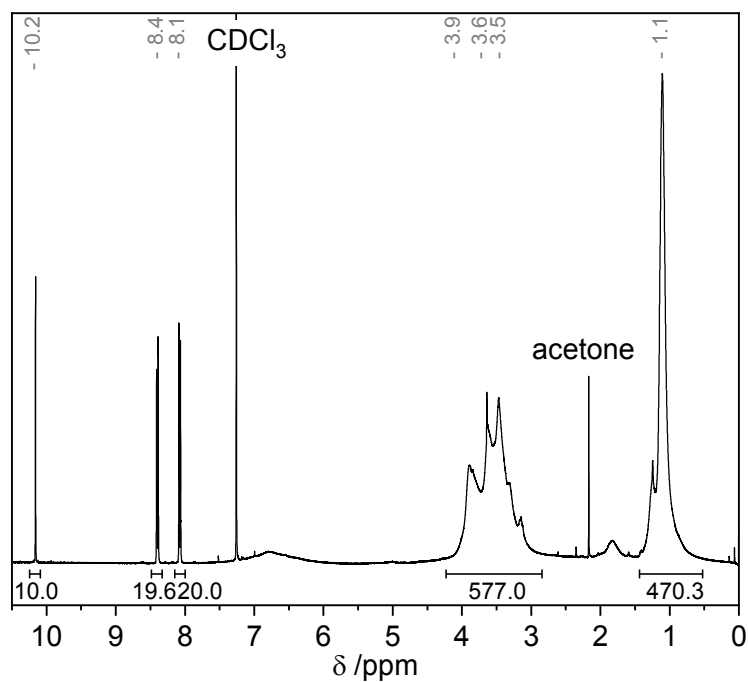


Figure A8. ^1H NMR spectrum of 11.2 mg modified SL oxypropylated with 5 wt% KOtBu.

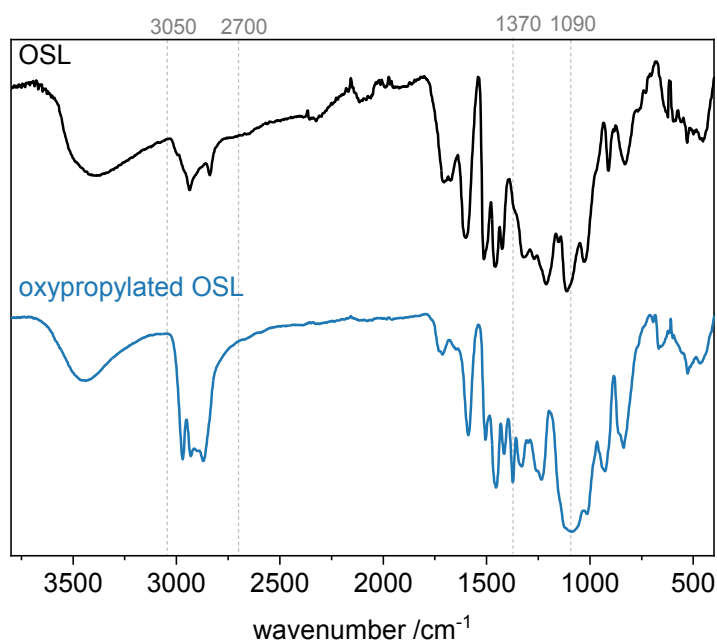


Figure A9. FTIR spectra of OSL (black) and of oxypropylated OSL (blue).

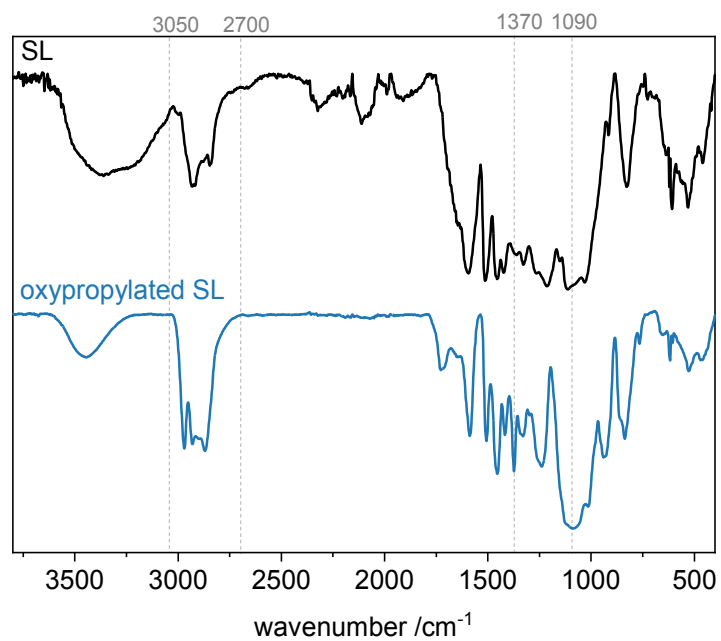


Figure A10. FTIR spectra of SL lignin (black) and of oxypropylated SL (blue).

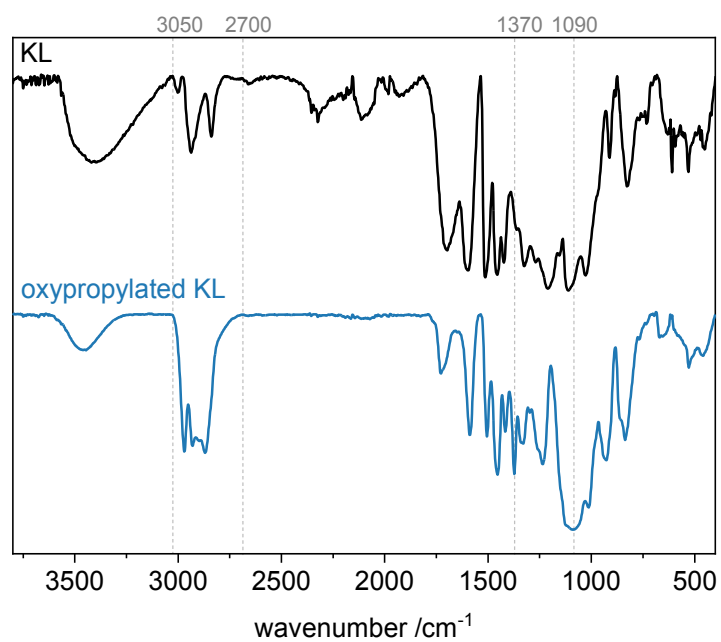


Figure A11. FTIR spectra of KL lignin (black) and of oxypropylated KL (blue).

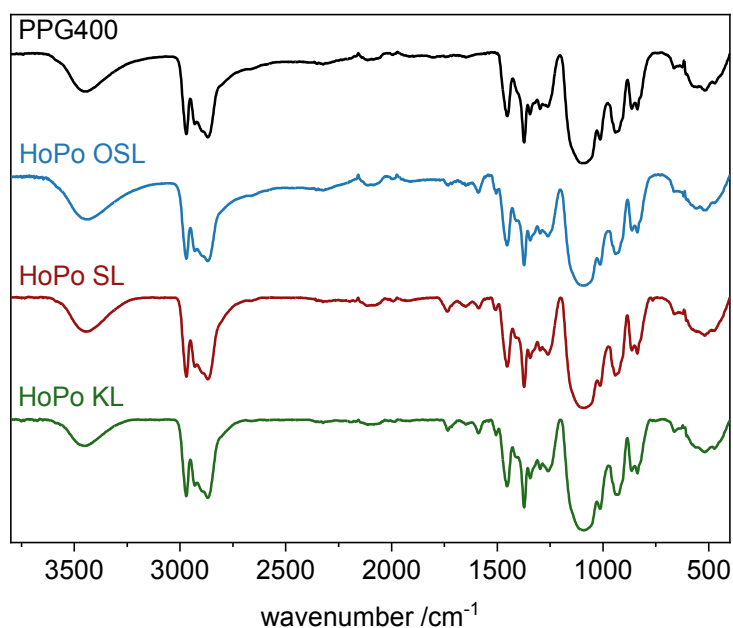


Figure A12. FTIR spectra of PPG400 (black) and homopolymers obtained in oxypropylation of OSL (blue) SL (red) and KL (green).

Table A1. Data on KL, SL and OSL.

	KL	SL	OSL
$M_n / \text{g} \cdot \text{mol}^{-1}$	3300	2800	3200
$M_w / \text{g} \cdot \text{mol}^{-1}$	11700	8800	5700
$OH_{\text{arom.}} / \text{mmol} \cdot \text{g}^{-1}$	2.5	1.2	3.3
$OH_{\text{total}} / \text{mmol} \cdot \text{g}^{-1}$	3.4	2.2	5.0

KL and SL are not soluble in organic solvents. Thus, a different setup was used for Size Exclusion Chromatography and data for M_n presented here differs from the values obtained in chapter 3.3.2.

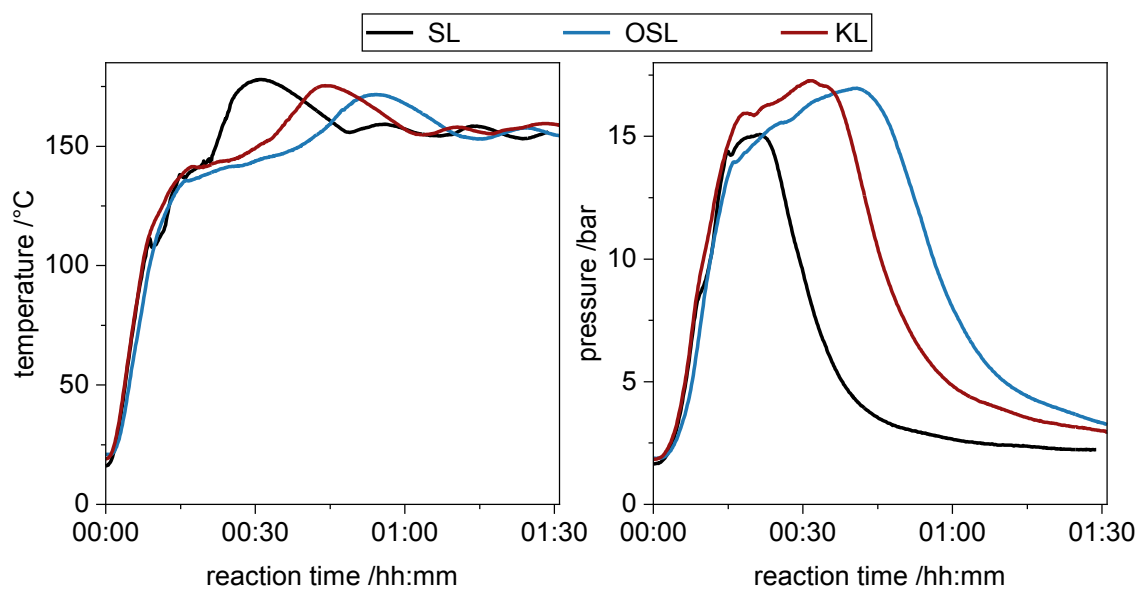


Figure A13. Temperature profile (left) and pressure profile (right) of oxypropylation of SL (black), OSL (blue) and KL (red) with 5 wt% KOtBu.

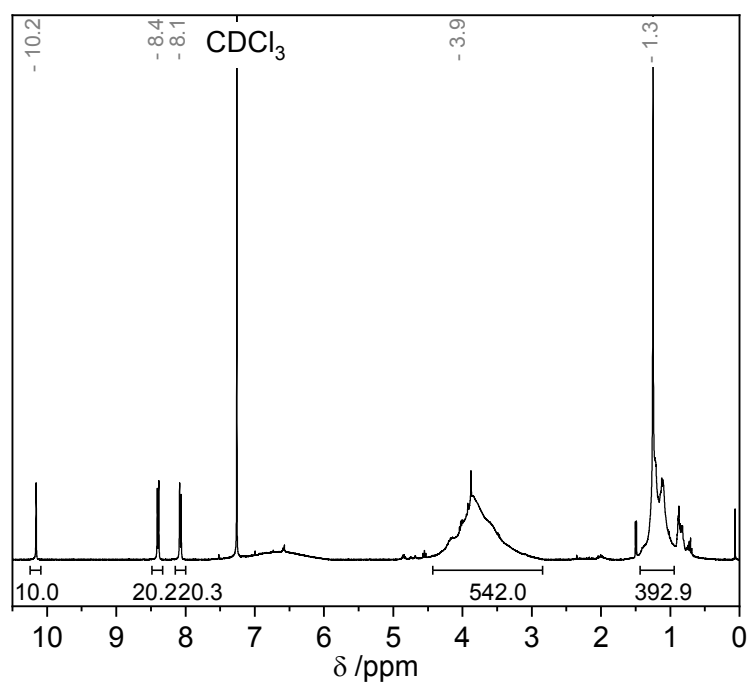


Figure A14. ¹H NMR spectrum of 14.7 mg modified OSL oxypropylated with cPC and KOtBu.

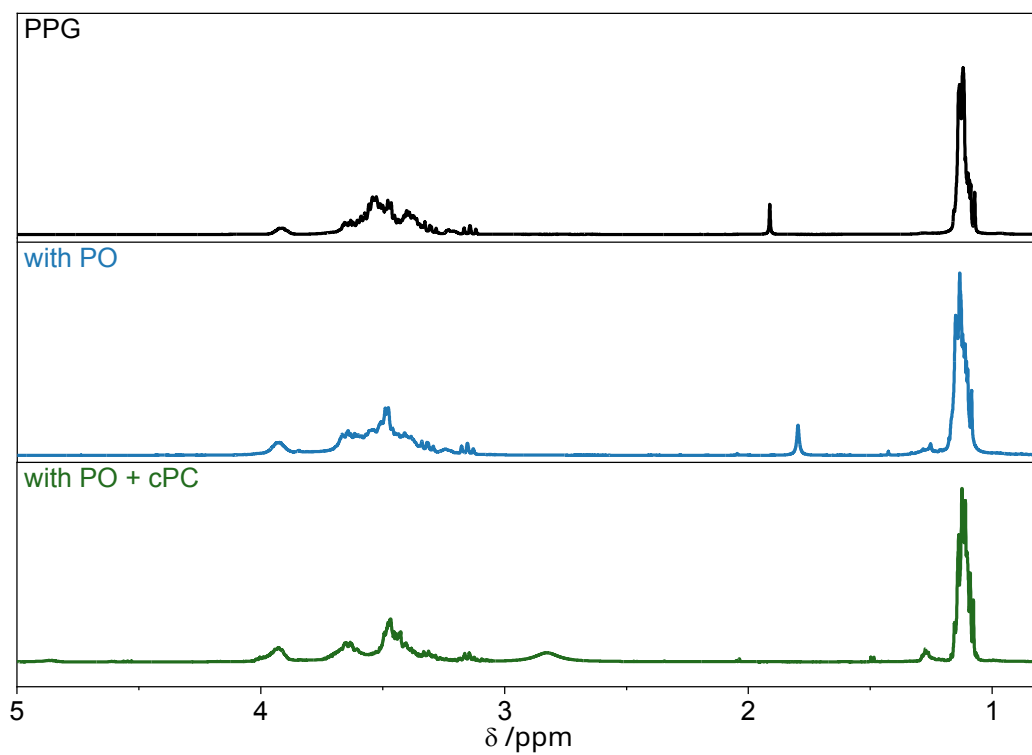


Figure A15. ^1H NMR spectra of commercially available PPG 400 (black), homopolymer after oxypropylation with PO (blue) and homopolymer after oxypropylation with PO + cPC (green).

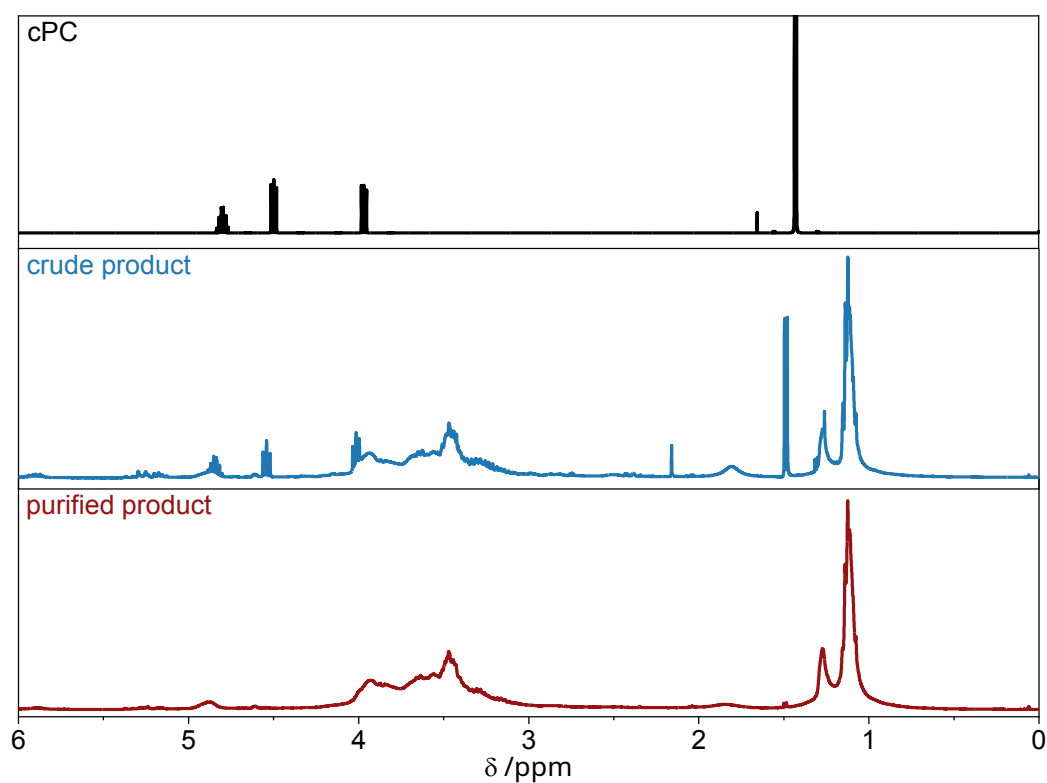


Figure A16. ^1H NMR spectra of cPC (black), crude reaction product (blue) and purified reaction product of oxypropylation of OSL with PC and cPC.

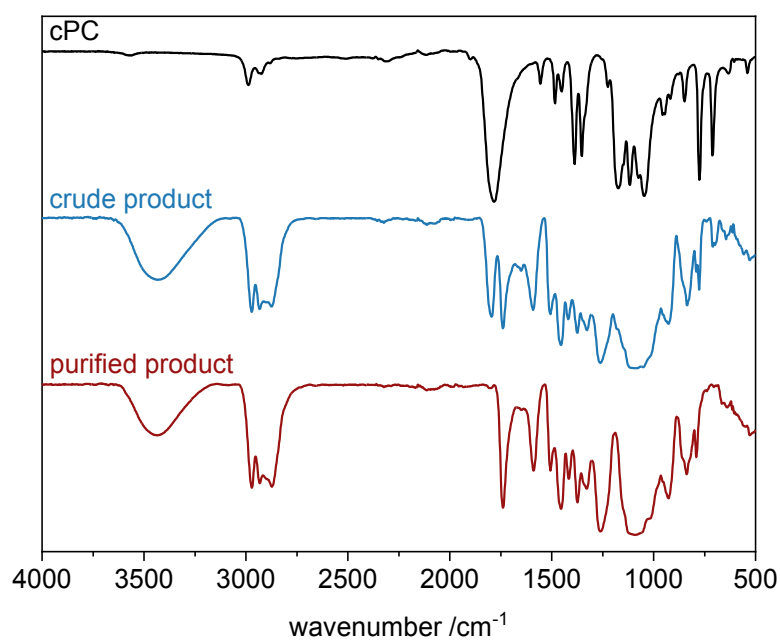


Figure A17. FTIR spectra of cPC (black), crude reaction product (blue) and purified reaction product of oxypropylation of OSL with PC and cPC.

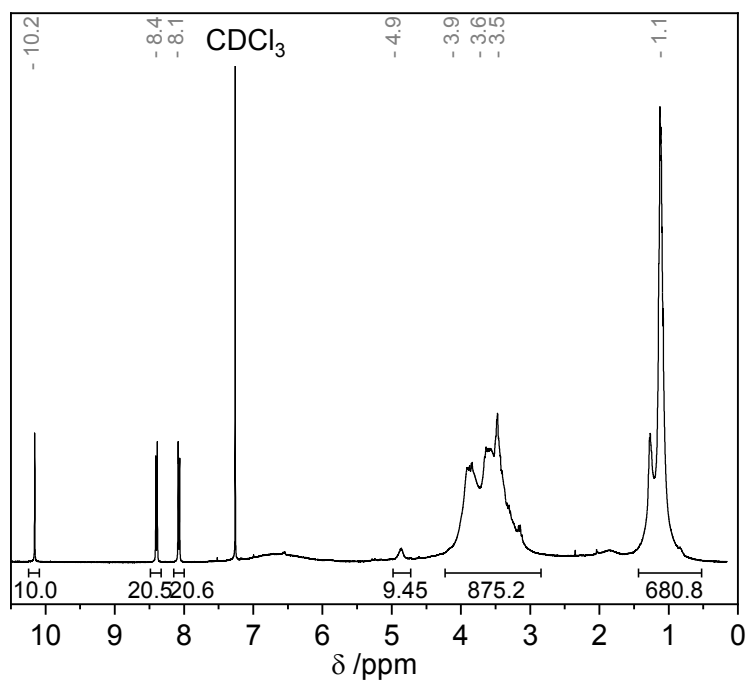


Figure A18. ¹H NMR spectrum of 16.2 mg modified OSL oxypropylated with 5% cPC.

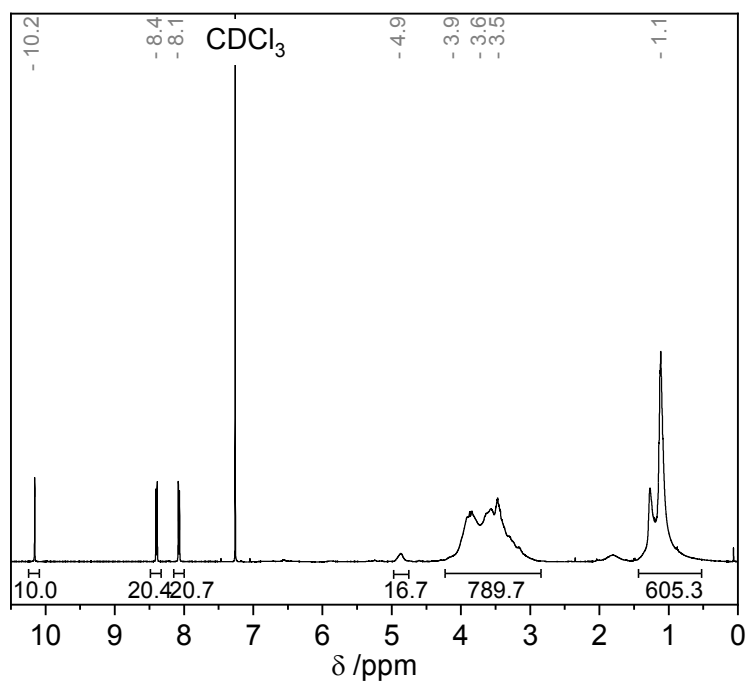


Figure A19. ¹H NMR spectrum of 15.7 mg modified OSL oxypropylated with 10% cPC.

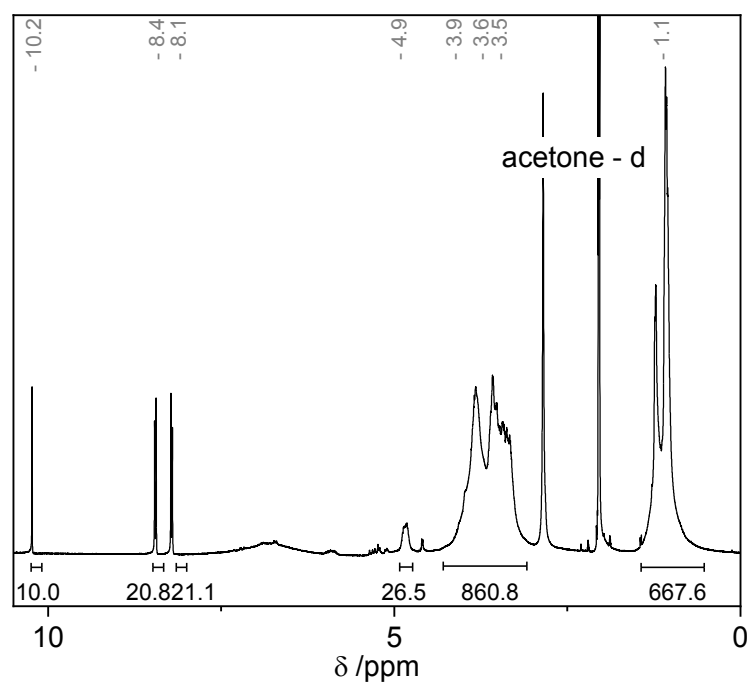


Figure A20. ^1H NMR spectrum of 15.0 mg modified OSL oxypropylated with 15% cPC.

Table A2. Experiment plan for Design of Experiments with DMSO fraction, M/C and M/F.

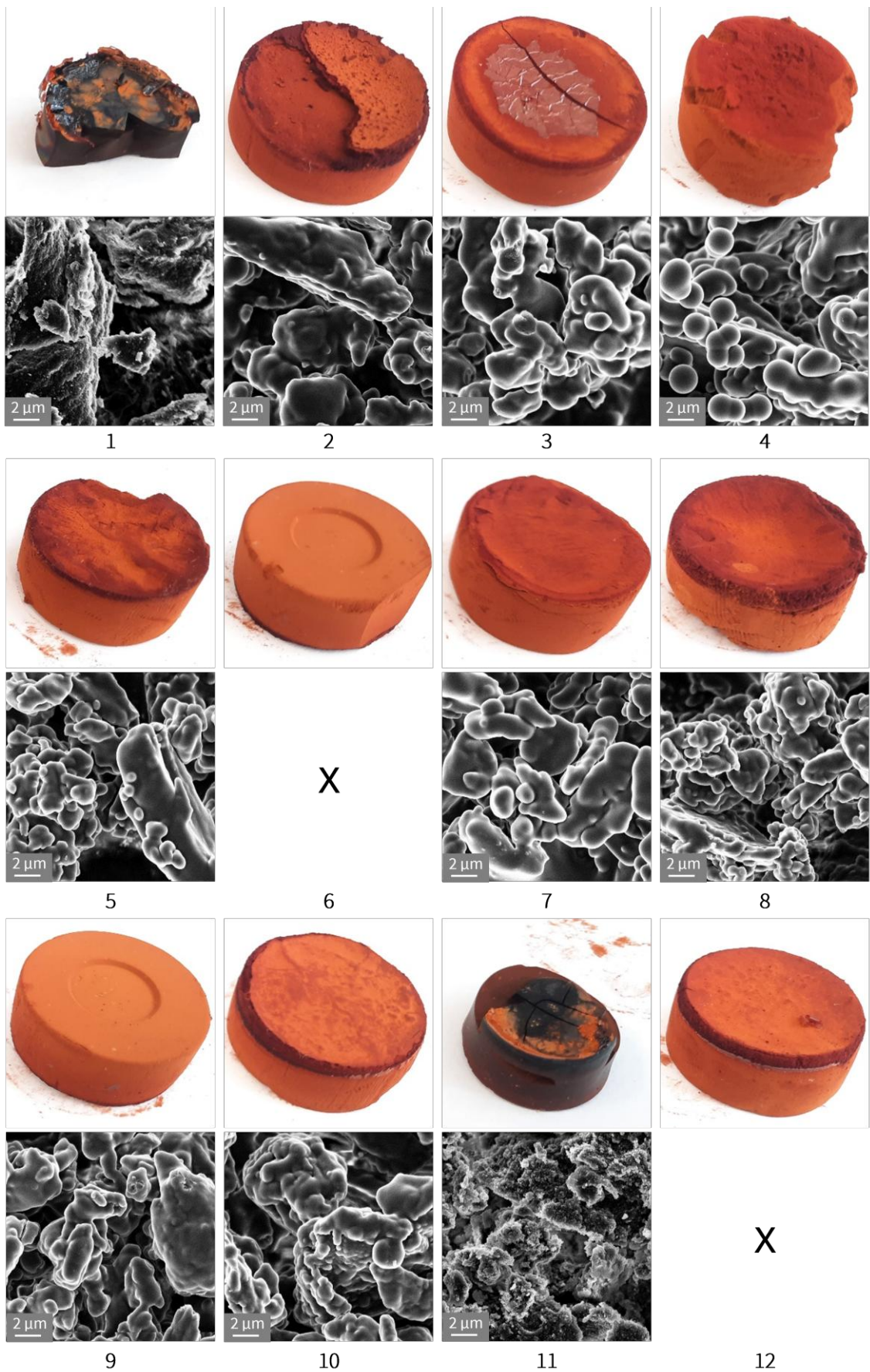
run	DMSO fraction <i>/wt%</i>	M/C	M/F
1	50.0	25.3	0.91
2	25.0	63.2	0.89
3	25.2	25.2	0.70
4	0.0	25.0	0.50
5	0.0	63.1	0.70
6	25.1	63.1	0.71
7	0.0	25.3	0.90
8	0.0	101	0.76
9	25.0	63.7	0.71
10	25.0	101	0.71
11	50.1	25.5	0.51
12	25.1	62.9	0.70
13	49.9	63.5	0.71
14	50.1	101	0.50
15	25.0	63.4	0.70
16	24.9	63.7	0.51
17	25.0	63.1	0.70
18	50.1	101	0.90
19	0.0	101	0.89
20	25.1	63.2	0.71

Table A3. Responses (gelation time, shrinkages, overall quality) for Design of Experiments.

run	gelation time /min	shrinkage /%	overall quality
1	45	41	1
2	30	7.5	5
3	20	7.5	4
4	10	7.5	2
5	10	2,5	3
6	30	7.5	5
7	10	2,5	4
8	20	2,5	3
9	30	7.5	5
10	60	5.0	5
11	30	43	1
12	45	7.5	5
13	180	41	1
14	180	38	1
15	30	7.5	5
16	30	7.5	5
17	60	7.5	5
18	1000	39	1
19	60	2.5	3
20	60	5.0	5

Table A4. Coded factors of the model equation describing gelation time as determined by Design of Experiments.

Coded factors	
-2.11	
1,45	M/C
0,8416	M/F
1,68	DMSO content
0,9426	M/C · M/F
1,01	M/C · DMSO content
0,7557	M/F · DMSO content



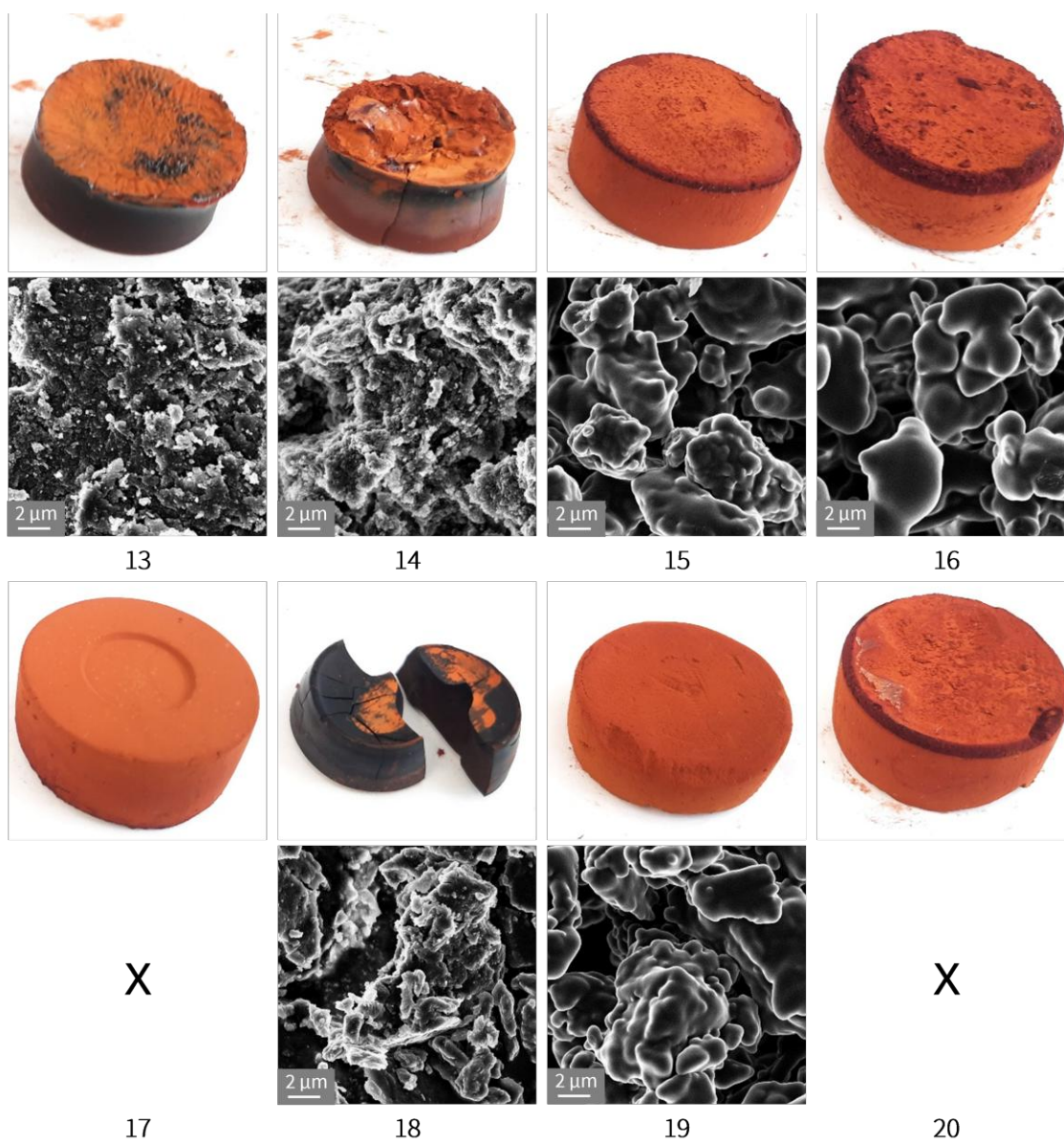


Figure A 21. Photos and SEM images of dried gels prepared for DoE.

Publications

Parts of this thesis have been presented at conferences:

Synthesis of Lignin Containing Resorcinol Formaldehyde Aerogels with Tailored Pores

P. Weidmann, Meyer, R. S. A. Meyer , I. Smirnova, G. A. Luinstra

Poster presentation at Macromolecular Colloquium, February 20-22, 2019, Freiburg, Germany.

Acid Catalyzed Lignin-Resorcinol-Formaldehyde Aerogels: Influence of Solvents on Particle Morphology

P. Weidmann, T. Duhm, R. S. A. Meyer , I. Smirnova, G. A. Luinstra

Poster presentation at EPF European Polymer Congress, June 26 – July 1, 2022, Prague, Czech Republic.

Acknowledgements

Ich möchte mich bei Prof. Dr. Gerrit A. Luinstra für die Möglichkeit bedanken, meine Doktorarbeit in seinem Arbeitskreis anzufertigen.

Dr. Robert Meyer danke ich für die fachliche Unterstützung während der gesamten Promotion.

Bei allen Partnern im Projekt POLIGOM, insbesondere bei den Arbeitsgruppen von Prof. Dr. Irina Smirnova and Prof. Dr. Falk Lieber bedanke ich mich für die gute Zusammenarbeit.

Frederik Leube, Torben Duhm und Tim Domroes gilt mein Dank für ihre Unterstützung im Labor im Zuge ihres Praktikums/Bachelorarbeiten.

Für zahlreiche Analytik bedanke ich mich bei Dr. Felix Scheliga (GPC), Frau Walther und Frau Woelken (SEM) sowie dem NMR-Service der Uni Hamburg.

Bei Hans und Hannah bedanke ich mich für das Korrekturlesen.

Ein riesiges Dankeschön geht an die Kollegen aus dem AK Luinstra, wegen denen ich trotz allem Frust jeden Tag gerne in die Uni gefahren bin. Die zahlreichen geselligen Runden mit euch haben dafür gesorgt, dass ich in den letzten Jahren nicht verrückt geworden bin. Im Besonderen danke ich meinen Lieblingskollegen Hannah und Hauke! Es bedeutet mir viel, dass ihr von meinen Kollegen zu meinen Freunden geworden seid und wir mit Sicherheit lange über die Promotion hinaus in Kontakt bleiben.

Zuletzt möchte ich mich bei allen Menschen bedanken, die mich während meines gesamten Studiums außerhalb der Uni begleitet haben. Ihr habt mich unterstützt und motiviert, aufgebaut und getröstet, aber auch mal kritisiert und mir so geholfen, über mich hinauszuwachsen. Vor allem habt ihr mich in genau den richtigen Momenten daran erinnert, dass sich das wirklich wichtige meist außerhalb der Uni abspielt. Ohne jeden einzelnen von euch wäre ich nicht diejenige, die ich heute bin – danke!

Declaration of Academic Integrity

I hereby declare on oath and affirm that this doctoral dissertation is my own work and that I have not used any aids and sources other than those indicated. If electronic resources based on generative artificial intelligence (gAI) were used in the course of writing this dissertation, I confirm that my own work was the main and value-adding contribution and that complete documentation of all resources used is available in accordance with good scientific practice. I am responsible for any erroneous or distorted content, incorrect references, violations of data protection and copyright law or plagiarism that may have been generated by the gAI.

Hamburg, 26.06.2025



Place, Date, Signature